

**Synthesis, Characterization and Biological Applications of
Phyto-assisted Chitosan Nanocomposites**



By

BEENISH

Department of Biochemistry

Faculty of Biological Sciences

Quaid-i-Azam University

Islamabad, Pakistan

2023

**Synthesis, Characterization and Biological Applications of
Phyto-assisted Chitosan Nanocomposites**



A dissertation submitted in the partial fulfillment of the requirements

for the degree of

Doctor of Philosophy

in

Biochemistry / Molecular Biology

Submitted By

Beenish

Department of Biochemistry

Faculty of Biological Sciences

Quaid-i-Azam University

Islamabad, Pakistan

2023

This thesis is dedicated to my beloved
family especially my husband, kids, my
parents and siblings

For their countless sacrifices to help me
complete this PhD journey

Author's Declaration

I **Beenish** hereby state that my PhD thesis, titled **“Synthesis, Characterization and Biological Applications of Phyto-assisted Chitosan Nanocomposites”** is my own work and has not been submitted previously by me for taking any degree from

Department of Biochemistry, Faculty of Biological Sciences, Quaid-i-Azam University, Islamabad, Pakistan.

Or anywhere else in the country/world.

At any time if my statement is found to be incorrect even after my graduation, the University has the right to withdraw my Ph.D degree.

Student/Author Signature: _____



Ms. Beenish
Date: June 26, 2024

Plagiarism Undertaking

I solemnly declare that research work presented in the PhD thesis, titled **“Synthesis, Characterization and Biological Applications of Phyto-assisted Chitosan Nanocomposites”** is solely my research work with no significant contribution from any other person. Small contribution/help wherever taken has been duly acknowledged and that complete thesis has been written by me.

I understand the zero-tolerance policy of the HEC and **Quaid-i-Azam University, Islamabad**, towards the plagiarism. Therefore, I as an Author of the above titled thesis declare that no portion of my thesis has been plagiarized and any material used as reference is properly referred/cited.

I undertake that if I am found guilty of any formal plagiarism in the above titled thesis even after award of PhD degree, the University reserves the right to withdraw/revoke my PhD degree and that HEC and the University has the right to publish my name on the HEC/University website on which names of students are placed who submitted plagiarized thesis.

Student/Author Signature: _____



Ms. Beenish

Date: June 26, 2024

Certificate of Approval

This is to certify that the research work presented in this thesis, entitled: “**Synthesis, Characterization and Biological Applications of Phyto-assisted Chitosan Nanocomposites**” was conducted by **Ms. Beenish** under the supervision of Prof. Dr. Bushra Mirza.

No part of this thesis has been submitted anywhere else for any other degree. This thesis is submitted to the Department of Biochemistry, Faculty of Biological Sciences, Quaid-i-Azam University, Islamabad, Pakistan in partial fulfillment of the requirements for the **Degree of Doctor of Philosophy** in the field of Biochemistry from Department of Biochemistry, Faculty of Biological Sciences, Quaid-i-Azam University, Islamabad, Pakistan.

Ms. Beenish

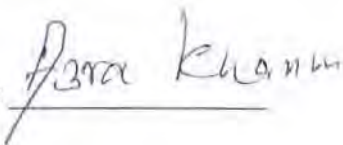
Signature: 

Examination Committee:

1. External Examiner:

Prof. Dr. Azra Khanum


University Institute of Biochemistry & Biotechnology
PMAS. Arid Agricultural University, Rawalpindi

Signature: 

2. External Examiner:

Prof. Dr. M. Jawad Hassan

Head of Department of Biological Sciences
National University of Medical Sciences
NUMS, Rawalpindi

Signature: 


3. Supervisor:

Prof. Dr. Bushra Mirza

Signature: 

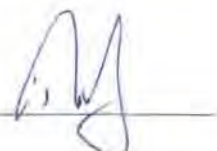
4. Co-Supervisor:

Dr. Nosheen Akhtar (NUMS Rwp)

Signature: 

5. Chairman:

Prof. Dr. Iram Murtaza

Signature: 

Dated:

June 26, 2024

CONTENTS

ACKNOWLEDGMENTS	i
LIST OF FIGURES	iii
LIST OF TABLES	vi
LIST OF ABBREVIATIONS	vii
ABSTRACT	ix

Chapter 1	Introduction and Literature Review	
1.1	Biopolymer based food packaging	1
1.2	Biopolymers	1
1.3	Chitosan	4
1.4	Active packaging	5
1.5	Nanocomposites	7
1.6	Methods of film preparation	13
1.7	Physical properties and characterization of chitosan films	14
1.8	Bioactive properties of chitosan films for food packaging	18
1.9	Plant extracts as additives in chitosan nanocomposite films	19
1.10	Selection of plant extracts	20
1.11	Selection of nano fillers	26
1.12	Aims and Objectives	27
Chapter 2	Screening, Biological Activities and Molecular Docking of the Plant Extracts	
2.1	Introduction	28
2.2	Materials and Methods	30
2.2.1	Plant collection	30

2.2.2	Plant extract preparation	30
2.2.3	Phytochemical analysis	31
2.2.4	<i>In vitro</i> biological activities	32
2.2.5	Molecular docking analysis	34
2.3	Results	34
2.3.1	Percent yield	34
2.3.2	Phytochemical analysis	35
2.3.3	In vitro biological activities	37
2.3.4	Molecular docking analysis	43
2.4	Conclusion	45
Chapter 3	Synthesis and Characterization of Phyto-assisted Chitosan Nanocomposites	
3.1	Introduction	47
3.2	Materials and Methods	49
3.2.1	Materials	49
3.2.2	Extraction of keratin from chicken feathers	49
3.2.3	Preparation of nano keratin	49
3.2.4	Extract and polyphenols preparation	50
3.2.5	Film Preparation	50
3.2.6	Physical, mechanical and barrier properties	51
3.2.7	Structural properties	53
3.2.8	Thermal properties	54
3.2.9	Statistical analysis	55
3.3	Results	55
3.3.1	Screening and optimization of contents in film preparation	55
3.3.2	Physical mechanical and barrier properties	58
3.3.3	Structural properties	65
3.3.4	Thermal properties	74
3.3.5	Conclusion	81

Chapter. 4	<i>In vitro</i> Biological Activities of Phyto-assisted Chitosan Nanocomposites	
4.1	Introduction	82
4.2	Materials and Methods	83
4.2.1	Total phenolic content	83
4.2.2	Antioxidant activity	83
4.2.3	Antibacterial activity	84
4.2.4	Antifungal activity	84
4.2.5	Food quality analysis	85
4.3	Results	85
4.3.1	Total phenolic content	85
4.3.2	Antioxidant activity	87
4.3.3	Antibacterial activity	87
4.3.4	Antifungal activity	87
4.3.5	Relationship analysis between DPPH scavenging and antimicrobial activity	88
4.3.6	Food quality analysis	90
4.4	Conclusion	92
Chapter. 5	Biodegradability and Toxicity	
5.1	Introduction	93
5.2	Materials and methods	95
5.2.1	Materials	95
5.2.2	Biodegradation studies	95
5.2.3	Toxicity studies	95
5.3	Results	97
5.3.1	Biodegradability analysis	97
5.3.2	Characterization of degraded films	99
5.3.3	Toxicity studies	107
5.4	Conclusion	111
Chapter. 6	Discussion	
6.1	Discussion	112
6.2	Screening, <i>in vitro</i> activities and molecular docking of plant extracts	112

6.3	Synthesis and characterization of phyto-assisted chitosan nanocomposites	115
6.4	<i>In vitro</i> biological activities of phyto-assisted chitosan nanocomposites	122
6.5	Biodegradability and toxicity	125
	Conclusion	130
	Future Perspectives	130
	References	132
	Appendix	149
	List of Publications	150

ACKNOWLEDGEMENTS

I am grateful for all the bounties that **ALLAH** Almighty has showered on me which enabled me to complete this thesis. Countless salutations upon the **Holy Prophet HAZRAT MUHAMMAD (Sallalloho Allaihe Waalahe Wassalam)** the city of knowledge for enlightening with the essence of faith in Allah and guiding the mankind, the true path of life.

I feel highly privileged in taking opportunity to express my deep sense of gratitude to my supervisor **Prof. Dr. Bushra Mirza**, Department of Biochemistry, Faculty of Biological Sciences, Quaid-i-Azam University (QAU), Islamabad for her kind guidance and valuable suggestions throughout the study and presentation of this manuscript. I am thankful to her for her inspiration, reassurance and counseling from time to time. I wish to express my most sincere thanks to Dr. Irum Murtaza, Chairman, Department of Biochemistry for extending the research facilities to accomplish this work. I am thankful to Dr. Muhammad Tahir Waheed for their support and help during my research work. I want to say special thanks to **Dr. Ihsan-ul-Haq** who provided immense help and his lab facilities in completion of my PhD research.

I would like to thankfully acknowledge Higher Education Commission, Pakistan (HEC) for providing the Faculty Development Program (FDP) scholarship and financial support during my research in Pakistan and Canada. I am extremely grateful to **Dr. Aman Ullah** at the Department of Agricultural, Food and Nutritional Science, University of Alberta., Canada for providing research facilities to carry out my research project in his laboratory and also for his immense help, suggestions and guidance in writing articles. I am also indebted to **Dr. Nosheen Akhtar** for her inspiration, reassurance and counseling from time to time to complete this research project.

It is my pleasure to mention my laboratory members Amirah, Punita, Kiki, Karren, Zubair, frage, for their great cooperation and support during my stay at University of Alberta, Edmonton, Canada. I believe that without their help my PhD project may not have been furnished so quickly and nicely. I would like to extend my deepest appreciation to those people, who helped me in one way or another during my stay at Department of Biochemistry, QAU, Islamabad, Pakistan and Edmonton, Canada. I wish to convey my gratitude to all of them specially Faheem baig, Shabana, Rimsha, Iqra,

Atiqa, Mehreen, Mehmand, Neelam, Rabia, Sara, Zunaira, Waleed, Sidra, Uroosa, yusra, Maria, Sundas and Umair (Canada), Kamran (Canada), Muhammad Arsalan (Canada), Momina (Canada) for their continued encouragement, moral support and necessary guidance. Special thanks to Irshad Khan, Amir and Ramzan for assisting me in various ways during my research work. I'll always remember the cooperation and help of Biochemistry office staff M. Tariq, M. Maqsood, M. Fayyaz and M. Shahzad. I would like to pay very special tribute to my lab fellows Irum, Samina, Furrukh and Afshan. Words fail me to express my appreciation to my dearest mother and father, sisters (Sundas and Fariha) and brothers (Bilal and Jamal khanzada) and my loving husband **Nadeem Ahmed Khanzada** and kids (**Abdullah and Meerab**) whose constant love and sacrifices enabled me to complete this PhD journey.

Beenish

LIST OF FIGURES

S. #	Title	Page
Fig. 1.1	Classes of biopolymers	3
Fig. 1.2	Mechanism of biodegradability in biopolymers	4
Fig 1.3	Structure of chitosan	5
Fig. 1.4	Active packaging systems in food	6
Fig 1.5	Structure of nano crystalline cellulose	9
Fig 1.6	Cross linking of chicken feather keratin with glutaraldehyde	12
Fig 1.7	<i>Cinnamomum zeylanicum</i>	21
Fig 1.8	<i>Cinnamomum tamala</i>	22
Fig 1.9	<i>Amomum subulatum</i>	22
Fig 1.10	<i>Trigonella foenum graecum</i>	23
Fig 1.11	<i>Mentha piperita</i>	24
Fig 1.12	<i>Coriandrum sativum</i>	25
Fig 1.13	<i>Lactuca sativa</i>	25
Fig 1.14	<i>Brassicca oleraceae var italic</i>	26
Fig 2.1	HPLC profile of the plant extracts	37
Fig 2.2	Total reducing power of the plant extracts	38
Fig 2.3	Total antioxidant activity of the plant extracts	39
Fig 2.4	Dose response curve of plant extracts showing highest and lowest DPPH scavenging percentage	40
Fig 2.5	Minimum inhibitory concentration (MIC) of the plant extracts	42
Fig 2.6	Graphical representation of polyphenols binding modes in fungal proteins.	45
Fig 3.1	Optimization of different components of chitosan films	56
Fig 3.2	Schematic representation of film preparation	57
Fig 3.3	Photographs of prepared films	58
Fig 3.4	Tensile strength (stress) and percent elongation (strain %) of extract incorporated films	59

Fig 3.5	Tensile strength (stress) and percent elongation (strain %) of polyphenol incorporated films	61
Fig 3.6	Water vapor permeability and opacity of polyphenol incorporated films	62
Fig 3.7	UV transmittance of extract incorporated films	63
Fig 3.8	UV transmittance of polyphenol incorporated films	63
Fig 3.9	Percent water solubility, swelling and moisture content	64
Fig 3.10	FTIR analysis	66
Fig 3.11	XRD analysis	68
Fig 3.12	XPS survey spectra	69
Fig 3.13	High resolution C1s spectra	70
Fig 3.14	SEM analysis of CNC and NK reinforced extract incorporated composites	72
Fig 3.15	SEM analysis of CNC reinforced polyphenol incorporated composites	73
Fig 3.16	SEM analysis of CNC and NK reinforced extract incorporated composites	73
Fig 3.17	TEM analysis	74
Fig 3.18	TGA analysis of CNC and NK reinforced extract incorporated composites	75
Fig 3.19	TGA analysis of CNC reinforced polyphenol composites	77
Fig.3.20	TGA analysis of NK reinforced polyphenol composites	78
Fig.3.21	DSC Analysis	79
Fig.3.22	DMA Analysis	80
Fig 4.1	Total polyphenol content and DPPH assay of films	86
Fig 4.2	Anti-bacterial and antifungal Zone of inhibition of films	88
Fig 4.3	Plates showing antibacterial zones of films	89
Fig 4.4	Plates showing antibacterial zones of films	89

Fig 4.5	Percent weight loss of baby carrots packaged with extract incorporated films	90
Fig 4.6	Baby carrot packaging with extract incorporated films	90
Fig 4.7	Percent weight loss of baby carrots packaged with polyphenol incorporated films	91
Fig 4.8	Baby carrot packaging with polyphenol incorporated films	92
Fig 5.1	Soil and lysozyme degradation of extract incorporated films	98
Fig 5.2	Soil and lysozyme degradation of polyphenol incorporated films	98
Fig 5.3	SEM images of degraded extract incorporated films	99
Fig 5.4	SEM images of degraded polyphenol incorporated films	100
Fig 5.5	FTIR Analysis of degraded extract incorporated films	101
Fig 5.6	FTIR Analysis of degraded polyphenol incorporated films	102
Fig 5.7	TGA analysis of soil degraded films	103
Fig 5.8	TGA analysis of lysozyme degraded films	104
Fig 5.9	DSC Analysis of degraded films	106
Fig 5.10	Hemo-compatibility Assay	107
Fig 5.11	Liver and blood biochemical parameters profile of film treated rats	110

List of Tables

S. #	Title	Page
Table 2.1	Percent yield of the plant extracts	38
Table 2.2	Total phenolic and flavonoid content of the plant Extracts	36
Table 2.3	Identification and quantification of polyphenols ($\mu\text{g}/\text{mg}$ of extract) by HPLC	38
Table 2.4	DPPH free radical scavenging activity of the plant Extracts	40
Table 2.5	Antibacterial assay	41
Table 2.6	Antifungal assay	43
Table 2.7	Binding affinities (in terms of k_d values) of polyphenols with fungal enzymes	44
Table 3.1	Mechanical and barrier properties of films	60
Table 3.2	Percent elemental composition of extract incorporated films	71
Table 5.1	Body weight changes of rats treated with films	108
Table 5.2	Hematological parameters of rats fed with films	109

LIST OF ABBREVIATIONS

ATCC	American Type Culture Collection
T.S	Tensile strength
E (%)	Percent elongation
CNC	Cellulose nano crystals
NK	Nano-keratin
CS	Chitosan
CS-control	Chitosan film only
CS-CNC	Chitosan with CNC only
CS-NK	Chitosan with NK only
CS-CNC-NK-EX1	Chitosan with CNC, NK and <i>C. tamala</i> extract
CS-CNC-NK-EX2	Chitosan with CNC, NK and <i>A. subulatum</i> extract
CS-CNC-NK-EX3	Chitosan with CNC, NK and <i>M. piperita</i> extract
CS-CNC-Q	Chitosan with CNC and quercetin
CS-CNC-R	Chitosan with CNC and rutin
CS-CNC-VA	Chitosan with CNC and vanillic acid
CS-NK-Q	Chitosan with NK and quercetin
CS-NK-R	Chitosan with NK and rutin

CS-NK-VA	Chitosan with NK and vanillic acid
TGA	Thermo-gravimetric analysis
DSC	Differential scanning calorimetry
FTIR	Fourier transform infra-red spectroscopy
DMA	Dynamic mechanical analysis
PHA	Poly-hydroxyalkanoates
IC50	The inhibitory concentration at 50%
TRP	Total reducing power
TAC	Total antioxidant activity
DPPH	2,2-diphenyl-1-picrylhydrazyl
WVP	Water vapor permeability
T _g	Glass transition temperature

Abstract

There is an increased demand for eco-friendly bio-degradable food packaging material to control the worldwide environmental crises arising due to petroleum derived plastic packaging. This study was designed in a contribution to make active chitosan films reinforced with two different types of nano fillers (cellulose nanocrystals and nano keratin) to increase the mechanical and barrier properties of chitosan films. Three ethanolic plant extracts (*Cinnamomum tamala*, *Amomum subulatum* and *Mentha piperita*) and their major polyphenols (quercetin, rutin and vanillic acid) were incorporated as additives to augment the antioxidant and antimicrobial properties of prepared films. Moreover, combinations of two nano fillers (synergistic effect of hybrid system) with plant extracts were evaluated for their effect on film properties. Tensile testing, thermo-gravimetric analysis, differential scanning calorimetry, dynamic mechanical analysis, water vapor permeability and opacity were used to evaluate the mechanical and barrier properties. Biodegradability of films was compared both in soil and lysozyme. The *in vitro* hemo-compatibility of films was checked on red blood cells. Acute oral toxicity effects of prepared films were analyzed *in vivo*. Baby carrot packaging was done with synthesized films and the effect of packaging on storage quality was assessed.

Screening of plants resulted in selection of *C. tamala*, *A. subulatum* and *M. piperita* for incorporation in chitosan films due to their highest total phenolic content, 70-80% free radical scavenging and moderate antimicrobial activities. Among polyphenols, quercetin, rutin and vanillic acid were selected due to their highest amount in the above extracts. Docking analysis predicted that selected polyphenols were one of the major reasons for the antimicrobial effect of these extracts via inhibition of specific enzymes.

Chitosan films were synthesized successfully via solvent casting and results showed that extract incorporated films reinforced with both nano fillers (CNC & NK) exhibited 59% increase in tensile strength of chitosan films. However, an increase of 63% was seen in tensile strength of CNC reinforced polyphenol composites. Extract incorporated films depicted excellent barrier properties (42% decrease in water vapour permeability), a two-fold increase in opacity, an enhanced thermal stability and glass transition temperature as compared to control chitosan films. Polyphenol composites displayed only 22% decrease in WVP and 38% increase in opacity. Extract incorporated

composites were found to be more thermally stable as compared to polyphenol composites.

Analysis of both extract and polyphenol incorporated films showed higher polyphenol content as compared to control which indicates correct incorporation of extract/polyphenol in the synthesized films. The films having higher TPC were found to have higher antioxidant activity. Synthesized films showed 70% free radical scavenging however the antimicrobial activity was found to be moderate. Among all combinations of nanocomposites films, *M. piperita* and quercetin loaded nanocomposite films displayed best DPPH scavenging and provided least weight loss of baby carrots while determining the food quality.

Biodegradability results showed that synthesized films (extract/polyphenol incorporated) displayed increased degradation in soil than lysozyme. CS-CNC-NK EX1 composites displayed 63% increased degradation than control chitosan films along with lower melting temperature and early degradation temperature in TGA and DSC analysis which suggest that chitosan film degradation highly depends on chemical modifications in their structure. The results of *in vitro* hemo-compatibility assay indicated the non-hemolytic to slightly hemolytic behavior of synthesized chitosan composites suggesting their non-toxicity. Moreover, acute oral toxicity analysis in rats also confirmed the non-toxic character of synthesized films as the oral ingestion of these films induced no significant change in body weight, hematological and biochemical parameters of blood as well as a normal functioning of liver and kidney was observed with no mortality.

In conclusion, we propose that incorporation of *C. tamala*, *A. subulatum* and *M. piperita* extracts and their polyphenols specifically quercetin to chitosan films in combination of CNC and NK as a hybrid nano fillers system can result in remarkably enhanced mechanical, barrier and biological properties of chitosan films for efficient use in food packaging.

Introduction and Literature Review
(Chapter # 1)

1.1 Biopolymer based food Packaging

There is a crucial role of food packaging in food preservation during the course of distribution process. The food packaging is mainly aimed at protecting the food from spoilage and to increase its shelf life (Shahid *et al.*, 2021). Traditional food packaging serves as an inert barrier where there is a negligible interaction of packaging material with food components. These traditional methods use metals (aluminum, tinfoil, foils) plastics and paper, that actually pose a significant risk towards environment due to their non-biodegradability (Fernandes *et al.*, 2022). Therefore, natural polymers are nowadays considered as an ecofriendly alternative by minimizing the environmental risk associated with synthetic polymers. Natural polymers consist on biodegradable films and coatings, which represent either thin films of edible/non-edible materials placed on the food product or spread as a coating respectively (Díaz-Montes & Castro-Muñoz, 2021). These films are composed of proteins, lipids, carbohydrates and their different blends to improve the packaging attributes.

Plastic packaging offers high mechanical and gas barrier properties (thus safety during storage and transportation), easy accessibility, scalability, low cost, ability to be molded into different dimensions by injection molding, but does not provide sustainability and biodegradability and have limited disposal methods (Ahmad & Sarbon, 2021). In addition to such environmental concerns, significant changes in food distribution, consumer demands for more convenient takeaways has impacted the food packaging (Gallego-Schmid *et al.*, 2019). Considering these issues, a food packaging material should be more natural, sustainable/bio-degradable, disposable as well as able to be recycled. These all qualities are offered by biopolymer based food packaging.

1.2. Biopolymer

Biopolymers are mainly derived from residuals of farming feed stocks, waste of marine food processing industry, animal sources or microbial sources. They contain the biological raw materials (i.e. starch, cellulose and bio-derived monomers (Gautam *et al.*, 2022)).

These polymers have the significant advantage of breaking down not only to their raw ingredients but also produce eco-friendly products such as CO₂ and water. Moreover, this kind of packaging is of great value in countries where waste is primarily managed by landfill (Awasthi *et al.*, 2022). Both edible films and coatings fall under the bio-based packaging technology. The most abundant biopolymers include cellulose, chitin and de-acetylated form of chitin i.e. chitosan. (Nasrollahzadeh *et al.*, 2021). These polymers are ordered into three classes. Polysaccharides consist of Cellulose, starch and chitosan that can be co-polymerized with other polymers to attain desired activities. Protein based polymers include albumin and gelatin whereas waxes, fatty acids, and vegetable oil-based polyesters come under lipid based polymers.

Biopolymer composites have been synthesized using biopolymers with reinforcements by suitable filler depending on its fiber type, structure and source. Some drawbacks of these biopolymers have also been noticed like, high water absorption, less moisture resistance, poor mechanical and barrier (gas/moisture) properties. Biopolymers based packaging is challenging towards practical packaging applications due to these poor properties of natural polymers at comparable levels to petroleum based packaging (Diyana *et al.*, 2021). Therefore, several strategies like nanotechnology, surface engineering, layer by layer assembly, chemical modification and blending with synthetic polymers are employed to improve the barrier properties of biodegradable packaging films to bring them to market and improve their scalability (Huq *et al.*, 2012). Partially degradable synthetic polymers can also be prepared by blending them with biopolymers, combining biodegradable constituents (such as starches), or adding bioactive components. The bio active components are then degraded to breakdown the polymer into smaller gears.

1.2.1. Biopolymer classification

Based on the origin, biopolymers are categorized into three main classes.

1. Biopolymers derived from proteins, lipids and polysaccharides
2. Biopolymers produced by microbial fermentation for example poly (hydroxy alkanoates) and pullulan.
3. Biopolymers chemically derived from monomers achieved by raw materials for instance poly (lactic acid).

A detailed classification of biopolymers was explained earlier (Vinod *et al.*, 2020) which is given below in figure 1.1.

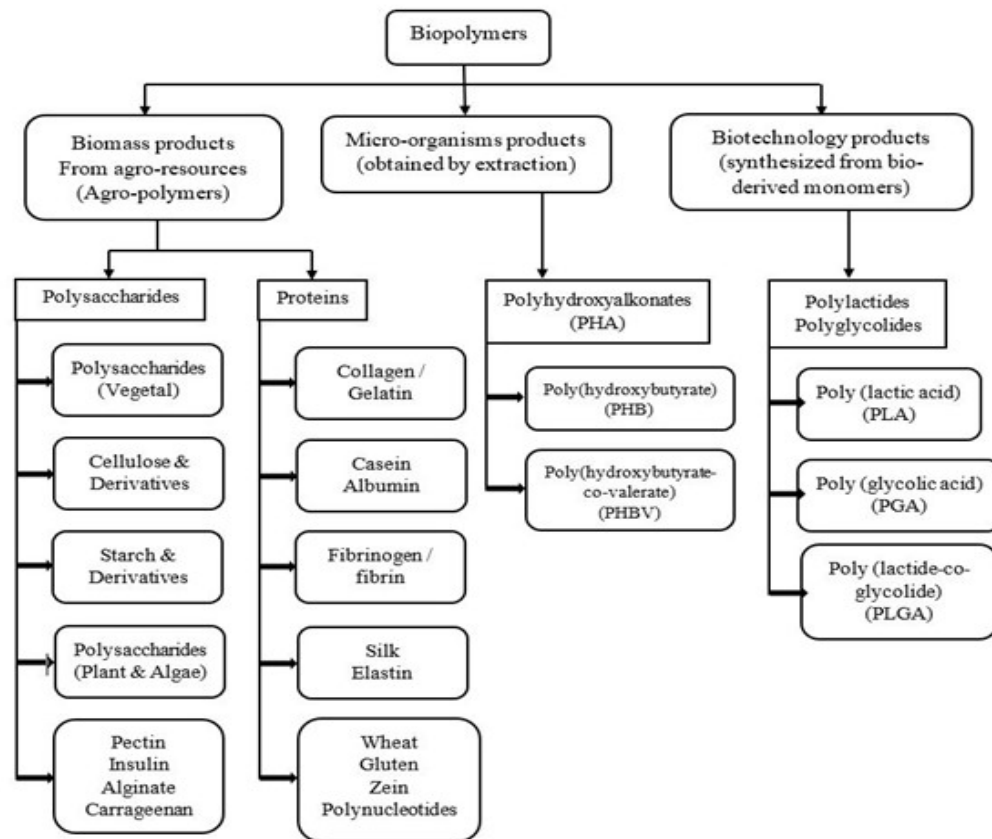


Fig 1.1 Classes of biopolymers (Source: Vinod *et al.*, 2020)

1.2.2 Biodegradability of biopolymers

The actual pluses of biopolymers are biodegradability and biocompatibility. The biopolymer degradation is dependent on several factors like environment, composition, polymer kind and bonds in between them. Following terms are used in biodegradability.

- Biodegradable: Due to the presence of microorganisms.
- Hydro-biodegradable: Due to presence of microorganisms and water.
- Photo-degradable: Due to light.
- Bio-erodable: Due to corrosion by regular abrasion.
- Compostable: Due to action of soil bacteria.

A bio-active medium containing either microorganisms, marine water or soil can cause the decomposition of biopolymers to carbon dioxide, methane, water and

other natural substances, both carbon dioxide and methane are beneficial as these are greenhouse gases. The figure 1.2 best describes the mechanism of biodegradability of bio polymers (Moustafa *et al.*, 2019).

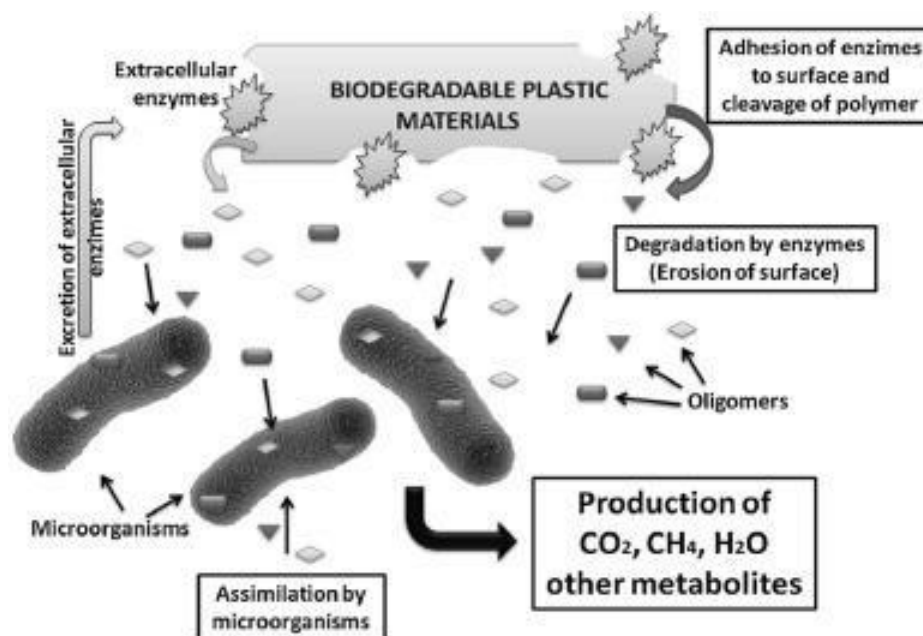


Fig 1.2 Mechanism of biodegradability in biopolymers

(Source: Moustafa *et al.*, 2019).

1.3 Chitosan

Among the various natural biopolymers (i.e. chitosan, cellulose, whey protein starch), chitosan has achieved great interest in recent decades. Chitosan and its derivatives are well known for their biodegradability, bio-compatibility, non-toxicity as well as metal chelating, antibacterial and antifungal properties (Bakshi *et al.*, 2020). It is considered as safe and biocompatible polymer for human dietary use and is also approved for wound dressing applications (Gruppuso *et al.*, 2022). Film forming characteristic of chitosan also suggest its use in synthesis of thin films for food packaging. Chitosan is a cationic polysaccharide extracted from de-acetylated chitin. It contains D-glucosamine units linked together with β - (1-4) and N-acetyl units of D-glucosamine. Its structure is shown in figure 1.3.

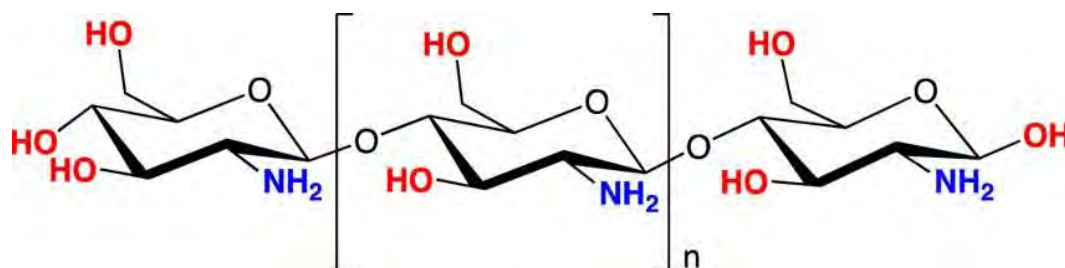


Fig 1.3 Structure of chitosan

Semi crystallinity of chitosan and its solubility in various acids like formic acid, citric acid and acetic acid makes it a good polymer for film synthesis (Zhu, 2021). Chitin for the synthesis of chitosan can easily be obtained from shell waste, various renewable resources and living organisms. Thus, Chitosan represents an easily available and cost effective polymer for food packaging (Yuan *et al.*, 2015). However, pure chitosan films have several limitations in food packaging industry for instance less mechanical strength, low thermal stability, brittleness and sensitivity to humidity (Haghighi *et al.*, 2020). Such limitations can be addressed by addition of nano-fillers, plasticizers, and/or cross-linking. One way to tackle these challenges is active packaging along with nano-reinforcement to improve the properties of chitosan films. Biopolymers like keratin (Tanase & Spiridon, 2014) and cellulose (Mujtaba *et al.*, 2017; Wildan & Lubis, 2021) when blended with chitosan, are reported to improve its packaging properties and food shelf life. Chitosan possess cationic and polar groups, which increase the compatibility of chitosan with other biopolymers. For example carbonyl, hydroxyl and amino groups in chitosan backbone enable the hydrogen bonds or dipole interaction with the corresponding functional groups (Bonilla *et al.*, 2018). Therefore, it has also been used as a drug delivery carrier of polymeric nanoparticles.

1.4 Active packaging

Active packaging is the deliberative incorporation of materials intended to improve the packaging conditions, to extend food shelf life and to maintain food sensory characteristics. These materials include free radical trappers, carbon dioxide absorbers/emitters, ethylene absorbers/emitters, antioxidant releasers, moisture absorbers and antimicrobial effect providers (Yong *et al.*, 2019). Antimicrobial systems, CO₂ emitters

and antioxidant releasers come under active release systems. Whereas moisture and ethylene absorbers, oxygen scavengers come under active scavenging system. Active packaging system is shown in figure 1.4.

As evident from literature, the most chitosan films made so far incorporate antioxidant /antimicrobial agents using chitosan as main matrix. It is predominantly due to high use of active components from natural resources such as phenolic compounds and essential oils from vegetables, legumes, fruits and seeds etc. Chitosan films with incorporation of gallic acid, Cinnamon, Eucalyptus globulus or clove bud have been synthesized so far (Hafsa *et al.*, 2016; Perdones *et al.*, 2014; Zarandona *et al.*, 2020). These active ingredients from natural plant extracts possess strong antioxidant and antimicrobial properties, therefore, their incorporation in pure chitosan films can help in improving shelf life of food product packaged with such films (Zhang J. *et al.*, 2019).

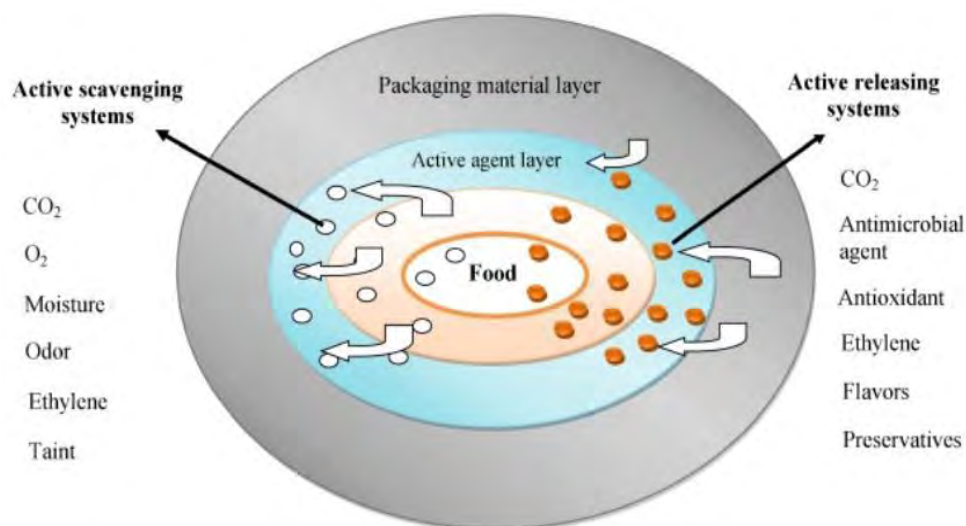


Fig 1.4 Active packaging systems in food (Source: Ahmed *et al.*, 2017)

Active packaging may consist of films or coatings which are described as under.

1.4.1 Films

Films can be demarcated as a thin (dried) biopolymer layer which is added separately, formed before and then can be applied on the product like a wrapper. It can be used as packaging or layer (Rodríguez *et al.*, 2020).

1.4.2 Coatings

Coatings refer to films formed, when their base is applied on the product surface after which drying occurs and thus, the coating formation (Kapetanakou & Skandamis, 2016).

1.5 Nanocomposites

Nanocomposites have two or more phases, a continuous phase consisting of essentially biopolymers like hydrocolloids i.e Polysaccharides, protein, pectin, starch etc. and a discontinuous phase having inorganic/organic filler i.e synthetic polymeric nano fibers, silicates, titanium dioxide, zinc oxide, carbon nanotubes, cellulose nanofibers and nanocrystals etc., with nanometer range dimensions (1–100 nm) (Arfat *et al.*, 2014; Zubair & Ullah, 2020). A variety of inorganic nanoparticles assist as additives to augment the performance of polymeric phase (John & Thomas, 2008) .

Reinforcement of materials using nano size particles is known as nano reinforcement. The interest of scientists in incorporation of nano fillers into polymer is increasing due to the attainment of potentially remarkable properties, as a result of nano metric dimensions.

1.5.1 Advantages of Nanocomposites

Combining nano fillers with polymers provides notable improvements in thermal, mechanical, gas and water resistance properties. Nano scale particles are obtained during dispersion which may demonstrate significant advantages to food product packaging, such as odor, appearance, flavor, compact packaging volume, prolonged shelf life as well as serve as carriers for antimicrobial or antioxidant agents and provide release of active constituents in a controlled way (Rhim & Ng, 2007).

Some extra benefits can also be achieved like transparency, low density, better surface properties, good flow and recyclability. The improvement of many characteristics depend on the major length scale and morphology of these materials. The nano fillers have size range from 1 to 100 nm range. Therefore, their uniform dispersion can bring about large surface area in between the constituents of composite. The molecular mobility and relaxation behavior is altered due to this increased interfacial area and thus

mechanical properties, thermal stability and melt viscosity are improved. However, this increased area can also lead to particle aggregation and dispersion problems of nano fillers (Sorrentino *et al.*, 2007). Small amounts (1-5 wt %) of nano fillers are reported to promote polymeric material properties, including improved tensile characteristics, high mechanical and barrier properties. While excessive use of nano fillers can cause nano toxicity, ultimately leading to various environmental and health issues (Das *et al.*, 2021). The weight of nanocomposites is less than orthodox biodegradable composites and this makes them competitive with addition of some additives (Hossain *et al.*, 2021). Moreover, nanocomposites can be biodegraded proficiently either by micro or macro organisms, photo chemical degradation (Avella *et al.*, 2005). Applications of these nanocomposites can solve the disposal problems and can provide packaging with improved properties.

The above mentioned advantages of nanocomposite system may provide new product advancement in food industry, such as particulate foods packaging, transporters for nutritional supplements and active agents (Ozdemir & Floros, 2004). However, the choice of type of biopolymer, nano filler and additive is important in property improvement of a nanocomposite based packaging film.

1.5.2 Cellulose Nano crystals as nano filler

Among a wide range of nano fillers, CNC is potentially admired for reinforcement of chitosan films due to its abundance, lightness, large surface area, sustainability and extraordinary mechanical properties. CNC is derived from cellulosic source (wood, bacteria) by acid hydrolysis and is attributed by a crystal rod-shaped nano scale particle formed as a stable aqueous colloidal suspension (Sacui *et al.*, 2014). Several reports on chitosan and CNC hybrid films have been published. While recently, chitosan bio-nanocomposites films reinforced with cellulose nano crystals (CNC) and glycerol were shown to improve barrier properties (Wildan & Lubis, 2021). In another study, grape pomace extract was used along with CNC in chitosan films to provide remarkable antioxidant, thermal and mechanical properties (Xu *et al.*, 2018). Addition of 3-5 % CNC to chitosan has been reported to accelerate the tensile power and barrier properties owing to the strong interaction between CNC and the chitosan matrix leading to a percolating network formation (Wildan & Lubis, 2021). Thermal resistance of chitosan is also reported to be unaffected by the addition of CNC whereas the chitosan

hydrophilicity increases. However, its crystallinity is boosted in the presence of CNC. Purity, good mechanical stability, controllable water capacity and gas-barrier properties are dominant properties of bacterial CNC (Xu *et al.*, 2020).

(a). Structure of CNC

When cellulose micro fibrils (consisting of highly amorphous as well as crystalline regions) are subjected to chemical or enzymatic treatment (like oxidation, treatment with sulfuric acid), these fibrils result in highly crystalline regions called cellulose nanocrystals (CNC). Rod like particles exhibiting high modulus, specific high strength, higher surface area and unique liquid crystalline characteristics represent CNC. As shown in figure 1.5, CNC structure comprise of large number of hydroxyl groups establishing a firm cellulose network with specific surface area. The highly abundant surface hydroxyl groups on CNC surface cause higher water permeability and thus pure CNC films are not effective in preventing water exchange therefore CNC is blended with other polymers for food packaging applications.

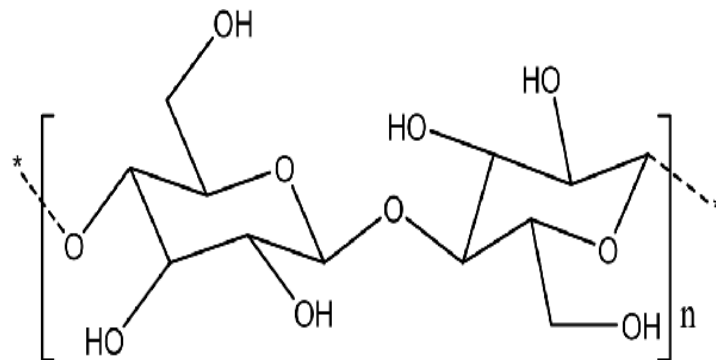


Fig 1.5 Structure of nanocrystalline cellulose

(b). CNC based composite films

Nano cellulose based composites have been prepared with both non-biodegradable (polyethylene/polypropylene) and biodegradable (Poly caprolactone (PCL), Poly lactic acid, Poly vinyl alcohol, Chitosan and Starch) polymers (López De Dicastillo *et al.*, 2021).

The reinforcement of CNC in polyvinyl alcohol (PVOH) matrix at different concentrations has been reported (Lee *et al.*, 2009). PVOH-CNC composites at 1%

CNC concentration showed 49% increase in tensile strength as compared to pure poly vinyl alcohol. However, tensile strength was decreased considerably at 3% and 5% CNC addition. In another study, PVOH composite reinforced by bacterial CNC was tested with tunable mechanical properties for medical device applications. The effect of different CNC and glycerol on tensile strength, young modulus, percent elongation and water vapor permeability of chitosan films has already been studied (Azeredo *et al.*, 2010). They reported highest mechanical strength and decreased WVP at 18% glycerol and 15% CNC concentrations. Another study reported sodium caseinate films reinforced with CNC by dispersing them into film solution. The synthesized films were found to be less transparent, more hydrophilic with almost doubled tensile strength and very less WVP at 3% CNC addition.

Recently, active films containing soy protein isolate were reinforced by CNC and zinc oxide nanoparticles, by both in situ and physical mixing. (Xiao *et al.*, 2020). The tensile strength, thermal and barrier properties were improved by CNC reinforcements. However, Zinc oxide contributed in inhibiting bacterial (*E. coli* and *S. aureus*) growth. Interestingly, CNC and Zinc oxide nanoparticles film hindered the relocation of zinc into food thus the formulated nanocomposite film displayed broad prospect in active packaging. A blend of PLA/PBAT/CNC nanocomposites was developed in which enhanced modulus beyond the glass transition temperature (T_g) of PLA was exhibited by films regardless of the preparation method (solvent casting/melt extrusion) (Sarul *et al.*, 2021). Biocompatible, mechanically strong and antibacterial nanocomposites were prepared in a hybrid PVA system including CNC and silver nanoparticles with reduced graphene oxide (Pal *et al.*, 2021).

1.5.3 Nano-Keratin as nano filler

(a). Keratin composite films

Eco-friendliness, biodegradability and sustainability of protein-based composites is a reason for their increased attention in food packaging industry. Different blend technologies are employed in order to improve their poor barrier properties. Chicken feathers serve as a natural source of keratin. Moreover, feathers are considered as a cost effective keratin source as feather waste is produced by poultry processing every year (Mumtaza & Munir, 2022). Feathers contain 90% keratin and 7% cysteine residues

which are responsible for alpha helix formation in keratin peptide chains through disulfide linkages. These disulfide bonds ease intermolecular crosslinking between protein chains. Moreover, the charged groups on polar amino acids helps in generation of a chemical gradient that helps in film's stabilization via hydrogen bonding, disulfide bridges and electrostatic attraction (Oluba *et al.*, 2022a).

Keratin has been isolated from chicken feather waste by acid and alkaline hydrolysis, oxidation or reduction by various researchers (Zahara *et al.*, 2021). Keratin extraction by sodium sulfite is economically favorable and preserves the protein secondary structure too. It also shows surface-active and emulsifying characteristics (Rajabinejad *et al.*, 2018).

Keratin–starch blended film enriched by avocado peel extract was prepared, characterized and assessed for antifungal activity. Results displayed that overall quality and spoilage induced weight loss was improved with extract loaded film packaging (Oluba *et al.*, 2022b). Keratin has been used as a starting material for synthesizing multilayer films i-e alternating keratin (anionic) and a polyelectrolyte (cationic) such as poly (vinyl alcohol) (Yang *et al.*, 2009).

(b). Limitation of keratin composite films

Despite of its strong protein structure, keratin shows brittleness during film formation. Therefore, keratin has been blended with starch and chitosan to improve its mechanical properties. Keratin bio composites when fabricated with starch, displayed poor resistance to water but exhibited gas barrier properties (when checked via gas permeation analyzer) and served as a protective coating over fruits surface (Oluba *et al.*, 2021). Analytically, chitosan displays a positive charge below its pK_a (~6.5) and isoelectric point of about 7.0–9.0 (Mohammed *et al.*, 2017) and thus, its complex with keratin via electrostatic interactions is most likely. Blends of chitosan and keratin suggested the mixing of chitosan with keratin due to fragile nature of keratin alone. These composite films displayed little enhancement in tensile strength and barrier characteristics in comparison to synthetic polymer based packaging (Tanabe *et al.*, 2002). Therefore, nano reinforcement in keratin might be a way to tackle this limitation.

(c). Nano keratin

Keratin based films have been stated to increase gas barrier properties to a great extent, however, there is a need to diminish the water sensitivity of keratin in order to improve overall functionality with other bio polymer combinations. Recently, urea coated keratin nanoparticles were prepared for use as fertilizers, as an alternative to challenging coating of bulk keratin (Sree *et al.*, 2021). Since bulk keratin undergoes denaturation when Urea reacts with peptide bonds which causes the weakening of protein intermolecular forces. Therefore, side chains of keratin were cross linked with glutaraldehyde to convert it into nano keratin, in order to make strong bond inside the protein structure as shown in figure 1.6.

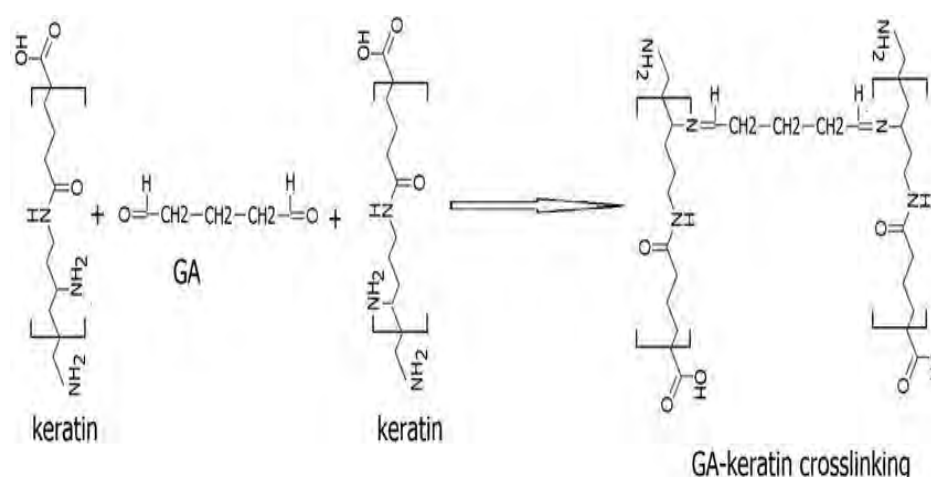


Fig 1.6 Cross linking of chicken feather keratin with glutaraldehyde

Nano-keratin formation not only helps to improve the surface area of keratin but also enhance its properties (Saravanan *et al.*, 2013). In another study keratin nanoparticles were synthesized from chicken feather keratin by crosslinking and incorporated in chitosan matrix for use as scaffolds in tissue engineering applications (Sree *et al.*, 2021). However, the use of nano keratin in chitosan films for food packaging is not explored yet. Therefore, we used a blend of nano keratin and chitosan in our study for development of bioactive food packaging films.

1.6 Methods of film preparation

Addition of nano fillers to chitosan matrix is reported by using several methods like solution mixing or solvent casting, in situ polymerization, melt blending/ compression molding etc (Chivrac *et al.*, 2009).

(a). Solvent-Casting

Solvent casting comes out to be the easiest technique to synthesize polymer composites. This method includes three stages for nanocomposites preparation. At first, nano fillers and polymers are dispersed in a suitable solvent via sonication / mechanical stirring (Okura *et al.*, 2014). Then filler solution is mixed with polymer solution and contents are allowed to heat at particular optimized temperature and stir for a certain time followed by sonication if required. This film forming solution is cast on aluminum plates, oven dried which results in generation of films of bio-nanocomposites.

This method is easy, convenient and low cost. There are several reports on using solvent casting for chitosan nanocomposites synthesis. Chitosan–gold-nanocomposites were fabricated using a solution-casting technique in 2015 (Regiel-Futyra *et al.*, 2015). Chitosan composite blend films with graphene oxide and cerium oxide (Panda *et al.*, 2022), montmorillonite and sepiolite (ChenXie & McNally, 2021) were also recently prepared by solvent casting.

(b). Compression molding

Compression molding is another less frequently used technique to prepare chitosan films. In this method, the polymer, filler, plasticizer with certain amount of deionized water are mixed well and placed in plastic bag for 24 hours at room temperature to hydrate the mixture. Next, the mixture is located between two heated aluminum plates that serve as a mold. These plates are kept in a carver press and heated at a particular temperature and pressure for a particular time period to achieve film formation (Silva *et al.*, 2021). Recently, chitosan films were prepared by thermo- compression using Aloe Vera as a cross linker and bioactive agent (Zarandona *et al.*, 2021).

(c). In situ polymerization

It involves uniform dispersion of filler into the monomer in the presence or absence of solvent. Then at a required temperature, curing agent is incorporated for polymer synthesis. Chitosan-poly acrylonitrile silver nanocomposites were formed by using this technique (Nageswar *et al.*, 2021).

(d). Electro spinning

It allows the generation of very thin films or nanocomposite fibers. Electro spinning is based on electric spinning, accelerated fluid stretching supported by immobilized charges on liquid surface. Electro spun Chitosan/Poly (ethylene oxide) based composites were prepared by this technique (Naseri *et al.*, 2014).

(e). Freeze drying

This method involves pouring a uniform blend of polymer plus filler into a copper mold followed by quenching the solution in liquid nitrogen. The polymer scaffold then undergoes freeze drying for removing the solvents (Zeng *et al.*, 2015).

1.7 Physical properties and characterization of Chitosan films**1.7.1 Mechanical Properties**

The maximum stress that a films can bear before breaking, when a force is applied using tensile machine is called tensile strength (Shah *et al.*, 2023). Maximum applied force is divided by the films' cross sectional area to calculate the tensile strength. However, percent elongation or elongation at break (E%) is the percent rise in length that a material will attain before it breaks. It is a measure of ductility of a material (Odagiri *et al.*, 2021). The tensile power of chitosan is directly related to its degree of acetylation as well as molecular weight (Ziani *et al.*, 2008). Moreover, the environment humidity and drying temperature can also have an impact on the mechanical and barrier properties of chitosan. Specifically, in case of acetic acid produced films, the tensile strength increases with increased storage at room temperature due to rearrangement of polymer chains (Zhong & Li, 2011). The choice of solvent can also affect the mechanical strength. The chitosan films prepared with lactic, citric acid or malic acid

were found to have less strength as compared to chitosan-acetic acid films (Dayarian *et al.*, 2014). Similarly, use of a specific plasticizer like glycerol is reported to produce mechanically strong films as compared to other plasticizers like oleic acid, sorbitol (Vlacha *et al.*, 2016).

In addition to these factors, incorporation of natural phenolics like gallic acid and protocatechuic acid into chitosan backbone has been reported to increase its strength (LiuMeng *et al.*, 2017). Nano fillers like cellulose nanocrystals alone or in combination with zinc oxide when dispersed in PVA and chitosan polymer mixture significantly boosted the tensile strength of these composites (Azizi *et al.*, 2014). Furthermore, addition of silver-montmorillonite antimicrobial nanoparticles in chitosan composite films also enhanced the mechanical strength owing to the interaction of silver particles with chitosan (Shameli *et al.*, 2011).

1.7.2 Barrier Properties

The barrier characteristics of chitosan can help in improving the nutritional value, extending the shelf life of food products mostly by offering protection from water and light. Water vapor permeability (WVP), Permeability to oxygen (OP) and UV resistance are important barrier attributes of chitosan (Cazón & Vázquez, 2020).

Recently, WVP and permeability to oxygen was seen to decline with increase in the Propolis extract concentration (Roy *et al.*, 2021). The protocatechuic acid addition in chitosan also revealed low moisture content and reduced WVP of chitosan films (LiuLiu *et al.*, 2017). Moreover, introduction of gallic acid, silver-MMT and Na-montmorillonite resulted a decline in WVP of chitosan films (Lavorgna *et al.*, 2014). The loading of sodium lactate in chitosan-polyvinyl alcohol/ montmorillonite films is has also been reported to improve carbon dioxide and oxygen barrier properties (Zhang *et al.*, 2017). Nano-cellulose addition along with tannic acid also resulted in films with reduced water solubility and moisture content (Leite *et al.*, 2021).

Chitosan films with CNC and grape pomace extract incorporation were found to have excellent UV barrier properties with increased opacity (Xu *et al.*, 2018). Increased opacity is highly desirable for light sensitive foods as these can prevent lipid oxidation induced by light. Incorporation of plant extracts in chitosan films has been reported by

various authors (Bonilla *et al.*, 2018) to help decrease the transparency and increase the opacity of films. Similar decrease in transparency was observed when green tea (Siripatrawan & Harte, 2010) and grape seeds extracts (Rubilar *et al.*, 2013) were added to chitosan film.

Thermal properties of chitosan films can be assessed by thermo gravimetric analysis (TGA) and differential scanning calorimetry (DSC). Thermal stability evaluation of films in TGA analysis has shown three consecutive weight loss steps. First weight loss occurs from 50°C to 100°C due to moisture loss, another sharp loss due to breakdown of several linkages in composites occur around 140°C to 395°C due to degradation of Chitosan and other components of film indicating the thermal degradation temperature (Xu *et al.*, 2018). The last weight loss occurs around 395–600 °C due to breakdown of char into low molecular weight gas products (Bonilla *et al.*, 2018). Thermal transition of chitosan composites is assessed by DSC analysis from 25°C to 300°C. Chitosan films display two endothermic peaks (at 109°C and 210°C) due to solvent evaporation and melting of crystalline structure (T_m) respectively) and one exothermic peak at 293°C due to chitosan decomposition.

Viscoelastic properties of composites are determined by Dynamic mechanical analysis (DMA). Glass transition temperature is determined by tan delta curve suggesting that how storage modulus and tan delta varies with temperature. Addition of different components like fillers and additives has been reported to affect the thermal and viscoelastic properties of chitosan composites (ChenXieTang *et al.*, 2021; Ilyas *et al.*, 2022).

1.7.3 Structural Properties

Various characterization techniques are used to observe the structure of chitosan nanocomposites which are discussed as under.

(a). Scanning electron microscopy (SEM)

SEM is based on using a focused electron beam for generation of various signals (like secondary electron, backscattered electrons, photons) at the sample surface to reveal the information regarding sample external morphology. It is used to investigate the

surface morphology of nanocomposites and distribution of nano fillers inside the polymer matrix (Kaur *et al.*, 2018; Wildan & Lubis, 2021).

(b). Transmission electron microscopy (TEM)

The working of TEM is based on using a particle beam of electrons in order to visualize the composites structure. In case of nanocomposites, extent of dispersion of nanoparticles either exfoliation or intercalation can be determined via TEM analysis.

Usually, three morphological categories can be observed in nanocomposites via TEM.

- 1. Micro-composites:** When molecules of polymer cannot penetrate in inter layer galleries, therefore, spacing between layers is unaltered which lead to similar properties as that of pristine state.
- 2. Intercalated nanocomposites:** When there is insertion of various polymer chains between interlayers along with a little bit expansion (2-8 nm) of d spacing.
- 3. Exfoliated nanocomposites:** Extensive penetration of polymer into layers of clay or other filler causes interlayers expansion (around 10 nm distance between layers) (Liu *et al.*, 2006).

(c). Fourier transform infrared spectroscopy (FTIR)

FTIR analysis is conducted to analyze different functional group present in nanocomposites. Study of these functional groups (such as peak shift and change in peak intensity) can reveal the important information regarding bonding between polymer and nano filler. (Wildan & Lubis, 2021).

(d). X-ray diffraction (XRD)

XRD analysis depicts the crystallinity of polymers and reveals the strength of interactions between polymer and nano fillers. Disappearance of nano filler characteristic peaks and appearance of new peaks has been reported to show dispersion of nano fillers in chitosan matrix by forming new bonds with the polymer. (Xu *et al.*, 2018).

(e). X-ray photon spectroscopy (XPS)

XPS survey helps to observe the surface elemental composition of bio-nanocomposites and a high resolution C1s spectra gives the idea of the specific chemical bonding between polymer and nano fillers (Scopelliti, 2021).

1.8 Bio active properties of chitosan films for food packaging**1.8.1 Antimicrobial Properties**

Chitosan films have intrinsic antimicrobial properties due to antimicrobial nature of chitosan. For example, baby carrots packaging by chitosan films has been shown to delay their microbial spoilage (Leceta Itsaso *et al.*, 2015). Moreover, addition of PVA, CNC/zinc oxide to chitosan films has also been reported to show antimicrobial activity against *S. choleraesuis* and *S. aureus* (Azizi *et al.*, 2014) Chitosan based coatings having propolis as an additive have been reported to inhibit *Escherichia coli*, *Salmonella enteritidis*, *Staphylococcus aureus* and *Pseudomonas aeruginosa* (Siripatrawan & Vitchayakitti, 2016). Good antimicrobial activity of vanillin based chitosan films were also reported where vanillin served as a cross linker (Stroescu *et al.*, 2015). Phenolic acid grafted chitosan films also displayed enhanced antimicrobial properties comparable to chitosan control. Pomegranate peel extract loaded chitosan films have also been shown to exhibit strong antibacterial properties (Mohebi & Shahbazi, 2017).

1.8.2 Antioxidant Properties

Chitosan films can be used as an active packaging to prevent oxidative damage of foods. Such as grafting of hydroxybenzoic acids (Liu *et al.*, 2018) as well as plant extracts addition (source of polyphenols and flavonoids) has been reported by various researchers to enhance antioxidant activity of chitosan films. For example, *Silybum marianum* L. extract (Liu *et al.*, 2018), grape pomace extract (Xu *et al.*, 2018), thyme extract and apple polyphenols (Sun *et al.*, 2017) incorporation to chitosan films has been shown to improve its antioxidant properties to a remarkable extent. Recently, lychee pericarp powder was added to chitosan films and was found to inhibit the browning of apple pieces as well as the polyphenol content of apple juice was reduced due to oxidation (polyphenol oxidase mediated) during storage (Jiang *et al.*, 2021).

1.9 Plant Extracts as additives in Chitosan nanocomposite films

It has been proved in various studies that natural plant extracts may serve as source of active agents in chitosan films not only to impart their antioxidant or antimicrobial effect into the films but can also improve other barrier properties. In some studies, addition of extracts like sweet potato extract, *Lycium barbarum* fruit extract and leaf *Pistacia terebinthus* extract to chitosan films resulted in decrease of both tensile strength and percent elongation (Wang *et al.*, 2015). However, addition of blackberry pomace extract, pomegranate peel extract and mango leaf extract showed increased tensile strength (Pirsa *et al.*, 2020; Rambabu *et al.*, 2019). Nevertheless, some extracts (black plum peel extract, black eggplant extract, propolis extract etc.) with higher flavonoid content have also displayed increase in both tensile strength and percent elongation (Siripatrawan & Vitchayakitti, 2016; Zhang X. *et al.*, 2019). It can be evidenced from these studies that high molecular weight components from extracts (such as polyphenols) can form hydrogen bonds (between amino/hydroxyl group of chitosan and polyphenols) and thus produce plasticizer effect and can either increase/decrease tensile strength (Flórez *et al.*, 2022).

Similarly, plant extract addition is reported to increase or decrease the permeability to water vapors. Intermolecular bonding interactions between extract and film matrix can influence the film's permeability to water vapors (Flórez *et al.*, 2022). Sometimes, addition of some extracts may weaken the interactions and can cause easy water movement through the film structure resulting in increased water vapor permeability. However, few studies suggest that hydrogen bonding interactions between chitosan and polyphenols can cause reduction in availability of hydrophilic groups, thus decrease the chitosan affinity towards water molecules (Kurek *et al.*, 2018).

Plant extracts with high polyphenol content are reported to impart free radical scavenging activity to chitosan films. For instance, chitosan blended with banana peel extract displayed up to 89% DPPH free radical scavenging activity. This is particularly due to hydrogen donating ability of polyphenols and flavonoids in extracts that lead to antioxidant activity of films (Zhang *et al.*, 2020). Regarding antimicrobial effect of extracts on films, green tea extract, apple peel extract, black plum peel extract and purple corn extract addition to chitosan remarkably improved its antimicrobial properties (Zhang J. *et al.*, 2019). Polyphenols of apple peel extract were found to

inhibit molds but did not show activity against yeasts. Many plant extracts have shown inhibitory effect on both gram positive and gram negative bacteria. Most common inhibitions were found to be against *E. coli*, *S. aureus*, *P. aeruginosa* and *B. subtilis* (Balti *et al.*, 2017; Flórez *et al.*, 2022). Extract addition also gives negligible UV transmittance to films, thus helps to inhibit lipid oxidation induced by UV light. A variety of plant extracts i-e *Ocimum tenuiflorum*, *Pistacia terebinthus*, *Carum copticum*, *Azadirachta indica*, mango leaf extract has been incorporated in chitosan matrix so far to offer extra bio-functional characteristics to chitosan films for use as eco-friendly packaging (Jafarzadeh *et al.*, 2020). However, an approach of blending the different nano-fillers and edible plant extracts (as additives) with chitosan for enhanced barrier properties is still under its way to explore more options.

1.10 Selection of Plant extracts

We selected four edible spices *Cinnamomum zeylanicum* (*C. zeylanicum*), *Cinnamomum tamala* (*C. tamala*), *Amomum subulatum* (*A. subulatum*), *Trigonella foenumgraecum* (*T. foenum graecum*) and four edible herbs i-e: *Mentha piperita* (*M. piperita*), *Coriandrum sativum* (*C. sativum*), *Lactuca sativa* (*L. sativa*), and *Brassica oleraceae var. italica* (*B. oleraceae*) for use as additives in chitosan nanocomposites synthesis. The most common herbs and spices were selected because of their easy availability, inexpensiveness, non-toxicity, frequent use as kitchen spices and salad, remarkable antioxidant and antimicrobial properties. Furthermore, there is lack of research on chitosan films incorporated with these natural extracts contributing to novelty of this project.

(a). *Cinnamomum zeylanicum*

C. zeylanicum bark is considered historical herbal medicine that possess remarkable curative and food flavoring properties. Cinnamon exhibits anti-inflammatory, antimicrobial, insecticidal, anti-mycotic and anticancer properties (Adarsh *et al.*, 2020). Mostly used as a kitchen spice this herb has been employed as a respiratory and digestive medicine in traditional ayurvedics. Eugenol and Cinnamaldehyde are main constituents of cinnamon bark.



Fig 1.7 *Cinnamomum zeylanicum*

Cinnamon bark extract has been used to photosynthesize selenium nanoparticles in chitosan bioactive nanocomposites (Alghuthaymi *et al.*, 2021). Recently, its essential oils have been used in chitosan films and have shown anti biofilm activity (Mouhoub *et al.*, 2022). Cinnamon extract loaded chitosan/gelatin electro spun nanofibers have also been prepared for biomedical applications (Ahmadi *et al.*, 2021).

(b). *Cinnamomum tamala*

C. tamala is a famous aroma spice and belongs to family ‘Lauraceae’. Its leaf extract has been used in traditional medicine for treating anorexia, diarrhea, colic, rheumatism and bladder disorders (Hassan *et al.*, 2016).

Its leaves have been proved to be antimicrobial, anti-helminthic and diuretic and also possess hypolipidemic and hypoglycemic properties (Agarwal *et al.*, 2019). Its leaves contain eugenol and sesquiterpenoids and can be used as a stimulant along with anti-biofilm, astringent, anti-flatulent and carminative properties (Mal *et al.*, 2018).



Fig 1.8 *Cinnamomum tamala*

Its essential oils have been encapsulated in chitosan nano emulsion via ion gelation technique and their antifungal activity against *Aspergillus flavus* was checked along with evaluation of their effect on stored millet shelf life (Singh B. K. *et al.*, 2022).

(c). *Amomum subulatum*

A. subulatum also known as black/greater cardamom, belongs to Zingiberaceae family and is mostly used in various Asian dishes, beverages and pickles etc. In old medicine systems, its fruits were considered as a cure to dyspnea, nausea, cough, inflammation, bleeding disorders etc.



Fig 1.9 *Amomum subulatum*

Studies have also reported the antioxidant (Drishya *et al.*, 2022), anti-inflammatory and anti-cancer (Sudarsanan *et al.*, 2021) properties of the *A. subulatum* dry fruits. Essential

oils of black cardamom has been reported to inhibit *E.coli* and *S.typhi* biofilm formation via inhibition of quorum sensing (Algburi *et al.*, 2021).

(d). *Trigonella foenum graecum*

T. foenum graecum also known as fenugreek, belongs to family Fabaceae, has been used as a traditional medicine, spice in culinary preparation, food stabilizer and emulsifier (Visuvanathan *et al.*, 2022).

Literature shows the antipyretic, anti-inflammatory and anti nociceptic activities of fenugreek leaves (Parvizpur *et al.*, 2006). Moreover, glycosides of its leaves have been reported to exert anti-obesity, anti-allergy, anti-inflammatory, anti-HIV activity, anti-tumor and anti-bacterial activities (Xiao, 2017).



Fig 1.10 *Trigonella foenum graecum*

The synthesis of chitosan coating loaded with fenugreek essential oil and its impact on storage of rainbow trout is already studied (Tooryan & Azizkhani, 2020).

(e). *Mentha piperita*

Commonly known as mint, *M. piperita* is traditionally used to improve digestion as well as its use in tooth paste, chewing gum and tea can also be seen. It belongs to Lamiaceae family and has been reported to exhibit antibacterial, antifungal, antiviral, antioxidant and anticancer properties.



Fig 1.11 *Mentha piperita*

M. piperita has been declared as a rich source of polyphenols such as rosmarinic acid, caffeic acid, protocatechuic acid glucoside, cinnamic acids and flavonoids such as rutin, catechin, 4'-methoxykaempferol-7-o-rutinoside (Gholamipourfard *et al.*, 2021). Moreover, *M. piperita* essential oils have been entrapped in chitosan-cinnamic acid nanogels and have depicted an enhanced antimicrobial activity (Beyki *et al.*, 2014).

(f). *Coriandrum sativum*

It belongs to family Apiaceae and is commonly used in salad dressings. Also known as Chinese parsley, *C. sativum* has been stated to have anti-diabetic, anti-fertility, antioxidant, anti-hyperlipidemic and hypotensive properties. Quercetin 3-glucoronide, Coumarins, Camphor, Linalool, Geraniol, Geranyl acetate are its main reported phytochemicals (Khan *et al.*, 2018).



Fig 1.12 *Coriandrum sativum*

C. sativum essential oils have been encapsulated in Chitosan nanomatrix as ecofriendly smart food preservative as they are reported to have potent antifungal and anti aflatoxigenic properties (Das *et al.*, 2019).

(f). *Lactuca Sativa*

Commonly known as Lettuce, *L. sativa* is a popular green leafy vegetable from Asteracea family and used raw in salad dressings (Viacava *et al.*, 2014).



Fig 1.13 *Lactuca sativa*

Its sensory characteristics, marketability, remarkable biological properties (antioxidant, anti-inflammatory) have led to its increased production and cultivation recently (Azarmi-Atajan & Sayyari-Zohan, 2020). There are reports of chitosan exogenous application to lettuce leaves to control its salinity (Zhang G. *et al.*, 2021).

However, literature lacks the incorporation of any lettuce extract to chitosan films for food packaging.

(g). *Brassicca oleraceae var italica*

Broccoli comes under brassicaceae family and is reported to be rich in health promoting compounds such as flavonoids, vitamin C and E and thus represent good source of antioxidants (Vasanthi *et al.*, 2009).



Fig 1.14 *Brassicca oleraceae var italica*

The demand for fresh broccoli has led researchers to produce several chitosan coatings enriched with various plant extracts to increase shelf life of broccoli (Alvarez *et al.*, 2013). However, there is no report of broccoli extract incorporation in chitosan films as additive.

1.11 Selection of nano fillers

We selected two different nano fillers i.e. cellulose nanocrystals and nano keratin, and studied the effect of their individual and mixed addition (synergistic) on chitosan films. The reason for selecting these fillers lies in their easy availability, cheap and green source (i.e. green trees and chicken feathers respectively) and higher compatibility with chitosan as discussed above.

1.12 Aims and Objectives

This study was carried out with following objectives.

1. Screening of edible herbs and spices and their respective polyphenols on the basis of their antioxidant and antimicrobial properties for incorporating them in chitosan nanocomposites
2. Synthesis of chitosan nanocomposite films incorporated with extracts/polyphenols and reinforced by CNC/ nano keratin by solvent casting technique
3. Analysis of mechanical, barrier, structural, thermal and viscoelastic properties of films
4. Evaluation of *in vitro* biological properties of films
5. Analysis of effect of packaging film on food quality
6. Biodegradability and toxicity analysis of films.

Screening, Biological Activities
and Molecular docking of the
Plant Extracts

(Chapter # 2)

2.1 Introduction

With rapidly growing environmental concerns of petroleum derived synthetic packaging, the development of biopolymer based coatings is receiving more attention by researchers nowadays (Oladzadabbasabadi *et al.*, 2022). The active packaging is gaining more popularity in food packaging industry due to its ability of minimizing food spoilage and improving food safety (Vilela *et al.*, 2018). Edible herbs and spices are considered as excellent source of active compounds to be responsible for providing various extra functions that a conventional packaging system usually don't have. For instance, plants extracts are rich in flavonoids and polyphenols which have antioxidant and antimicrobial properties (Bi *et al.*, 2019). These active compounds can react with functional groups of biopolymers through electrostatic linkages, hydrogen bonding (most commonly) or dipole-dipole interactions and thus become incorporated in the polymer matrix. The potential of loading phenolic compounds as well plant extracts in chitosan films has been explored by many researchers. For instance, polyphenols such as syringic acid, protocatechuic acid, quercetin, rutin and extracts of black and green tea, nettle extract, pomegranate peel extract, grape seed extract have been investigated for active packaging in chitosan films (Peng *et al.*, 2013; Wang X. *et al.*, 2019; Yang *et al.*, 2019).

Packaging films with incorporated antioxidants have gained much popularity since oxidation is the main process that can adversely affect the food quality (Souza *et al.*, 2017). There are some synthetic antioxidants such as butylated hydroxytoluene (BHT) and butylated hydroxyanisole (BHA) frequently incorporated in food packaging films. Although they offer low cost and high stability but have toxicological concerns (Siripatrawan & Harte, 2010). Therefore, plant extracts as well as their respective polyphenols can serve as a suitable and safe alternative to such synthetic antioxidants. Plant extracts exhibiting antioxidant activity through different *in vitro* assays (DPPH, total antioxidant capacity, reducing power assay) can be incorporated in packaging films to prevent oxidation (Bi *et al.*, 2019). Moreover, commercially available plant polyphenols known for best antioxidant activity can also be incorporated in biopolymer-based films. Due to their susceptibility to degradation the polyphenols cannot directly be added to food products. Nano entrapment of polyphenols (such as chitosan nano carriers) can not only prevent them from degradation but also prevents

their interaction with other food components. Chitosan based nano carriers are reported to improve the intestinal absorption of polyphenols (Hu *et al.*, 2017). Similarly, plant extracts or polyphenols having strong antimicrobial activities can also be incorporated in chitosan matrix to produce high quality packaging film offering resistance to microbial action. For example, elagic acid and caffeic acid are recently reported to inhibit *Candida auris* by modifying fungal cell wall (Hu *et al.*, 2017) .

Nowadays, in silico tools such as molecular docking is in common practice to predict the anti-microbial efficacy of phytobiotics (Rampone *et al.*, 2021). Therefore, target identification for particular polyphenol should be a major concern for emerging plant-based drugs. For instance, in silico studies have revealed superoxide dismutase, catalase, and isocitrate lyase as molecular targets for curcumin for treating *Paracoccidioidomycosis*, since curcumin is reported to affect the fungal plasma membrane by increasing the production of reactive oxygen species (Rocha *et al.*, 2021). Likewise, other plant polyphenols should be gauged for targeting specific bacterial or fungal enzymes through molecular docking analysis.

Hence, assessment of the plant extracts for antioxidant and anti-microbial potential should be prioritized for their incorporation in packaging films. Moreover, specific mechanism of action of the incorporated active compounds should be focused via molecular docking in order to use them as phyto-therapeutic agents in food packaging films. To support this idea, we selected four edible spices, including *C. zeylanicum*, *C. tamala*, *A. subulatum*, *T. foenumgraecum* and four edible herbs i.e. *M. piperita*, *C. sativum*, *L. sativa*, and *B. oleraceae* to evaluate the in vitro biological activities for incorporation in chitosan films. These common kitchen spices were selected due to their minimal/no toxicity, significant antioxidant and antimicrobial properties, and their frequent use in routine diet. A few studies have been reported on the incorporation of essential oils of these plants as additive in chitosan films (Liu *et al.*, 2022). However, there is no report of incorporating ethanol extracts of above-mentioned plants in chitosan nanocomposites. Therefore, active phytochemicals of plants were quantified using high-performance liquid chromatography (HPLC). Furthermore, molecular docking was performed to comprehend the underlying antimicrobial mechanism of detected polyphenols in order to use them as additive in chitosan nanocomposites.

2.2 Materials and Methods

2.2.1 Plant collection

Eight edible herbs and spices i.e. *C. zeylanicum*, *C. tamala*, *A. subulatum*, *T. foenum graecum*, *M. piperita*, *C. sativum*, *L. sativa*, and *B. oleraceae* respectively were obtained during September 2020 from the Bharakahu local market, Islamabad, Pakistan. Three dried spices i.e. *C. zeylanicum*, *C. tamala*, *A. subulatum* were recognized by Dr. Muhammad Zafar, Department of Plant Sciences, Quaid-i-Azam University, Islamabad. Remaining five plants i.e. *T. foenum graecum*, *M. piperita*, *C. sativum*, *L. sativa*, and *B. oleraceae* were submitted in Herbarium, Department of Plant Sciences, Quaid-i-Azam University, Islamabad under accession number 131371 to 131375 respectively.

2.2.2. Plant extract preparation

The herbs were washed with tap water and dried for three weeks. Dried spices and herbs were ground to powder and kept in air-tight bottles at room temperature. Fine powder (200 g) of each plant was macerated in analytical grade ethanol (1000 ml) for five days. Maceration was carried out to increase the contact between plant material and solvent and to soften plant's cell wall so that ethanol soluble phytochemicals may be released. The disruption of the plant cell wall was further enhanced by the sonication (after maceration) and thus release of phytochemicals was facilitated. Whatman #1 filter paper (Sigma, USA) was used to filter the extracts. Rotary evaporator (Buchi, Switzerland) was used to concentrate the extracts via vacuum evaporation and drying was done at 40 °C in a vacuum hood followed by storage at 15 °C. Percent recovery of the extracts was calculated by the following formula:

$$\text{Extract recovery} = \left(\% \frac{w}{w}\right) = \frac{A}{200} * 100 \quad \text{Eq. 2.1}$$

Where A refers to dry extract weight

2.2.3 Phytochemical analysis

(a). Total Phenolic Content (TPC)

TPC was measured by the Folin–Ciocalteu method as reported previously (Foo *et al.*, 2017). Briefly, 10 μ L (20 mg/mL in DMSO) of the extract was mixed with Folin–Ciocalteu reagent (tenfold diluted with water). Following a room temperature incubation of 5 minutes, 98 μ L of 6% sodium bicarbonate was added. This mixture was retained at 25 °C for 90 min and absorbance was measured at 630 nm using micro titer plate reader. The standard curve equation for gallic acid was obtained ($y = 0.0732x - 0.0205$) with R^2 value of 0.999. The assay was executed in triplicate and TPC was determined as mg of gallic acid equivalent (GAE) per gram of extract (mg GAE/g Extract).

(b). Total Flavonoid Content (TFC)

The TFC of the extracts was determined by aluminum chloride colorimetric assay, with some modifications (Ahmed *et al.*, 2017). Briefly, each extract stock (10 μ L from 20 mg/mL stock in DMSO), aluminum chloride (10 μ L; 10% w/v in H₂O), 1.0 M potassium acetate (10 μ L), and distilled water (170 μ L) were mixed and incubated at room temperature (30 min). The absorbance of the mixture was measured at 405 nm. The standard curve equation for quercetin ($y = 0.01x - 0.004$) was obtained and the resultant TFC was expressed in microgram equivalents of quercetin per gram Extract (mg QE/g Extract).

(c). High Performance Liquid Chromatography (HPLC) Analysis

Polyphenols were identified and quantified using HPLC analysis of the medicinal plants. An Agilent Chem station Rev. B.02–01-SR1 (260) based HPLC system, furnished with analytical column (Zorbex-C8 ; 4.6 x 250 nm, 5 μ m particle size) in combination with a diode array detector (Agilent technologies, Waldbronn, Germany) was used, following previously reported method (Nasir *et al.*, 2020). Wavelengths used to detect the standards were 257 nm for rutin, vanillic acid and plumbagin, 279 nm for catechin, syringic acid, coumaric acid, and emodin, 325 nm for caffeic acid, apigenin, luteolin, gentisic acid, and ferulic acid, while quercetin and kaempferol were analyzed at 368 nm. Different polyphenols were identified and quantified by comparing their UV

absorption spectra. The retention time of samples was compared with standards and the results were documented as $\mu\text{g}/\text{mg}$ extract.

2.2.4 *In vitro* biological activities

2.2.4.1 Antioxidant assays

(a). Total Reducing Power (TRP)

For reducing power assay, test extract (50 μL ; 20 mg/mL in DMSO) was mixed with 475 μL of phosphate buffer (0.2 mol/L, pH 6.6) and potassium ferricyanide (1% w/v in water). (Ahmed *et al.*, 2017). The mixture was incubated (20 min; 50 °C) and then 500 μL of tri-chloro acetic acid was added. Following centrifugation (3000 RPM) at room temperature (10 min), the upper layer (500 μL) was mixed with equal volume of distilled water and Iron (III) chloride (100 μL ; 0.1% w/v in water). After this, 200 μL was taken from this and absorbance was measured at 645 nm using microplate reader (Biotech, Elx-800, St. Louis, MO, USA). The assay was performed in triplicate. The chemicals and standards used in the assays were purchased from Sigma-Aldrich (St. Louis, MO, USA).

(b). Total Antioxidant Capacity (TAC)

Total antioxidant capacity was evaluated by the phosphomolybdate method (Younus *et al.*, 2019). An aliquot of 10 μL extract (20 mg/mL in DMSO) was added to 190 μL of reagent solution (0.6 M sulphuric acid, 28 mM sodium phosphate, and 4 mM ammonium molybdate solution in H_2O) in 96 well plate. After incubation for 90 min at 95 °C in the water bath, the reaction mixture was cooled at room temperature and absorbance was taken at 630 nm using microplate reader (Biotech, Elx-800, USA). Both TRP and TAC were expressed as the number of mg of vitamin C equivalents per gram of extract (vit. C eq/g).

(c). DPPH (2, 2-Diphenyl-1-picryl-hydrazyl radical) Free Radical Scavenging

Decolorization of purple-colored DPPH was used to measure the free radical scavenging activities of the extracts (Ahmed *et al.*, 2017; Younus *et al.*, 2019). Here, 190 μL of DPPH solution (in methanol) was added in each well (96 well plate) followed

by the addition of 10 μ L of four different dilutions (125, 250, 500, and 1000 μ g/mL) of each extract. Samples were kept in the dark at 37 °C (15 min) and absorbance was taken at 517 nm using microplate reader (Biotech, Elx-800, St. Louis, MO, USA). The assay was performed in triplicate and ascorbic acid served as a positive control in each experiment. Percentage free radical scavenging was derived from the given formula:

$$\% \text{ Scavenging} = \text{Abs}_{\text{neg}} - \text{Abs}_{\text{ex}} / \text{Abs}_{\text{neg}} \times 100 \quad \text{Eq 2.2}$$

Where:

Abs_{neg} = Absorbance of negative control

Abs_{Ex} = Absorbance of extract

The inhibitory concentration at which the test sample showed 50% scavenging (IC₅₀) was determined using Graph Pad Prism 5 software.

2.2.4.2 Antimicrobial assays

(a). Antibacterial assay

The antibacterial activity was assessed using disc diffusion assay (Ahmed *et al.*, 2017). The test bacterial strains cultures (i-e *Bacillus subtilis* (ATCC-6633), *Staphylococcus aureus* (ATCC-6538), *Pseudomonas aeruginosa* (ATCC-15442) and *E. coli* (ATCC-25922) were obtained from the Pharmacy department, Quaid-i-Azam University, Islamabad, Pakistan. Each bacterial strain (100 μ l) was streaked on nutrient agar respectively for antibacterial assay. Discs of filter paper loaded with test extract (5 μ L; 20 mg/mL), positive control (Ciprofloxacin, 20 μ g/mL), and negative control (DMSO) were employed on agar plates and incubated (24 h; 37°C). Afterwards, plates were observed for particular antibacterial zones of inhibition (mm) on specific time intervals. Ciprofloxacin was used as positive control.

(b). Antifungal assay

The antifungal activity of the extracts was evaluated by the agar disc diffusion method (Ahmed *et al.*, 2017), performed in triplicate. The spores of test fungal strains *Fusarium solani* (FCBP- 0291), *Mucor species* (FCBP-0300), *Aspergillus niger* (FCBP-0198),

and *Aspergillus flavus* (FCBP-0064) were procured from the department of Pharmacy, Quaid-i-Azam University, Islamabad, Pakistan. These strains were collected in solution (0.02% v/v tween 20 in water) and the turbidity was adjusted according to McFarland 0.5 turbidity standard. Then, fungal strain (100 μ L) was streaked on sabouraud dextrose agar. Discs of filter paper, impregnated with test extract (5 μ L; 20 mg/mL), positive control (Terbinafine, 20 μ g/mL), and negative control (DMSO) were employed on agar plates and incubated (24–48 h; 28 °C). Afterwards, the average diameter (mm) of the growth inhibition zone around all the discs was measured and recorded.

2.2.5 Molecular docking analysis

Molecular docking analysis was executed to predict the possible antifungal mechanism of the polyphenols, detected via HPLC analysis. Protein databank (PDB) was used to acquire 3D structures of fungal enzymes 14-alpha-demethylase and nucleoside di phosphokinase with PDB IDs 5FRB and 6K3H respectively. These two fungal enzymes i.e. CYP51 and NDK were selected for docking due to their significant role in sterol biosynthesis, spore development and pathogenesis in fungi respectively. A 3D structure CYP51B protein was modeled using Swiss Prot. Pub chem (<https://swissmodel.expasy.org/>). Pubchem was used to obtain structures of ligands (i.e. rutin, quercetin, apigenin, and kaempferol with PubChem IDs 5280805, 5280343, 5280443, and 5280863, respectively). Ligands and heteroatoms were removed and proteins were optimized and minimized using UCSF Chimera software. Docking was performed using the Pyrx-virtual screening tool, binding affinities were saved as CSV files and Discovery studio was used to visualize the final protein–ligand interactions (Baig *et al.*, 2020).

2.3 Results

2.3.1 Percent yield

Among spices, *C. zeylanicum* exhibited the highest percent yield, while *M. piperita* presented a highest yield among herbs. The percent yield of eight plant extracts is depicted in table 2.1.

Table 2.1 Percent yield of the plant extracts

S. No	Plant Name	Extract percent yield (%)
1	<i>C. zeylanicum</i>	26.5
2	<i>C. tamala</i>	18.8
3	<i>A. subulatum</i>	9.5
4	<i>T. foenumgraecum</i>	5.1
5	<i>M. piperita</i>	10.2
6	<i>C. sativum</i>	5.6
7	<i>L. sativa</i>	6.4
8	<i>B. oleraceae</i>	7.0

2.3.2 Phytochemical Analysis

(a). Total phenolic assay

The highest amount of TPC was exhibited by *C. tamala* (176.5 ± 1.5 mg GAE/g Extract). Among herbs, the highest TPC (136.2 ± 6.4 mg GAE/ g Extract) was quantified in *M. piperita*, as presented in Table 2.2. Phenolic content appeared to decline in the following order *C. tamala* > *M. piperita* > *C. zeylanicum* > *A. subulatum* > *L. sativa* > *T. foenumgraecum* > *B. oleraceae* > *C. sativum*.

(b). Total flavonoid assay

Among spices, *T. foenum graecum* represented the highest TFC while *M. piperita* depicted the highest TFC among herbs (Table 2.2). Extracts of *A. subulatum* and *B. oleraceae* displayed lowest amount of total flavanoids. The descending order of TFC among the extracts was *T. foenum graecum* > *M. piperita* > *C. zeylanicum* > *L. sativum* > *C. tamala* > *C. sativum* > *B. oleraceae* > *A. subulatum*

Table 2.2 Total phenolic and flavonoid content of the plant extracts

S. No	Plant	Total Phenolic content (mg GAE/ g Extract)	Total Flavonoid content (mg QE/ g Extract)
1	<i>C. zeylanicum</i>	82.4 ± 5.6	23.7 ± 0.1
2	<i>C. tamala</i>	176.5 ± 1.5	13.7 ± 0.3
3	<i>A. subulatum</i>	24.4 ± 0.1	2.5 ± 0.4
4	<i>T. foenumgraecum</i>	25.5 ± 0.3	28.8 ± 0.4
5	<i>M. piperita</i>	136.2 ± 6.4	26.8 ± 1.1
6	<i>C. sativum</i>	25.2 ± 0.8	11.6 ± 0.6
7	<i>L. sativa</i>	28.6 ± 3.2	15.3 ± 1.3
8	<i>B. oleraceae</i>	17.2 ± 3.2	2.3 ± 1.1

Data is represented as mean ± SD

(c). High-Performance Liquid Chromatography (HPLC) Analysis

Quantitative polyphenol detection was carried out using HPLC (using a total of 18 standards), by comparing chromatograms of samples with that of standards (Table 2.3). A total of 12 polyphenols were detected in studied plant extracts, i.e., rutin, kaempferol, vanillic acid, quercetin, apigenin, ferulic acid, catechin, gentisic acid, syringic acid, plumbagin, caffeic acid and emodin. The representative chromatograms are shown in Figure 2.1.

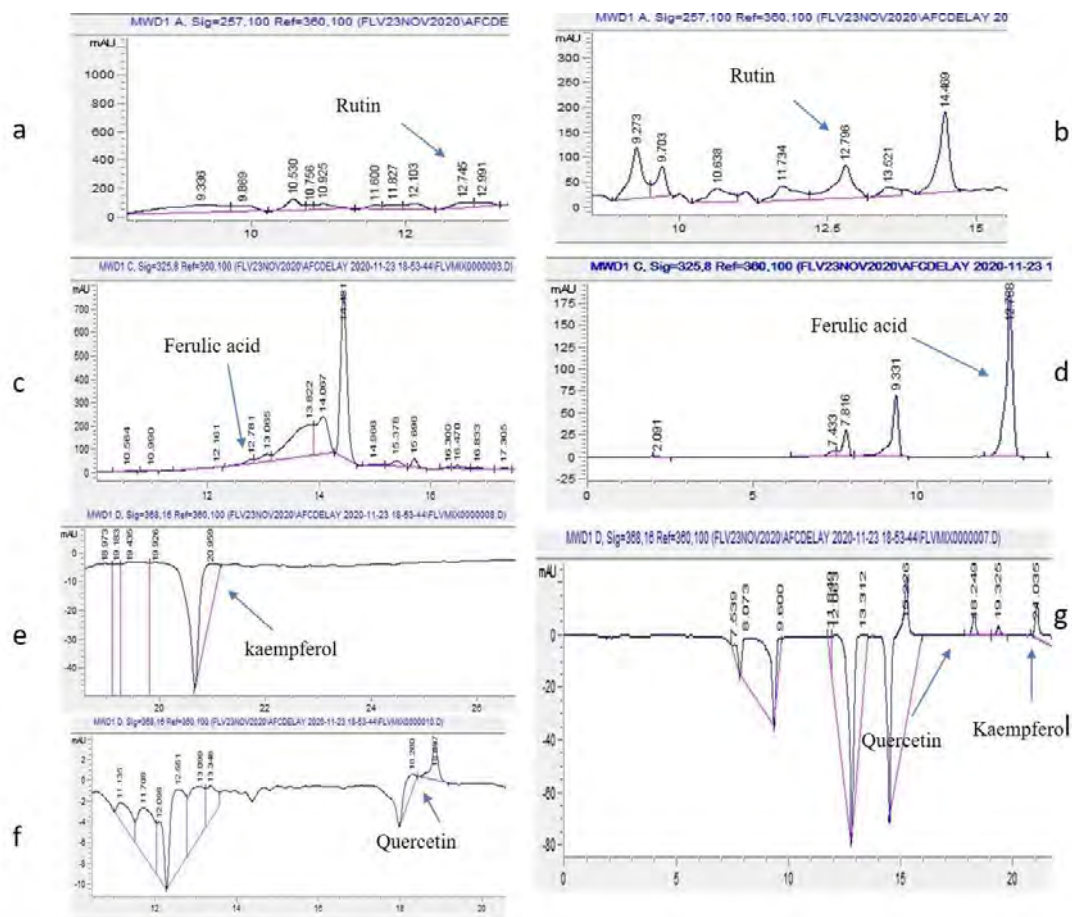


Figure 2.1. HPLC profile of the plant extracts

(a) *C. tamala* (b) standard (Rutin) (c) Ethanolic Extract of *M. piperita* (d) Standard (Ferulic acid) (e) Ethanolic extract of *C. zeylanicum* (f) Ethanolic extract of *A. subulatum* (g) Standard (Kaempferol and Quercetin)

2.3.3 *In vitro* biological activities

2.3.3.1 Antioxidant assays

(a). Total Reducing Power (TRP)

Total reducing power results indicated a wide range of reducing power of the extracts, ranging from 8.7 to 65.04 $\mu\text{g vit. C eq./mg Extract}$. The maximum TRP values were shown by *M. piperita* followed by *C. zeylanicum* and *C. tamala* as depicted in Fig 2.2.

Table 2.3. Identification and quantification of polyphenols ($\mu\text{g}/\text{mg}$ Extract) by HPLC.

Plant	Rutin (R)	Vanillic Acid (VA)	Quercetin (Q)	Ferulic Acid (FA)	Syringic Acid (SA)	Kaempferol (K)	Plumbagin (PL)	Apigenin (A)	Catechin(C)	Emodin (E)	Caffeic Acid (CF)	Gentisic Acid (GS)
<i>C. zeylanicum</i>	-	0.21 \pm 0.02	-	-	-	0.63 \pm 0.02	-	-	-	-	-	-
<i>C. tamala</i>	8.34 \pm 0.26	2.35 \pm 0.04	-	-	-	-	0.11 \pm 0.04	-	-	0.54 \pm 0.03	-	-
<i>A. subulatum</i>	-	0.21 \pm 0.01	0.85 \pm 0.03	-	0.2 \pm 0.04	-	-	-	-	-	-	-
<i>T. foenumgraecum</i>	6.32 \pm 0.03	-	1.35 \pm 0.04	-	0.24 \pm 0.06	-	-	0.53 \pm 0.03	-	0.05 \pm 0.002	-	-
<i>M. piperita</i>	4.3 \pm 0.05	-	-	3.01 \pm 0.26	0.22 \pm 0.07	-	-	-	-	-	0.43 \pm 0.04	-
<i>C. sativum</i>	3.44 \pm 0.06	-	-	-	-	-	-	-	-	-	0.27 \pm 0.02	1.01 \pm 0.22
<i>L. sativa</i>	3.07 \pm 0.11	-	-	-	-	-	-	-	0.55 \pm 0.03	-	0.37 \pm 0.04	-
<i>B. oleraceae</i>	0.84 \pm 0.03	-	-	-	-	-	-	-	-	-	-	-

Experiments were executed in triplicate and the data are presented as mean \pm standard deviation (SD).

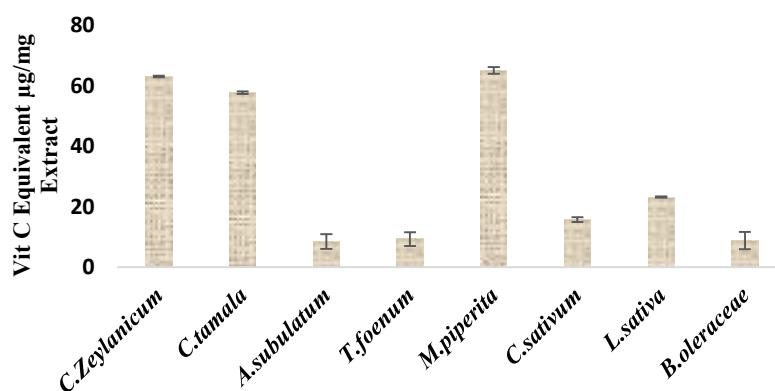


Fig 2.2 Total reducing power of the plant extracts

(b). Total anti-oxidant Capacity (TAC)

Results of TAC showed a wide range of values exhibited by the plant extracts, expressed as the number of ascorbic acid equivalents, from 5.58 to 48.4 mg vit. C eq /g extract as shown in figure 2.3.

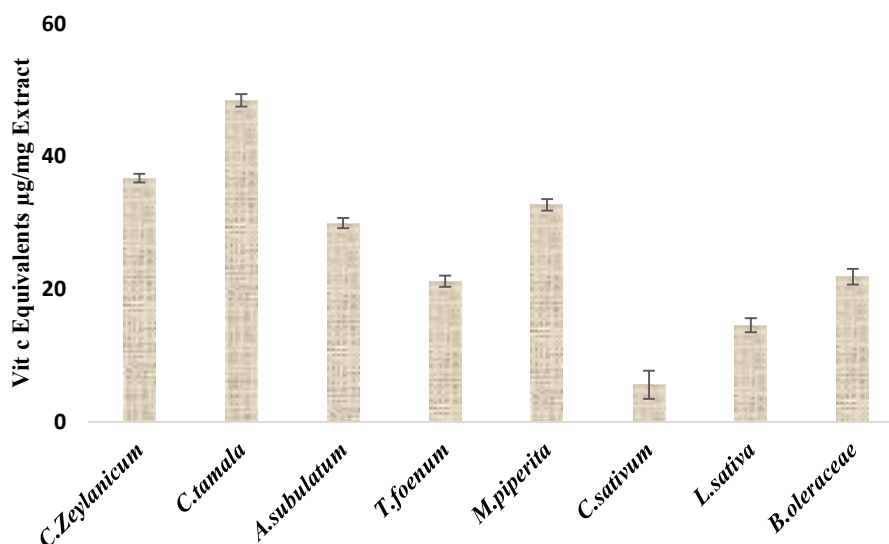


Fig 2.3. Total antioxidant activity of the plant extracts

(c). DPPH Scavenging Assay

Free radical scavenging potential of the extracts was evaluated through DPPH assay. Results displayed that *C. tamala* extract showed highest DPPH scavenging potential exhibiting IC₅₀ of 8.7 $\mu\text{g}/\text{ml}$, followed by *C. zeylanicum* with an IC₅₀ value of 25.4 $\mu\text{g}/\text{ml}$ and *M. piperita* with an IC₅₀ value of 124.9 $\mu\text{g}/\text{ml}$. However, *B. oleracea* extract showed least DPPH scavenging with an IC₅₀ value of 759.4 $\mu\text{g}/\text{ml}$ as shown in table 2.4. Ascorbic acid served as positive control showed IC₅₀ (0.01 mg/ml) for DPPH radical. The dose response curves of plant extracts showing highest and lowest DPPH free radical scavenging are shown in Figure 2.4.

Table 2.4. DPPH free radical scavenging activity (IC₅₀ µg/ml) of the plant extracts

S. No	Plants	IC ₅₀ (µg/ml)
1	<i>C. zeylanicum</i>	25.4 ± 2.0
2	<i>C. tamala</i>	8.7 ± 0.9
3	<i>A. subulatum</i>	283.4 ± 4.9
4	<i>T. foenum graecum</i>	485.9 ± 6.6
5	<i>M. piperita</i>	124.9 ± 8.2
6	<i>C. sativum</i>	250.9 ± 13.9
7	<i>L. sativa</i>	221.6 ± 2.1
8	<i>B. oleraceae</i>	759.4 ± 2.5

Experiments were executed in triplicate and the data is presented as mean ± standard deviation (SD).

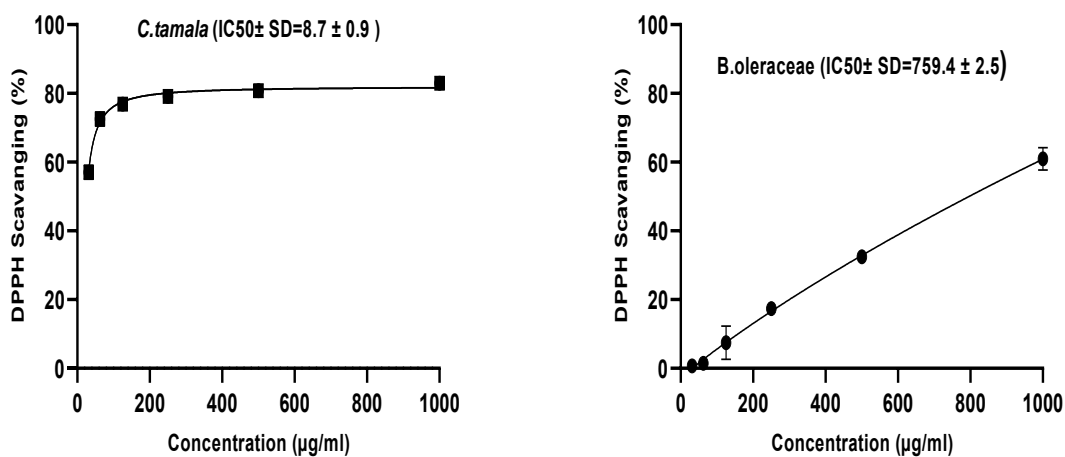


Fig. 2.4. Dose response curve of plant extracts showing highest and lowest DPPH scavenging percentage

2.3.3.2 Antimicrobial assays

(a). Antibacterial assay

The disc diffusion assay was used to measure the inhibition zones which were recorded in mm. The highest antibacterial zones of inhibition were seen in case of *C. tamala* (i.e. 9 mm), *L. sativa*, *B. oleraceae* (7.66 mm) and *A. subulatum* (7.06 mm) against *P. aeruginosa* and *S. aureus* respectively (Table 2.5).

Table 2.5. Antibacterial assay

S. No	Plants	Zones of inhibition (mm) at 200µg/ml			
		<i>P. aeruginosa</i>	<i>E. coli</i>	<i>S. aureus</i>	<i>B. subtilis</i>
1	<i>C. zeylanicum</i>	---	5.33 ± 0.57	5.66 ± 0.57	---
2	<i>C. tamala</i>	9.13 ± 0.15	6.66 ± 0.57	---	---
3	<i>A. subulatum</i>	---	5.33 ± 0.57	7.06 ± 0.11	---
4	<i>T. foenumgraecum</i>	---	---	6.33 ± 0.57	---
5	<i>M. piperita</i>	5.31 ± 0.31	---	---	5.66 ± 0.57
6	<i>C. sativum</i>	5.93 ± 0.05	6.33 ± 0.57	6.33 ± 0.57	---
7	<i>L. sativa</i>	---	6.33 ± 0.57	7.66 ± 0.57	---
8	<i>B. oleraceae</i>	---	5.33 ± 0.57	7.66 ± 0.57	---
9	<i>Ciprofloxacin</i>	18.33 ± 0.57	21.66 ± 0.57	19.83 ± 0.28	20.33 ± 0.57

--- Not detected

However, slight inhibition i-e 5.33 mm and 6.33 mm were shown by *C. zeylanicum*, *A. subulatum* and *B. oleracea* against *E. coli* and *T. foenum graecum* and *C. sativum* against *S. aureus* respectively. Furthermore, broth dilution was carried out in order to calculate MIC of only those extracts which displayed zones of inhibition at 200 µg/ml. It is evident from fig.2.4 that lowest MIC (≤ 100 µg/ml) was depicted by most of the plant extracts against *E. coli*. Interestingly, *T. foenum graecum* was also found to inhibit all bacterial strains at ≤ 100 µg/ml except *B. subtilis*.

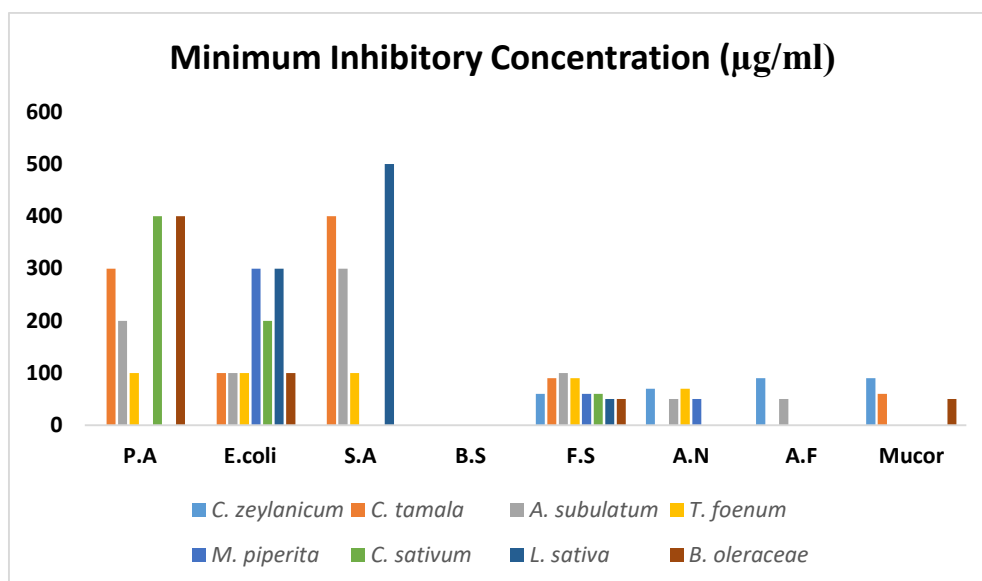


Fig.2.5 Minimum inhibitory concentration (MIC) of the plant extracts

b). Antifungal assay

The antifungal potential of the extracts was assessed against four pathogenic fungal strains. Results showed that all studied plant extracts inhibited the growth of *F. solani*. *C. zeylanicum* inhibited the growth of all fungal strains, with a maximum zone of inhibition (13 mm) against *F. solani*. *A. subulatum* exhibited antifungal activity against *Fusarium solani*, *Aspergillus niger*, and *Aspergillus flavus*.

Minimum inhibitory concentration was calculated by disc diffusion assay by again loading extracts on filter paper discs at lower concentrations i-e first screening at 100 µg/ml and then 90, 80, 70, 60 and 50 µg/ml. Fig 2.4 displays that *A. subulatum* and *M. piperita* were found to exert antifungal effect even at very low concentration i-e 50 µg/ml against *A. niger*.

Table 2.6. Antifungal assay

S. No	Plants	Zones of inhibition (mm) at 200µg/ml			
		<i>F. solani</i>	<i>A. niger</i>	<i>A. flavus</i>	<i>Mucor species</i>
1	<i>C. zeylanicum</i>	13.0 ± 0.5	10.0 ± 0.15	8.1 ± 0.15	10.0 ± 0.15
2	<i>C. tamala</i>	11.3 ± 1.05	-----	-----	7.1 ± 0.12
3	<i>A. subulatum</i>	13.6 ± 0.17	7.1 ± 0.1	5.0 ± 0.05	-----
4	<i>T. foenum graecum</i>	9.3 ± 0.5	7.1 ± 0.2	-----	-----
5	<i>M. piperita</i>	10.0 ± 0.1	6.0 ± 0.1	-----	-----
6	<i>C. sativum</i>	7.6 ± 0.3	-----	-----	-----
7	<i>L. sativa</i>	9.3 ± 0.4	-----	-----	-----
8	<i>B. oleraceae</i>	8.3 ± 0.57	-----	-----	9.2 ± 0.05
9	<i>Terbinafine</i>	20 ± 0.98	22 ± 1.03	23 ± 1.04	22 ± 1.02

---Not detected

2.3.4 Molecular docking

To predict the antifungal mechanism of action of the plant extracts, the docking interactions of their common polyphenols were analyzed against two important fungal enzymes. Among all polyphenols, rutin showed the greatest affinity for 14-alpha demethylase (CYP51) and nucleoside diphosphokinase (NDK) with the lowest K_d (dissociation constant) values of -9.4 and -8.9, respectively (Table 2.7).

Results showed that rutin interacted with fungal 14-alpha demethylase by forming hydrogen bonds with tyrosine 90 (Figure 2.5 a), while, quercetin formed two hydrogen bonds with histidine 415 and cystine 417 (Figure 2.5 b). Binding affinity was estimated to be -9.4 and -8 for rutin and quercetin, respectively (Table 2.7). Binding affinity for interaction with 14-alpha demethylase, were found to be increased in the following order: rutin > catechin > quercetin > kaempferol > vanillic acid > ferulic acid. Rutin and kaempferol showed the highest binding affinity for fungal nucleoside diphosphokinase with K_d -8.9 and -8.2 , respectively. Rutin and kaempferol both interacted with nucleoside diphosphokinase by forming hydrogen bonds with arginine C:19 and glutamine D:147 (Figure 2.5d, 2.5e), while rutin also showed interaction with arginine C:19, glutamate: 30, glycine A: 20, asparagine: 21, and serine D: 27 (Figure 2.5d).

Table 2.7 Binding affinities (in terms of K_d values) of polyphenols with fungal enzymes

Polyphenol	14-alphaDemethylase (CYP51)	Nucleoside Diphosphokinase (NDK)
Rutin	-9.4	-8.9
Quercetin	-8	-7.8
Kaempferol	-7.9	-8.2
Vanillic acid	-5.7	-5.6
Ferulic acid	-6.1	-5.9
Catechin	-8.1	-7.7

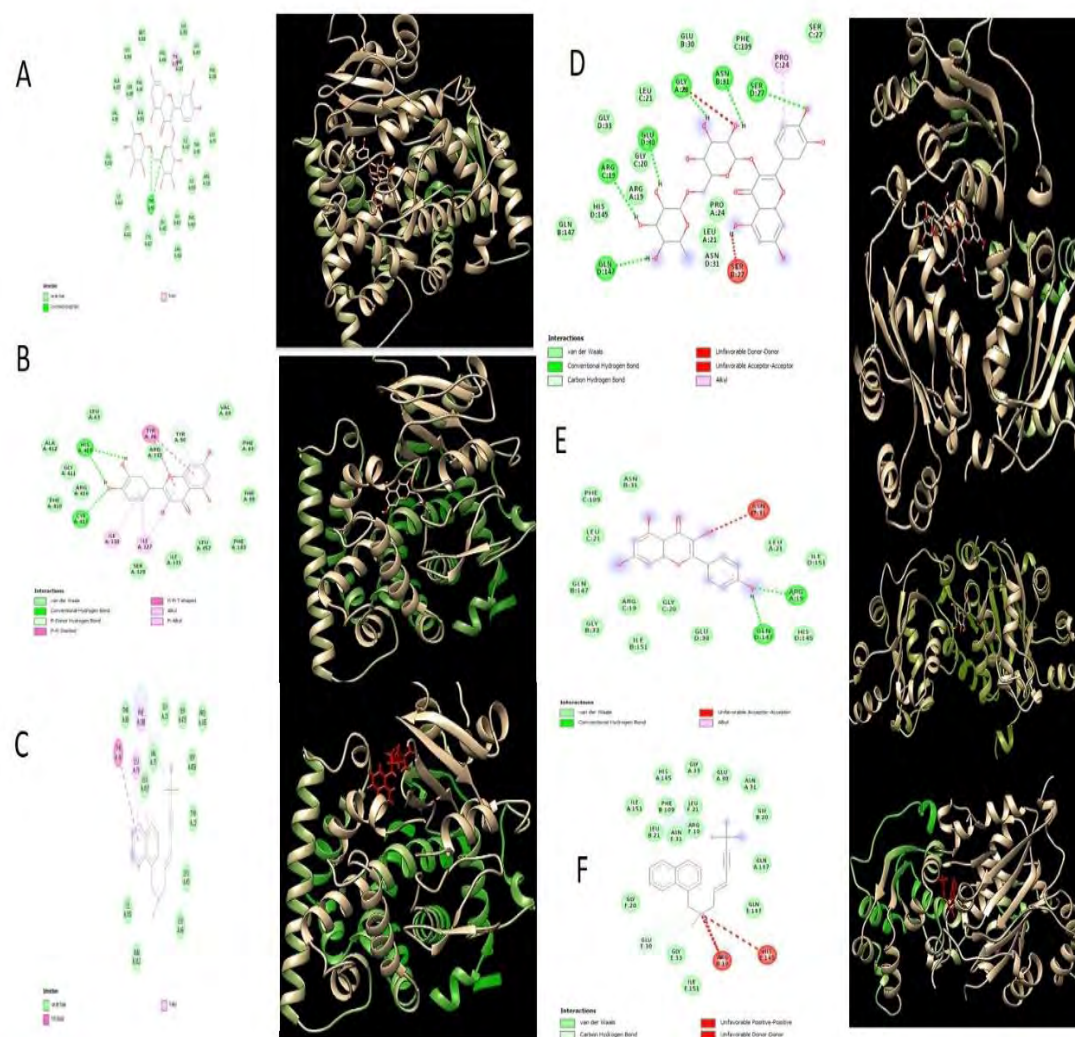


Figure 2.6. Graphical representation of polyphenols binding modes in fungal proteins. (A) Rutin with 14 alpha demethylase (CYP51). (B) Quercetin with CYP51. (C) Terbinafine with CYP51. (D) Rutin with nucleoside diphospho kinase (NDK). (E) Kaempferol with NDK. (F) Terbinafine with NDK.

2.4 Conclusion

In vitro biological assays of ethanolic plant extracts were carried out to select the plants with significant activities in order to be incorporated in chitosan films. Our results demonstrate that *C. tamala* exhibited strong antimicrobial activities, lowest IC₅₀ values (ie 8µg/ml) in DPPH free radical scavenging, highest total antioxidant activity and strong reducing power. Moreover, *A. subulatum* and *M. piperita* displayed good antimicrobial activities, highest TPC as well as 84% scavenging in DPPH assay. Therefore, on the basis of these results these three plant extracts were selected for final

incorporation in chitosan films. In addition to this, the main polyphenols of these plants i.e. rutin, vanillic acid and quercetin as identified by HPLC results were also selected for individual incorporation in chitosan films. The Docking results showed that common plant polyphenols present in these plants may be one of the major reasons for their antimicrobial effect via inhibition of specific enzymes. Lowest K_d values of rutin (as this polyphenol was found in highest concentration in *C. tamala*) for fungal enzymes positively correlate with lowest IC₅₀ of this plant extract in DPPH assay. Overall, these plant extracts and their respective polyphenols can be used as additive in chitosan films to impart their antioxidant and antimicrobial properties to improve the shelf life of food products

Synthesis and Characterization of
Phyto-assisted Chitosan
Nanocomposites

(Chapter # 3)

3.1 Introduction

Food and Agriculture Organization of the United Nations (FAO) has recently proposed active packaging as an eminent way to improve food's quality during storage and transportation specially after facing Covid-19 challenges (Ashraf *et al.*, 2021). Active food packaging films based on biopolymers are designed in a contribution to protect food from detrimental effect of ultra violet rays, chemicals or microbial contamination or water vapors (Hiremani *et al.*, 2022). Chitosan active films are being given more focus nowadays due to its film forming property, nontoxicity, biodegradability, bio-functionality, chemical stability and strong antimicrobial properties (Sameen *et al.*, 2021). Chitosan, derived from de-acetylated chitin; is a linear polysaccharide containing D-glucosamine units linked together with β - (1-4) bond and N-acetyl units of D-glucosamine (Kumar *et al.*, 2019). However, low thermal stability low mechanical properties, brittleness and humidity sensitiveness are major draw backs of pure chitosan films (Haghighi *et al.*, 2020). Biopolymers like keratin (Tanase & Spiridon, 2014) and cellulose (Mujtaba *et al.*, 2017; Wildan & Lubis, 2021), when blended with chitosan, are reported to improve its packaging properties and food shelf life. Other biopolymers can become compatible with chitosan, due to presence of cationic and polar groups. For instance carboxyl, amino and hydroxyl groups in chitosan backbone facilitate the hydrogen bonds or dipole interaction with the analogous functional groups (Bonilla *et al.*, 2018).

Another way to improve properties of chitosan films is the addition of antimicrobial/antioxidant plant extracts and the incorporation of nano fillers in chitosan matrix. Different nano fillers such as nano clay (montmorillonite MMT) (Qin *et al.*, 2015), cellulose nanocrystals (CNC) (Xu *et al.*, 2018), cellulose nano fibers (Phan *et al.*, 2019), and carbon nanotubes (Cao *et al.*, 2009) are reported to enhance barrier and mechanical characteristics of chitosan films. Various carboxyl and hydroxyl groups are introduced into cellulose molecule of modified nano cellulose constructing both amorphous and crystalline areas simultaneously so making it an efficient nano filler (Isogai, 2021) for reinforcement in composite films. Crosslinking the side chains of keratin helps to convert it into nano keratin to improve its surface area and to enhance its properties (Sree *et al.*, 2021). However, the effect of the influence of nano filler either nano cellulose or nano keratin is greatly determined by the nature of both the

reinforcing agents and the polymer matrix (López De Dicastillo *et al.*, 2020; Taherimehr *et al.*, 2021). Chitosan bio-nanocomposites films reinforced with cellulose nano crystals (CNC) and glycerol were shown to improve barrier properties (Wildan & Lubis, 2021). In another study, grape pomace extract was used along with CNC in chitosan films to provide antioxidant, thermal and mechanical properties (Xu *et al.*, 2018). Urea coated nano keratin composites were used as fertilizers and in another study keratin nanoparticles were synthesized from chicken feather keratin by crosslinking and used in chitosan matrix for use as scaffolds in tissue engineering use (Sree *et al.*, 2021). However, the use of nano keratin in chitosan films for food packaging is not explored yet. Literature also suggests that synergistic effect of mixing two nano fillers in chitosan matrix may give pronounced barrier properties as compared to using one filler (Tang *et al.*, 2008).

For adding bioactive properties to chitosan films, variety of plant extracts i.e. *Ocimum tenuiflorum*, *Pistacia terebinthus*, *Carum copticum*, *Azadirachta indica*, *mango leaf extract* have been incorporated in chitosan matrix (Jafarzadeh *et al.*, 2020). Polyphenols incorporation can also aid in bioactive chitosan films formulations. Quercetin (3,3',4',5,7-pentahydroxyflavone) and rutin (3,3',4',5,7-pentahydroxy flavone-3-rhamnoglucoside) are yellow colored, water insoluble solids possessing potent antioxidant, antibacterial and anticancer properties (Paudel *et al.*, 2022; Rubini *et al.*, 2020). Vanilla beans are rich in vanillic acid (4-Hydroxy-3-methoxybenzoic acid; vanillin oxidized form), that is not only an approved food additive but also exhibit various pharmacological activities (Chatterjee *et al.*, 2015). As per literature, vanillic acid was grafted on amino groups of chitosan (Chatterjee *et al.*, 2015), quercetin loaded chitosan nanoparticles were used to prepare chitosan packaging film (Roy & Rhim, 2021b) and rutin has been used in gelatin/chitosan films (Roy & Rhim, 2021a), PHA/chitosan blend film (Narasagoudr *et al.*, 2020) and chitosan/graphene films (An *et al.*, 2013). Overall, an approach of blending the different nano fillers and edible plant extracts (as additives) with chitosan for enhanced barrier properties is still under its way to explore more options.

Therefore, in current work, a synergistic approach of blending chitosan with two nano fillers along with additive effects of extracts and polyphenols was applied. Biodegradability was provided to films by chitosan blending part. Barrier properties

were upgraded by adding CNC and nano-keratin while three ethanolic plant extracts i.e. *C. tamala* (C.T), *A. subulatum* (A.S) and *M. Piperita* (M.P) and three respective polyphenols (rutin, vanillic acid and quercetin) were used as additives (as a rich source of polyphenols) to impart antioxidant and antimicrobial properties. Effect of different concentrations of CNC, nano keratin, plant extracts and polyphenols were observed to assess their impact on film properties. As per our literature survey, there is no report on use of nano keratin and cellulose nano crystals reinforced chitosan films with or without incorporating the above-mentioned plant extracts/selected polyphenols.

3.2 Materials and Methods

3.2.1 Materials

Chitosan (CAS No. 9012-76-4, 50-190 kDa; low molecular weight) was procured from sigma Aldrich. Alberta Innovates Technology Futures (AITF) provided the CNC. The poultry feathers were collected from Sofina Foods Edmonton. Ethanol ($\geq 95\%$, CAS No. 64-17-5), n-hexane (CAS No.110-54-3, $\geq 95\%$), glycerol (CAS No.56-81-5, 99.6%), glacial acetic acid (CAS No.64-19-7, $\geq 95\%$), were acquired from Sigma-Aldrich and used as received.

3.2.2 Extraction of keratin from chicken feathers

Initially, Chicken Feathers were washed with soap and water. Fume hood drying was carried out at room temperature for 4 days. Residual moisture was removed by oven-drying them at 50 °C for 8 h. Feathers were then processed and crushed via Fritsch Mill with 0.25 mm sieve size (Laval Canada, Pulverisette 15). After processing, feathers were extracted with hexane for lipids removal and then dried and kept at room temperature for preparation of nano keratin (NK). Keratin was extracted from dried chicken feathers following a previously reported method (Kaur *et al.*, 2018).

3.2.3 Preparation of nano keratin

Nano keratin was synthesized using cross linking method (Saravanan *et al.*, 2013). Firstly, 100 mg of isolated chicken feather keratin was dissolved in deionized water (2 ml) and then absolute ethanol (8 ml) was mixed under continuous stirring. Afterwards, 8% glutaraldehyde (1 μ l) was incorporated to cross link the keratin molecules to

synthesize nano keratin. The solution was then stirred for 24 hours. The keratin nanoparticles were obtained by 20 minutes' centrifugation (20,000 rpm) followed by several cycles of washing to eliminate unreacted glutaraldehyde. The obtained nanoparticles were freeze dried and subjected to further characterization.

3.2.4 Extract and Polyphenols preparation

Quercetin (CAS No.117-39-5), vanillic acid (CAS No. 121-34-6) were bought from Sigma-Aldrich and rutin (CAS No. 207671-50-9) was bought from Thermo-fisher scientific and used as received. Selected plant extracts of *C. tamala*, *A. Subulatum* and *M. Piperita* were prepared as described in chapter 2.

3.2.5 Film preparation

Solvent casting method was employed for films synthesis. Glacial acetic acid (1 % v/v) was used to dissolve chitosan powder (2 % w/v). It was then magnetically stirred for 6 hours at 90°C and cooled to room temperature. After optimization, (20 %, w/v) glycerol served as plasticizer in all films. The chitosan solution was mixed with varying concentrations of CNC (0, 1, 3, 5 and 7 %, w/v) and/or nano keratin (0, 0.1, 0.3 and 0.5 % w/v) suspensions, stirred at 70°C for 2 hours with 300 rpm speed and sonicated for 30 minutes to achieve nanoparticle dispersion. For extract incorporated films, ethanolic plant extracts of *C. tamala*, *A. subulatum* and *M. piperita* were added at varying (0.5, 1 and 1.5%, w/v) concentrations to chitosan/CNC/NK film solution, sonicated for 30 minutes and stirred at 70°C for 2hours at 300 rpm. However, for polyphenol loaded films, 1% (w/v) polyphenol solution (rutin, vanillic acid and quercetin) was mixed to film solution, stirred at 50°C for 2 hours with a speed of 300 rpm and sonicated for 30 minutes to achieve homogenous film forming solution. Subsequently, the film solution was decanted on aluminum plates, and oven-dried at 40°C for 24 hours. Conditioning was carried out at 25°C and relative (50%) humidity for 1 day (before peeling them off from plates) for further evaluation. The films were designated as under

- CS-control (Chitosan film only)
- CS-CNC (Chitosan with CNC only)
- CS-NK (Chitosan with NK only)
- CS-CNC-NK-EX1 (Chitosan with CNC, NK and *C. tamala* extract)

- CS-CNC-NK-EX2 (Chitosan with CNC, NK and *A. subulatum* extract)
- CS-CNC-NK-EX3 (Chitosan with CNC, NK and *M. piperita* extract)
- CS-CNC-Q, CS-CNC-R, CS-CNC-VA (Chitosan with CNC and quercetin/
rutin/vanillic acid)
- CS-NK-Q, CS-NK-R, CS-NK-VA (Chitosan with NK and quercetin/
rutin/vanillic acid)

3.2.6 Physical, mechanical and barrier properties

(a). Film Thickness

The three different locations of films were selected to measure films thickness using a digi-Max vernier caliper purchased from USA-Sigma-Aldrich. An average of three thickness readings was calculated and used for determining the mechanical properties of films. Most of the films thickness was of 80-90 μm .

(b). Mechanical Testing

An autograph AGS-X (Shimadzu, Canada) armed with 1000 N load cell (static) was utilized in observing the TS and % E of bio-nanocomposite films (ASTM D882-02). Rectangle pieces (50×5 mm) of films were used for mechanical testing. An initial grid separation of 3 cm and 50 cm/ min (cross head speed) was fixed. Peak load was divided to original cross-sectional area of sample to calculate tensile strength (T.S). Percent elongation (% E) was calculated by observing the percent changes in specimen length between the grips. Three replicates were measured for accuracy.

(c). Water vapor permeability (WVP)

Film's water permeability was checked by an already reported method (Zubair & Ullah, 2020) with some modifications. The film samples with an exposed area of $1.95 \times 10^{-3} \text{ m}^2$ were placed in a permeation cell previously filled with anhydrous calcium hydride (0 % relative humidity). The cell was placed back in desiccator filled with saturated solution of sodium chloride (75% relative humidity). The cell weight was noted daily till 6 days.

$$WVP = (WVTR - L)/\Delta P \quad \text{Eq. 3.1}$$

Where WVTR= water vapor transmission rate

L= Film thickness

ΔP = Difference in partial water vapor pressure across the sides of film

(d). UV Transmittance and Opacity

Prepared films were assessed for their optical properties by measuring the film absorbance via Optizen spectrophotometer (UV visible) from 200 nm to 800 nm wavelength range. Films pieces of 1x4 cm² were placed directly in the test cell of spectrophotometer against a blank cell. The percent transmittance and film opacity were calculated by the following formulas.

$$\%T = \text{antilog} (2 - \text{absorbance}) \quad \text{Eq.3.2}$$

$$\text{Opacity} = \text{Absorbance}_{600} / \text{Film thickness} \quad \text{Eq. 3.3}$$

(e). Water solubility

Gravimetric method was used for solubility studies. Film pieces of 1x4 cm² were weighed as m₁. Afterwards, samples were oven dried at 105 °C (1 day) to obtain a constant dry mass (m₂). It was followed by soaking the film samples in distilled water (25 °C for 24 h) and then taking them out after achieving a constant mass (m₃). Again, samples were oven dried for one day (105 °C) to achieve a constant weight (m₄). Following formulas were used to calculate water solubility, swelling degree and moisture content. $((m_2 - m_4)/m_4) * 100$

$$\text{Water solubility (\%)} = \left((m_2 - \frac{m_4}{m_4}) * 100 \right) \quad \text{Eq. 3.4}$$

$$\text{Swelling (\%)} = \left((m_3 - \frac{m_2}{m_2}) * 100 \right) \quad \text{Eq. 3.5}$$

$$\text{Moisture content (\%)} = \left((m_1 - \frac{m_2}{m_2}) * 100 \right) \quad \text{Eq. 3.6}$$

3.2.7 Structural Properties

(a). Fourier Transform Infrared (FTIR) Spectroscopy

The functional group changes of bio nanocomposite films were determined using Bruker Alpha Optics FTIR from Esslingen, Germany. A wave number range of 400-4000 cm^{-1} was selected for sample spectra analysis and OPUS software (version 6.5) was used. Before placing thin film sample, Clean ATR crystal spectra were recorded as background. Spectra processing was done using OMNIC (Nicolet) spectra software.

(b). X-ray Diffraction (XRD)

XRD of chitosan films was executed with a Rigaku Ultima IV (diffraction unit) at 38 kV and 38 mA. A Cu $K\alpha$ radiation source was used with 0.154 nm wavelength (λ). The XRD data was calculated at 5° to 45° (2θ) and 0.02° (step size). X-ray beam angle of incidence on the sample is designated as θ . Specimens of bio-nanocomposite films (1.5 x 1.5 cm) were directly placed on XRD grid to scan their diffraction pattern.

(c). X-ray Photoelectron Spectroscopy (XPS)

Elemental survey spectra and high resolution C1s spectra of chitosan nanocomposite films were determined via XPS. Specimen powders were evaluated using a UK based Kratos Analytical ULTRA spectrometer equipped with a source of Aluminum $K\alpha$ X-ray. Lower than 3×10^{-8} Pa base pressure was used in the analytical chamber. For charge compensation an electron flood gun with a power of 150 W and an aperture slot of $400 \times 700 \mu\text{m}^2$. Au 4f peaks resolution was 0.70 and Ag 3d peaks were set at 0.55 eV. For recording spectra, 160 eV (pass energy) was utilized and high-resolution scanning (40 eV) was done. Data processing was done by Origin software.

(d). Scanning Electron Microscopy (SEM)

The external (surface) morphology of bio-nanocomposites was examined by Zeiss Sigma 300 VP-FESEM, functioning at 20 kV. Gold/copper coating was done using (Anatech Ltd) hummer sputter coater 6.2 before placing samples on grid.

(e). Transmission Electron Microscopy (TEM)

The chitosan films were observed for structure insights by “FEI Morgagni 268 TEM”. TEM was operated at 80 kV and provided with CCD camera (Gatan Orius). The polymer resin embedding was done for each sample and 80 nm thick slices of films were set ready by ultra-microtome. A sample slice piece was positioned on a copper support grid for examination and uranyl acetate and lead citrate staining was performed.

3.2.8 Thermal Properties

(a). Thermo-gravimetric Analysis (TGA)

The chitosan nanocomposite films were examined for their thermal stability by thermogravimetric analyzer i.e. TA Instruments, Q50, USA following nitrogen stream. All film’s temperature reached to 600 °C from 25°C. Heating rate was selected at 10 °C/min and around 8 and 10 mg sample size was used. Sample weight loss was determined in terms of temperature changes.

(b). Differential Scanning Calorimetry (DSC)

Examination of thermal properties of chitosan nanocomposites was carried out using TA Instruments, DSC Q100 (USA) using nitrogen. For temperature and heat flow calibration, we used pure indium. All films were examined at temperature of 25°C to 300°C and a heating rate (10°C/min) was set. 5-10 mg weight samples were pressed in aluminum pans.

(c). Dynamic Mechanical Analysis (DMA)

The viscoelastic behavior was analyzed via Q800 dynamic analyzer (TA Instrument) using nitrogen flow at 1 Hz frequency and 15 μm amplitude. Film’s length and width was recorded and then heating started at -50°C and stopped at 200°C at 3°C/min heating rate. The loss modulus (E''), storage modulus (E') and loss tangent ($\tan \delta$) were noted down in terms of temperature. The temperature peak value of which $\tan \delta$ was recorded as glass transition temperature (T_g).

3.2.9 Statistical Analysis

Triplicate samples were used in all experiments. Statistix 8.1 software was used to evaluate significant differences in mechanical and barrier properties data.

3.3 Results

3.3.1 Screening and Optimization of Contents in Film Preparation

(a). Plasticizer Optimization

Different concentrations of glycerol (10%, 20% and 30%) were investigated for the preparation of chitosan bio-nanocomposite films. 20% Glycerol found to be suitable plasticizer for composite films as it provided highest tensile strength (Fig 3.1). Furthermore, the other parameters including temperature and time (stirring and sonication) were also optimized for solvent casting before implementing the actual experiments.

(b). Nano-filler Optimization

Two different nano fillers i.e. CNC and nano keratin were investigated for their optimal concentration to be used in bio-nanocomposite films. Different concentrations of CNC (1%, 3%, 5% and 7% w/v) were checked, among them 3% was found to be optimal on the basis of excellent mechanical properties. Varying nano keratin concentrations (0.5%, 1%, 0.3% and 1.5% w/v) were used in composite films (Fig 3.1). 0.3% nano keratin was selected for use in bio-nanocomposite films preparation as it gave highest tensile strength.

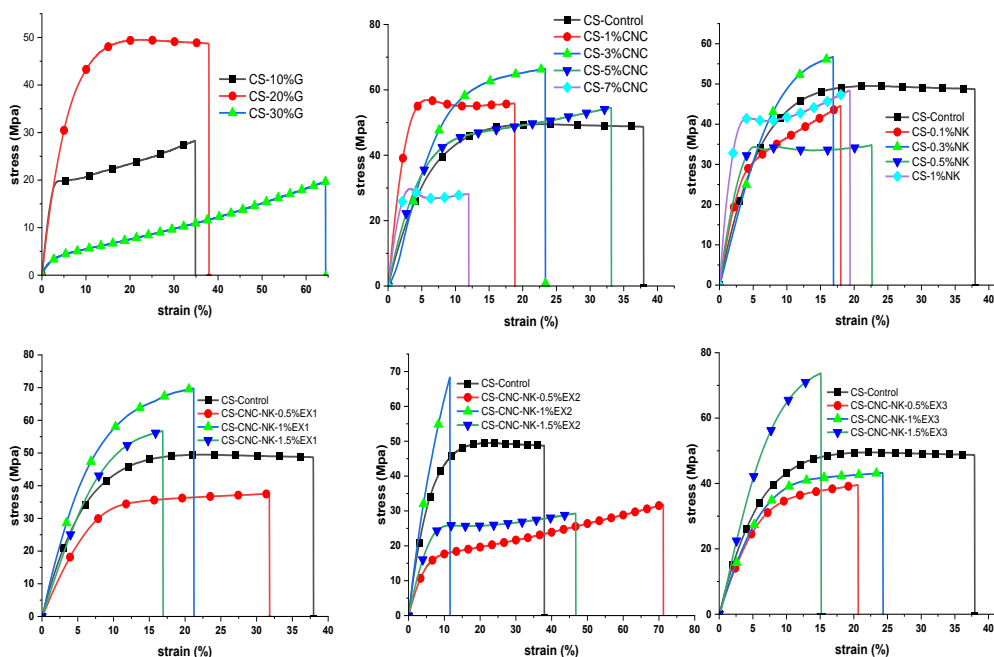


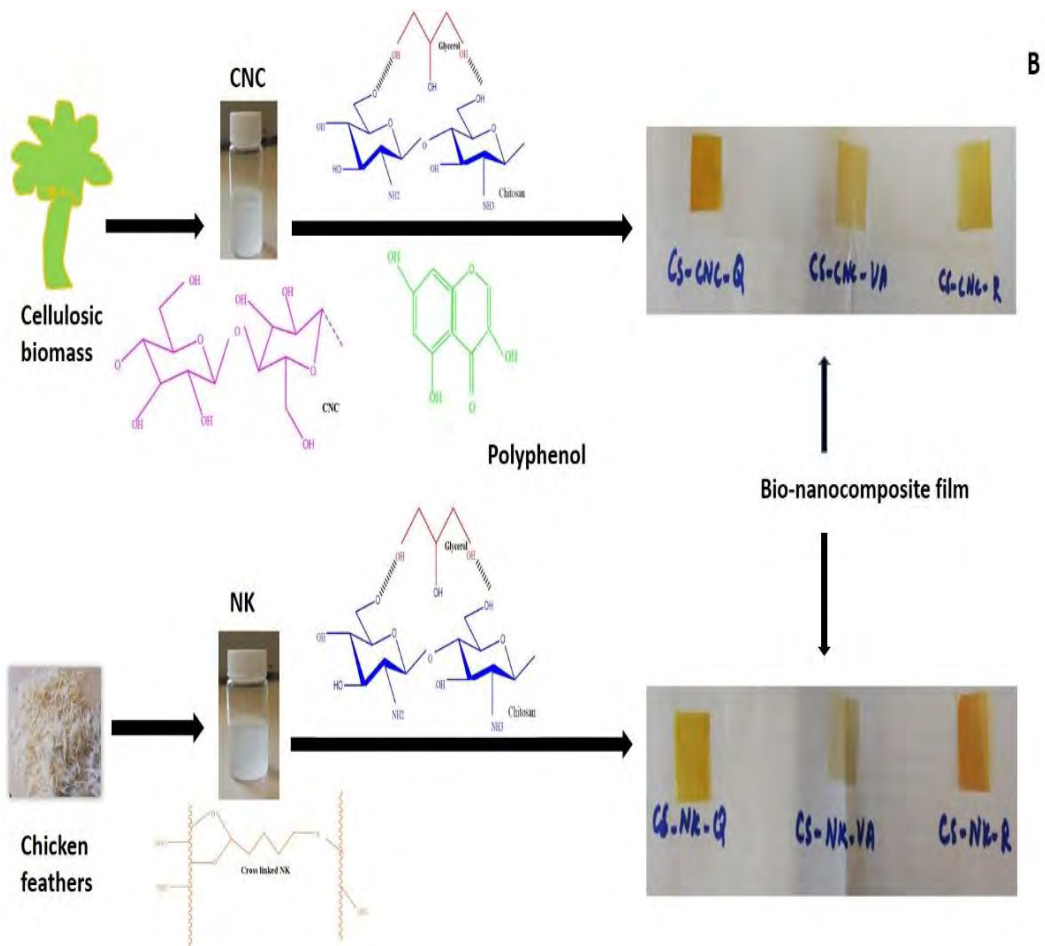
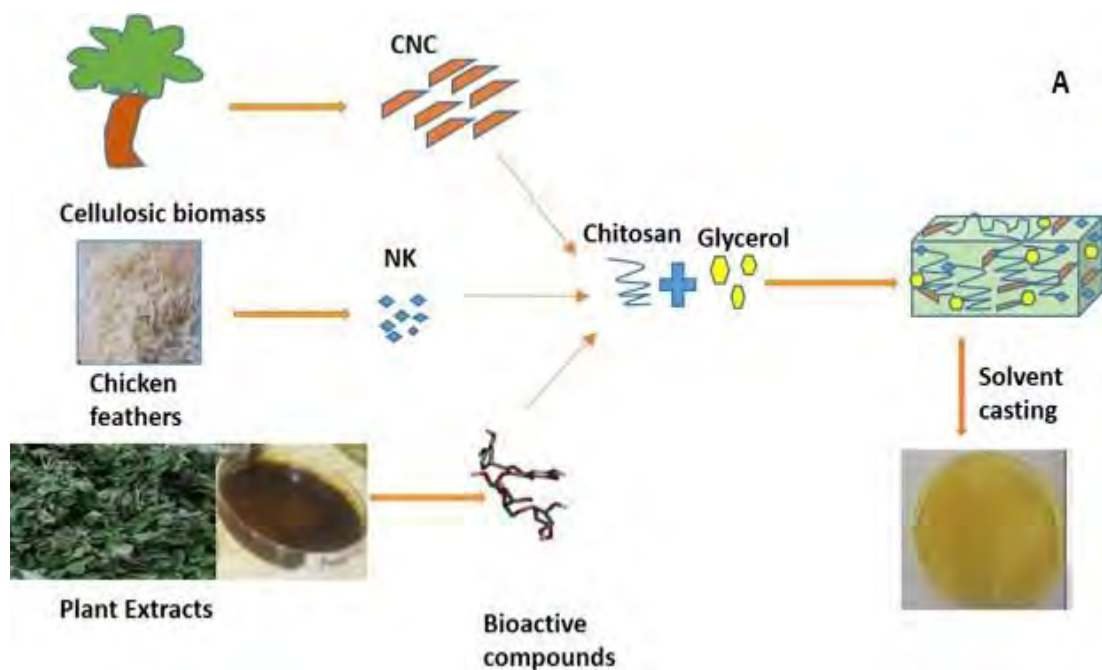
Figure 3.1. Optimization of different components of chitosan films

- a): glycerol%, b): CNC%, c): NK %, d): *C. tamala* (EX1) %
 e): *A. subulatum* (EX2) % and f): *M. piperita* (EX3) %

(c). Extract Optimization

Three different plant extracts (*C. tamala*, *A. subulatum*, *M. piperita*) were optimized for use as additives in chitosan composite films. Each extract was mixed at a concentration of 0.5%, 1% and 1.5% to check at which concentration best mechanical strength is achieved (Fig 3.1). 1.5% was found to be the best for *M. piperita* (EX3) and 1% concentration for *C. tamala* and *A. subulatum* i-e (EX1 and EX2) to be used in all film blends.

The below schematic representation (Fig 3.2) shows step wise synthesis of (a) extract and (b). polyphenol incorporated Chitosan nanocomposites films.



3.2 Schematic representation of film preparation

3.3.2 Physical, mechanical and barrier properties

(a). Film Thickness

All films thickness was found in the range of 0.08-0.12 mm. The photographs of extract loaded and polyphenol loaded films are given as under (Fig 3.3).

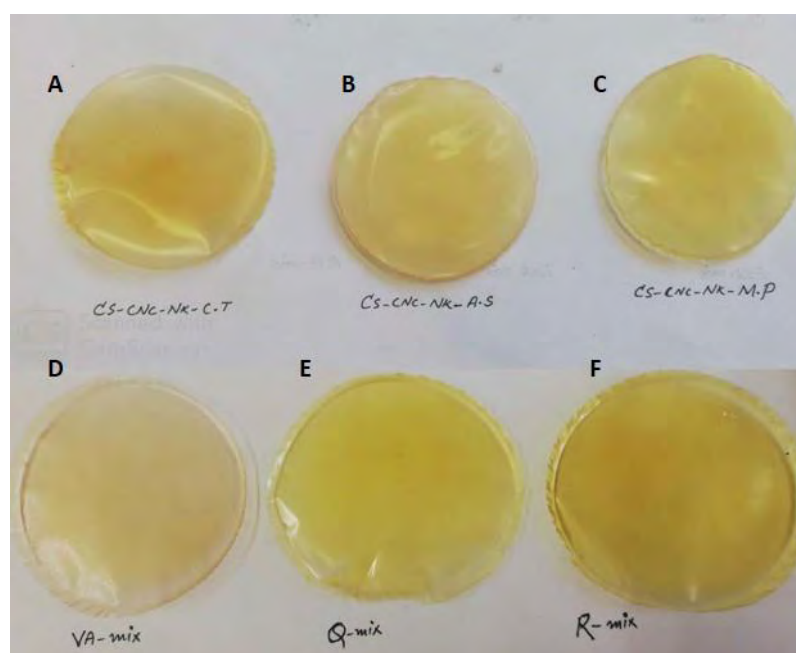


Fig 3.3 Photographs of prepared films (a), (b) and (c). Extract incorporated films, (d), (e) and (f). polyphenol incorporated Chitosan films reinforced with CNC/NK.

(b). Mechanical testing of extract loaded films

Predominantly, films with 3% CNC-CS demonstrated significantly high T.S (65.5 Mpa) when compared with CS-control films (44.6 Mpa) and CS-NK films (53.2 Mpa). However, % E was seen to be gradually increased by addition of nano-keratin to chitosan in CS-NK films. After optimization, 20% glycerol, 3% CNC, 0.3% NK, 1.5% *M. piperita* and 1% *C. tamala* and 1% *A. subulatum* (as shown in Fig 3.1) were used in all blends. T.S of chitosan nano-composites was increased (61%) by adding CNC in chitosan films blended with extracts, although there was no significant effect of NK addition on T.S of Chitosan films incorporated with extract (Table3.1).

Furthermore, synergistic addition of two nano fillers (without extract) was found to decrease the tensile strength (Fig 3.4), however, the addition of extract improved the tensile strength of chitosan films (59%) reinforced by both CNC and NK.

Figure 3.4 Tensile strength (stress) and percent elongation (strain %) of extract incorporated films

Extract incorporated films with both CNC and NK gave better mechanical and barrier testing results while extracts films with one nano filler (either CNC or nano keratin) did not show good mechanical and barrier properties therefore only the results of mixed reinforcement in case of extract incorporated films are discussed.

(c). Mechanical testing of polyphenols loaded films

In case of polyphenol incorporated films, when CNC was added to quercetin/ rutin/ vanillic acid mixed chitosan solution then tensile strength was increased (69%) as compared to chitosan control while % elongation didn't change to a significant extent (Fig 3.5). Contrastingly, nano keratin reinforced polyphenol incorporated chitosan films showed only 38% increase in T.S and % E was decreased as compared to control.

Table 3.1. Mechanical and barrier properties of films

S. N	Films	Thic kness (mm)	Tensile strength (Mpa)	Elongation at break (% E)	WVP (gmm/m ² d k Pa) x10 ²	Opacity
1	Control (CS)	0.09	44.68±4.32 ^c	34.39±5.01 ^b	8.84±0.04 ^d	1.41±0.005 ^g
2	CS-CNC	0.09	65.59±0.90 ^b	24.46±3.21 ^{bc}	5.31±0.02 ^{hi}	2.65±0.005 ^b
3	CS-NK	0.09	53.24±3.03 ^c	20.17±4.68 ^{cd}	8.19±0.11 ^e	1.05±0.005 ^h
4	CS-CNC-EX1-	0.09	68.36±8.09 ^b	18.21±0.15 ^{cd}	6.00±0.116 ^g	1.56±0.005 ^f
5	CS-CNC-EX2	0.09	67.88±1.36 ^b	22.83±2.48 ^{cd}	5.65±0.07 ^{gh}	1.87±0.005 ^{cd}
6	CS-CNC-EX3	0.09	80.11±1.57 ^a	23.82±8.91 ^{bcd}	5.62±0.09 ^h	1.85±0.005 ^d
7	CS-NK-EX1	0.12	50.74±0.76 ^c	59.33±0.33 ^a	12.4±0.26 ^b	1.34±0.005 ^g
8	CS-NK-EX2	0.12	50.71±0.72 ^c	59±0.90 ^a	14.48±0.11 ^a	1.73±0.005 ^e
9	CS-NK-EX3	0.10	42.24±2.56 ^c	49±2.45 ^a	10.4±0.08 ^c	1.05±0.005 ^h
10	CS-CNC-NK-EX1	0.11	65.28±7.78 ^b	20±2.15 ^{cd}	6.58±0.07 ^f	2.73±0.05 ^a
11	CS-CNC-NK-EX2	0.09	70.62±0.98 ^{ab}	13.54±1.66 ^d	5.18±0.01 ⁱ	1.66±0.005 ^e
12	CS-CNC-NK-EX3	0.11	71.24±2.45 ^{ab}	14.94±0.38 ^{cd}	5.08±0.17 ⁱ	1.92±0.007 ^c

^{a-c} Mean of three replicates ± standard deviation. (P > 0.05)

Same column means following same letter are not significantly different

Fig 3.5 Tensile strength (stress) and percent elongation (strain %) of polyphenol incorporated films.

(a).CS (chitosan control), CS-CNC-VA, CS-CNC-Q, CS-CNC-R (b). CS, CS-NK-VA, CS-NK-Q, CS-NK-R

(d). Water vapor permeability (WVP) of extract loaded films

The essential characteristic of a food packaging film is a decreased permeability to water vapors in order to enhance the shelf life. WVP of bio-nanocomposite films ranged from 5.08 to 8.84 (g mm/m²d k Pa x 10²). Presence of extracts in CS-NK films individually enhanced the permeability to water vapors while extract incorporated CS-CNC films exhibited reduction in WVP (Table 3.1). However, when both CNC and NK were blended in chitosan film incorporated with extract, the 42% decrease in water permeability of the bio-nanocomposite film was achieved (especially in case of CS-CNC-NK-EX3 and CS-CNC-NK-EX2) as compared to control.

(e). Water vapor permeability (WVP) of polyphenol loaded films

In current study, all polyphenol incorporated films displayed slightly low WVP (ranging from 6.87 to 8.74 (g mm/m²d k Pa x 10²) as compared to chitosan control films (8.84 g mm/m²d k Pa x 10²) (Fig 3.6). Quercetin incorporated film reinforced by CNC displayed the least WVP followed by VA-CS-CNC films. However, NK reinforced polyphenol loaded films depicted higher WVP as compared to CNC reinforced films.

Fig 3.6 Water vapor permeability and opacity of polyphenol incorporated films

(f). UV Barrier Properties

Opacity values were calculated in order to evaluate film transparency. Higher opacity values indicate lower transparency (Merino *et al.*, 2018). Table 3.1 shows that chitosan control film demonstrated the least opacity (1.41 ± 0.005) (highest transparency). Addition of CNC increased the film opacity to 88% (i.e. 2.65 ± 0.005) while effect of nano keratin addition was not found to be significant. Addition of extract in individual CNC and NK film had no significant effect on opacity. In contrast, when both CNC and nano keratin were mixed with chitosan-extracts film solution their opacity was found to be doubled especially with *C. tamala* (EX1) (2.73 ± 0.05). Extract incorporated films with both CNC/NK displayed negligible UV transmittance as shown in fig 3.7(a).

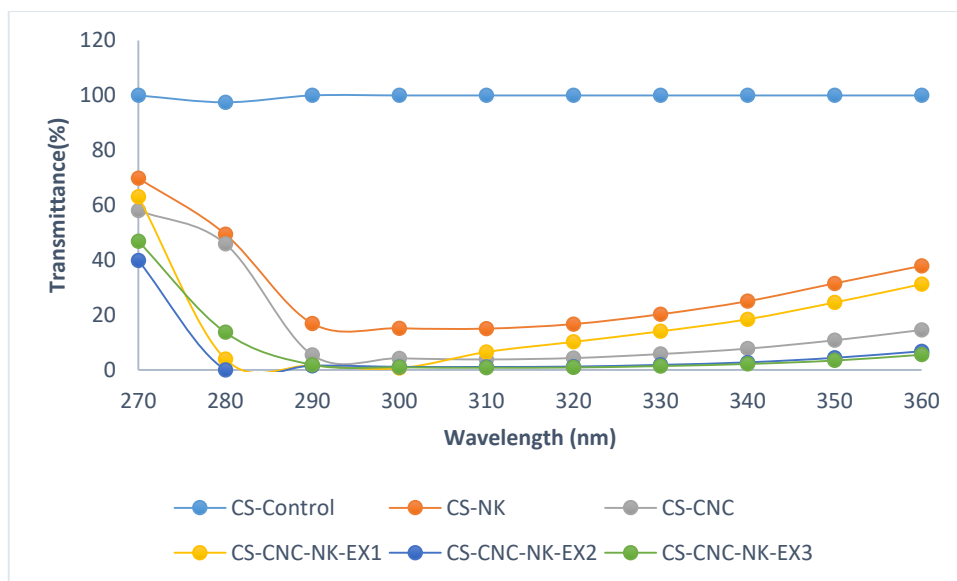


Fig 3.7 UV transmittance of extract incorporated films

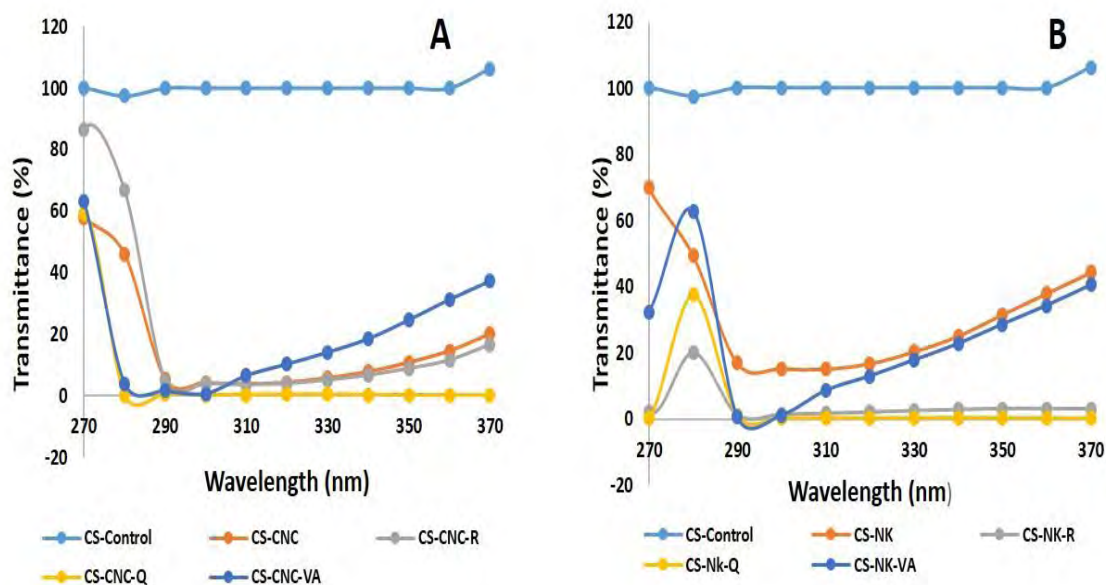


Fig 3.8 UV transmittance of polyphenol incorporated chitosan composites

(a). CNC reinforced and (b). NK reinforced composites

Almost 38% increase in opacity values and negligible UV transmittance was achieved when CNC and quercetin were mixed in chitosan matrix (Fig 3.8a). In contrast, polyphenol incorporated films reinforced by nano keratin were found to have low

opacity as compared to neat chitosan and depicted 19-60% UV transmittance in UV region (Fig 3.8b).

(g). Water solubility, swelling and moisture content of films

The water solubility, moisture and swelling values for the bio-nanocomposite films (incorporating both nano filler and extract) were found to be much lower (17%, 52% and 7.79%, respectively) as compared to control films (20%, 66% and 11.8% respectively). Films with nano-keratin, chitosan and glycerol showed highest moisture content (16.39%) followed by chitosan control films (11.8%). Highest % swelling was seen in case of control chitosan (66%) followed by nano keratin film (56%). However, all films with both nanoparticles and extract demonstrated quite low swelling and least moisture content as compared to control (Fig 3.9a).

Fig 3.9 Percent water solubility, swelling and moisture content (a) CS, CS-CNC, CS-NK, CS-CNC-NK-EX1, CS-CNC-NK-EX2, CS-CNC-NK-EX3 (b) CS, CS-CNC-VA, CS- CNC-Q, CS-CNC-R, CS-NK-VA, CS-NK-Q, CS-NK-R

In case of polyphenol incorporated films, least moisture content was exhibited by CS-CNC-R films. Moreover, CNC reinforced polyphenol incorporated films displayed less water solubility and moisture content as compared to NK reinforced films. Interestingly, the swelling percentage of NK reinforced films was found to be quite low as compared to control and CNC films (Fig 3.9b).

3.3.3 Structural Properties

(a). Fourier Transform Infrared (FTIR) Spectroscopy

All bio-nanocomposite films displayed the representative peaks at 556.6, 1037.9, 1331.7, 1419.4, 1578.6, 1652, 288.5, 2941.5 and 3280.2 cm^{-1} . Hydrogen bonding interactions in CS-CNC-NK-EX composites represent a noteworthy increase in peak intensity and a broader OH peak at 3280.2 cm^{-1} (as compared to control film). Moreover, the intensity and sharpening of the peaks at 1578.6 (Amide II) slightly increased in presence of extracts, particularly in case of EX3. Moreover, C=O stretching vibration as obvious in control film (1648 cm^{-1}), CS-CNC-NK-EX1 (1641 cm^{-1}) and CS-CNC-NK-EX2 (1659 cm^{-1}) was absent in CS-CNC-NK-EX3 film. FTIR results were found in accordance with tensile strength of films as CS-CNC-NK-EX3 film (having highest tensile strength) exhibited higher peak intensity followed by CS-CNC-NK-EX2 (Fig 3.10a).

The main functional group peaks observed in CNC reinforced polyphenol composites were 1024.3 cm^{-1} , 1389.5 cm^{-1} , 1538.5 cm^{-1} , 1626 cm^{-1} , 2893 cm^{-1} and 3264 cm^{-1} respectively (Fig 3.10b). The sharp increase in intensity of OH group vibrations and peak shift from 3341 cm^{-1} (neat chitosan) to 3264 cm^{-1} was found in rutin incorporated CNC reinforced chitosan composite. An increase in intensity, sharpening of amide –II peak and slight shift (1546 to 1538.5 cm^{-1}) was observed in case of all CNC-polyphenol loaded composites. However, NK reinforced polyphenol films depicted peak shifts of OH group vibrations (3341 cm^{-1} to 3291.3 cm^{-1}), C-H stretching vibrations (2893 to 2866 cm^{-1}), amide I vibrations (1603 in neat NK) to 1579 cm^{-1} , Amide III vibrations (1327 in neat NK to 1389.5 cm^{-1}), NH bending (1513 to 1497 cm^{-1}) and C-O stretching vibrations (1024.3 to 1001.4 cm^{-1}) (Fig 3.10c).

Fig.3.10 FTIR analysis

(a). Chitosan control film and Extract loaded CNC and NK reinforced composites (b). CNC reinforced polyphenol composites and (c). NK reinforced polyphenol composites

Moreover, Peak intensity of vanillic acid incorporated NK composites was found to be low as compared to rutin and quercetin which displayed highest intensity and peak shift in case of OH vibration and NH bending.

(b). X-ray Diffraction analysis (XRD)

XRD results disclosed that Chitosan powder had two peaks at 10.9° and 20.8° while after making films second peak was markedly broadened and shifted to 22.6° (Fig 3.11a). Cellulose nano-crystals depicted three specific peaks at $2\theta=15^\circ$, $2\theta=22.4^\circ$, $2\theta=34.6^\circ$ owing to crystalline structure of cellulose. In case of CNC films these peaks were shifted to 9.4° , 20° (i-e characteristic peaks of chitosan) and 26.9° respectively representing both the chitosan and CNC characteristic peaks. However, NK powder displayed two peaks at 9.6° and 19.7° which were shifted to 10.6° and 20.8° during film formation.

Disappearance of CNC and NK own peaks and sharp appearance of characteristic chitosan peaks was noted in XRD analysis. Mixing both the nanoparticles along with extract didn't affect the crystalline structure in case of CS-CNC-NK-EX2 and CS-CNC-NK-EX1 films but most noticeable differences were observed in case of CS-CNC-NK-EX3 films in which at 34.6° particular CNC peak disappeared (showing more dispersion of CNC) and major shift in peak was seen along with appearance of a new peak at 7.05° which shows additional crystallinity regions.

In case of CNC reinforced polyphenol incorporated composites, main chitosan peaks were observed to be shifted to 9.14° and 19.48° (Fig 3.11 b) while all CNC peaks were disappeared. Particularly, in case of quercetin incorporated nanocomposites a new peak appeared at 12.2° is suggested to belong to quercetin.

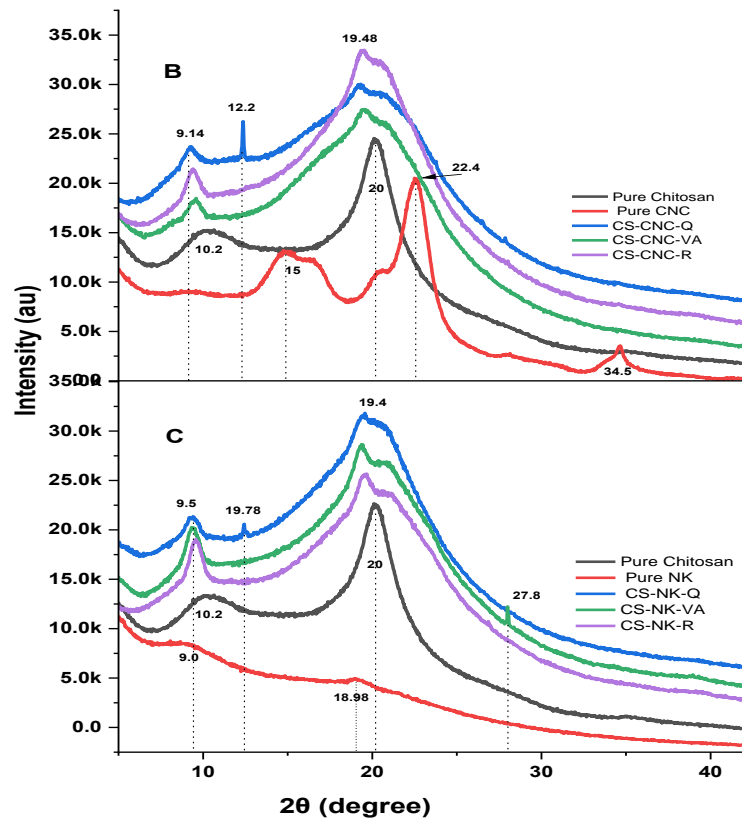


Figure 3.11. XRD analysis

(a). Pure Chitosan, CNC, NK powders, CS film, CNC film, NK film and Extract loaded CNC and NK reinforced composites films. (b). CNC reinforced polyphenol loaded chitosan composites and (c). NK reinforced polyphenol composites.

In case of nano-keratin reinforced composites, chitosan peaks were shifted to sharp peaks at 9.5° and 19.48° (Fig 3.11 c) while both nano keratin peaks (9° and 18.98°) were disappeared displaying the nano keratin dispersion in these films. Interestingly, quercetin and vanillic acid incorporated composites exhibited new peak at 19.78° and 27.8° which shows the presence of additional crystalline portions in these composites.

(c). X-ray Photoelectron Spectroscopy (XPS)

XPS survey displayed the surface elemental composition of bio-nanocomposites and a high resolution C1s spectra to estimate the chemical bonding. It can be seen from survey spectra (Figure 3.12) that chitosan control as well as chitosan reinforced by CNC, nano keratin and extracts exhibited carbon, oxygen and nitrogen as the key elements with binding energy of 284.07, 530.5 and 398.07 eV respectively. All nano-composites exhibited different intensities.

Figure 3.12. XPS Survey spectra of films

Figure 3.13. High resolution C1s spectra

(a). CS-CNC-NK-EX2, (b).CS-NK, (c).CS-CNC (d). CS

Table 3.2 Percent elemental composition of extract incorporated films

Samples	C1s	O1s	N1s
CS	62.39	30.44	5.88
CS-CNC	63.07	29.94	5.38
CS-NK	61.01	29.51	5.91
CS-CNC-NK-EX1	65.14	28.87	4.59
CS-CNC-NK-EX2	61.12	31.42	6.27
CS-CNC-NK-EX3	63.81	27.68	5.05

A gradual increase in carbon was seen by the addition of CNC in chitosan while addition of nano keratin increased the percentage of nitrogen in chitosan bio-nanocomposite (Table 3.2). Gradual increase in oxygen and nitrogen atoms was obvious in case of CS-CNC-NK-EX2.

High resolution C1s spectra (Figure 3.13) reveals that CNC when mixed with chitosan exhibited a surface modification and CS-CNC displayed four peaks at BE 285.17, 283.5, 282.19 and 284.12 eV. However, CS-CNC-NK-EX2 also depicted the presence of an additional peak at 286.98 eV.

(d). Scanning Electron Microscopy (SEM)

Bio-nanocomposites were analyzed by SEM to study the surface morphology and distribution of cellulose nanocrystals and nano keratin in chitosan matrix as depicted in Figure 3.14, 3.15 and 3.16. It can be noticed from SEM analysis that control chitosan film surface exhibited a smooth surface as compared to a rough/irregular surface in all bionanocomposites. The cross-section analysis shows roughness in chitosan nanocomposites incorporated with extracts and polyphenols as compared to neat chitosan control.

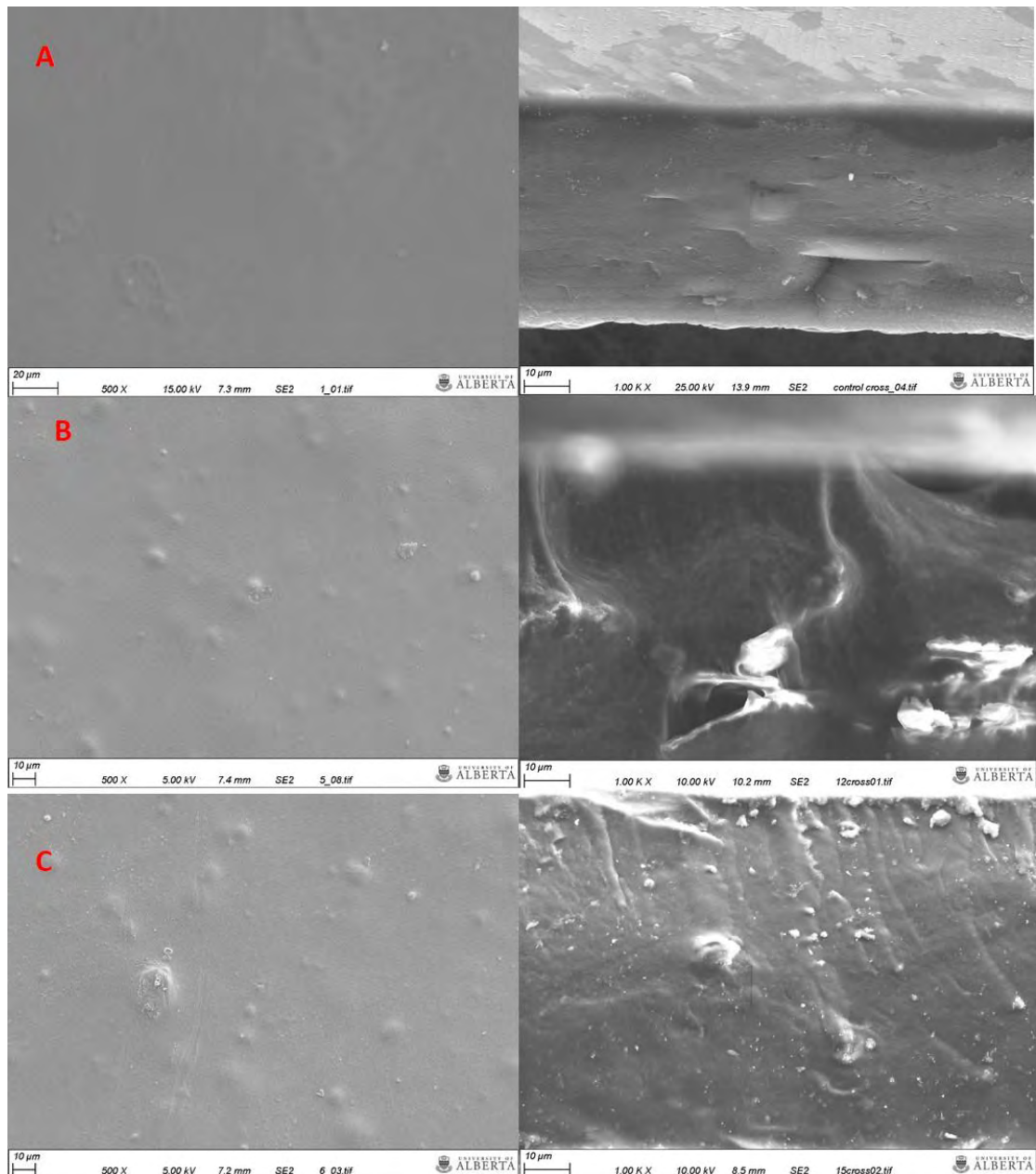


Figure 3.14 SEM analysis of CNC and NK reinforced extract incorporated composites

surface (left) and cross section (right) of
a). CS, b). CS-CNC-NK-EX2, c).CS-CNC-NK-EX3

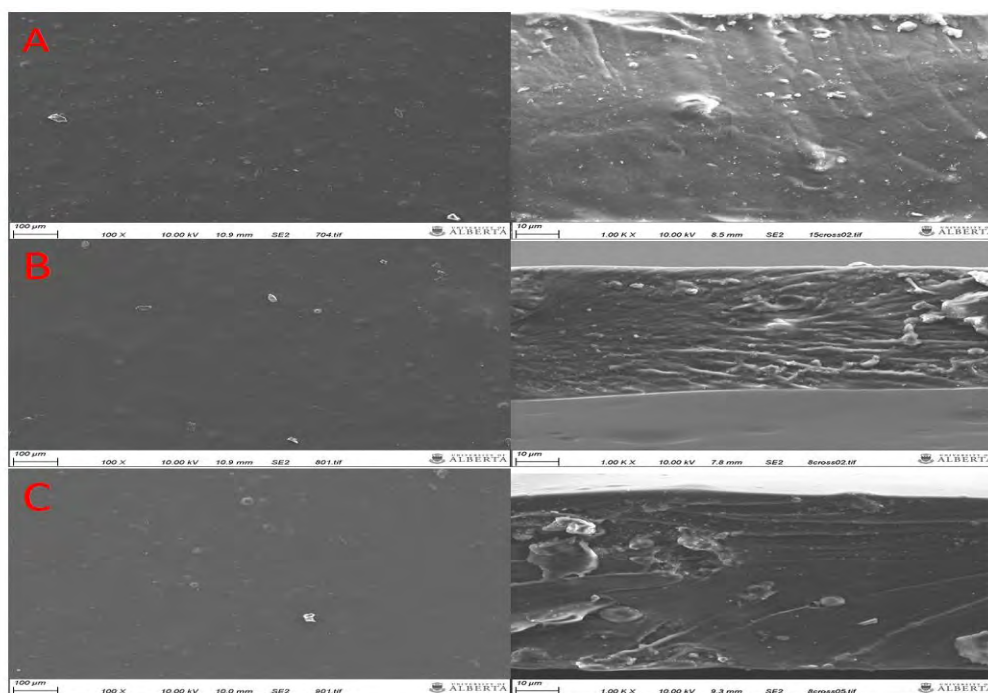


Fig 3.15 SEM analysis of CNC reinforced polyphenol composites

Surface (left) and cross section (right) a).CS-CNC-Q, b). CS-CNC-VA, c). CS-CNC-R

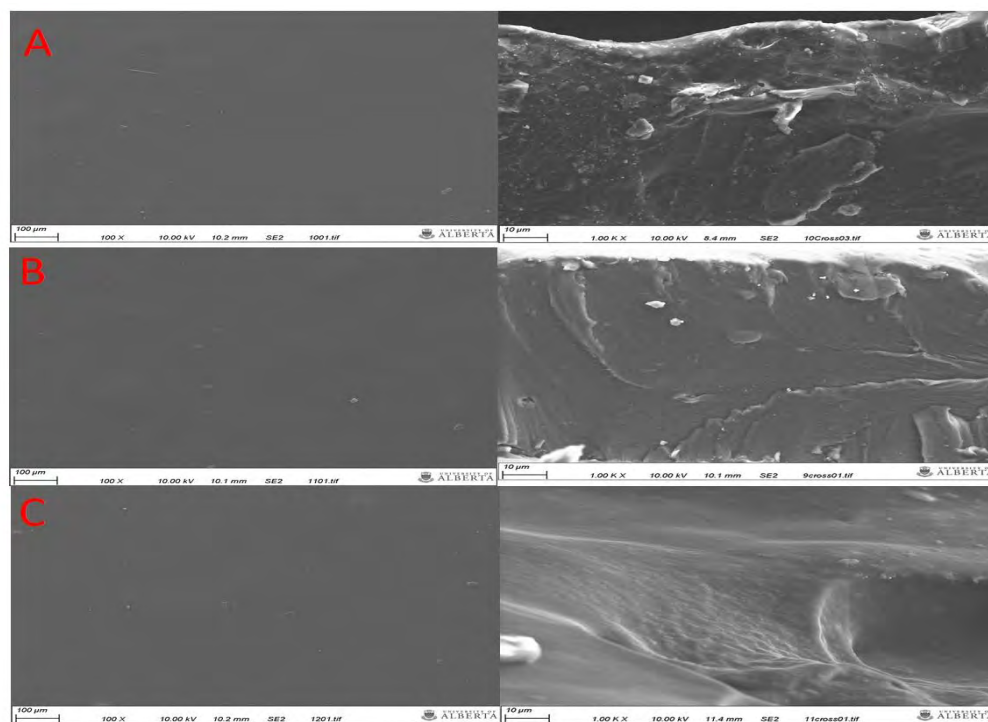


Fig 3.16 SEM analysis of NK reinforced polyphenol composites

Surface (left) and cross section (right) of. a). CS-NK-Q, b). CS-NK-VA, c). CS-NK-R

(e). Transmission Electron Microscopy (TEM)

To observe the incorporation of CNC and NK in matrix and to see the extent of their dispersion TEM analysis was done. Fig 3.17 represents the TEM images of bio-nanocomposites, the clear and dark regions represent both the exfoliation and intercalation of cellulose nanocrystals and nano keratin in chitosan matrix.

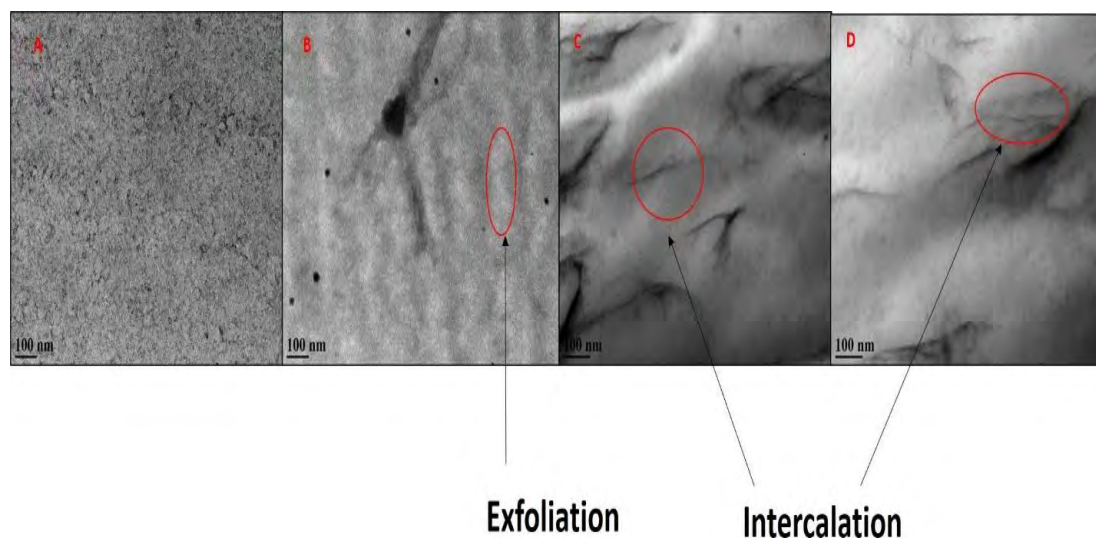


Figure.3.17 TEM analysis

a). CS b). CS-CNC-NK-EX1 c). CS-CNC-NK-EX2 and d). CS-CNC-NK-EX3

Presence of dark lines of CNC threads were seen in both CS-CNC-NK-EX2 and CS-CNC-NK-EX3, however control image does not depict such dark lines. Moreover, both intercalation and exfoliation of CNC and nano keratin was seen in all composites (as marked in Fig 3.17).

3.3.4 Thermal Properties

(a). Thermo-gravimetric Analysis (TGA)

Variations in thermal stability of different chitosan blends were examined as a temperature function by TGA and differential thermo-gravimetric analysis (DTG). All chitosan films exhibited three weight loss points at 50-100 °C, 140 to 395 °C, 395–600 °C respectively.

In case of extract incorporated films, least weight loss was seen in case of CS-CNC-NK-EX3 films. Moreover, 70% weight loss of control films occurred at 275° C while CS-CNC-NK-EX3 composite films displayed 70% loss at a delayed temperature i.e. at

287° C showing the stronger interaction of CNC, NK and EX3. The DTG curve for CS-CNC-NK-EX3 films shows the maximum weight loss at a delayed temperature (293°C) than other nanocomposite films (Fig 3.18)

In contrast, reinforcement by one nano filler (either CNC/NK) showed a delayed temperature peak at 285°C). Effect of individual nano reinforcements of extract incorporated films on thermal stability is not given here as it didn't show significant results.

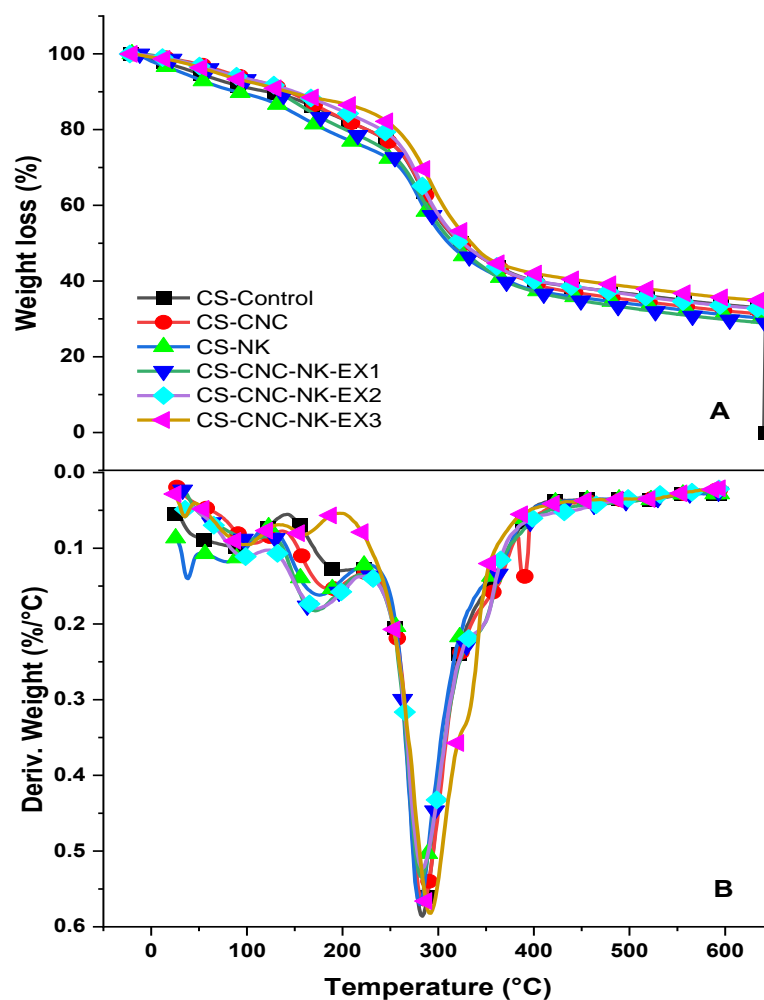


Figure 3.18 TGA Analysis of CNC and NK reinforced extract incorporated composites

(a) TGA, (b) DTG

TGA results of Polyphenol composites indicated that addition of quercetin and rutin increased maximum thermal degradation temperature of chitosan-CNC film (283.1 to 286.9°C) while vanillic acid film displayed T_{max} at slightly lower temperature (Fig 3.19). Polyphenol incorporated CNC films show 70% weight loss at 1°C higher temperature than control. Nano keratin reinforced polyphenol composites also displayed good thermal stability as compared to control (Fig 3.20). Quercetin and vanillic acid incorporated films showed maximum thermal degradation temperature at slightly delayed temperature i.e. 284.2°C. Furthermore, 70% weight loss for polyphenol films was seen at a delayed temperature (281.7°C) as compared to neat chitosan (275 °C). Higher char residue was obtained in case of CS-NK-VA films (34%) showing good thermal stability.

(b). Differential Scanning Calorimetry (DSC)

Films' thermal transition was checked via DSC analysis at 25° C to 300°C. Control chitosan film exhibited two peaks at 109° C and 210° C (endothermic) and peak at 293° C (exothermic). Figure 3.21 (a) shows that both nano filler blended films depicted delayed moisture peak (120°C and 150°C) in case of CS-CNC-NK-EX3 and CS-CNC-NK-EX2 respectively). As higher T_m (i.e. 250°C) was achieved for CS-CNC-NK-EX3 and CS-CNC-NK-EX2 films. However, reinforcement with one nano filler (either CNC/NK) in presence of extract was not found to have significant differences in T_m .

Figure 3.19 TGA Analysis of CNC reinforced polyphenol composites.
(a) TGA, (b) DTG

Figure 3.20. (a) TGA Analysis of NK reinforced polyphenol Composites.
(a) TGA, (b) DTG

DSC analysis of CNC reinforced polyphenol films (Fig 3.21b) depicted that quercetin/ rutin/ vanillic acid incorporated films reinforced by CNC showed a delayed moisture peak (109°C in control film to 113°C in polyphenol incorporated film) melting at lower temperature (204°C in CS film to 181.8°C in CS-CNC-Q film) was observed in all composites. Similarly, DSC analysis of nano keratin reinforced polyphenol films also displayed a slightly more reduction in T_m (175.7°C) (Fig 3.21 c).

Therefore, extract incorporated films reinforced with both nano filler (CNC & NK) were found to be more thermostable than polyphenol loaded composites.

Fig.3.21. DSC analysis

(a) CS, CS-CNC, CS-NK, CNC and NK reinforced extract incorporated composites (b). CNC reinforced polyphenol composites and (c). NK reinforced polyphenol composites

(c). Dynamic Mechanical Analysis

The films' viscoelastic behavior was observed via DMA, suggesting that how storage modulus and tan delta varies with temperature. Fig 3.22 (a) depicts that the storage

modulus (E') values steadily drop in all blends which is the characteristic of the thermoplastic materials. The EX3 incorporated chitosan film (i.e. CS-CNC-NK-EX3) exhibited at higher value of storage modulus (E') as compared to other blends. An improvement in glass transition of all blends was seen as evident from fig. 3.22 (b). Particularly, CS-CNC-NK-EX3 films exhibited two transition peaks at 25°C and 170°C as compared to 0°C and 140°C of control, thus represented higher stability of synthesized films.

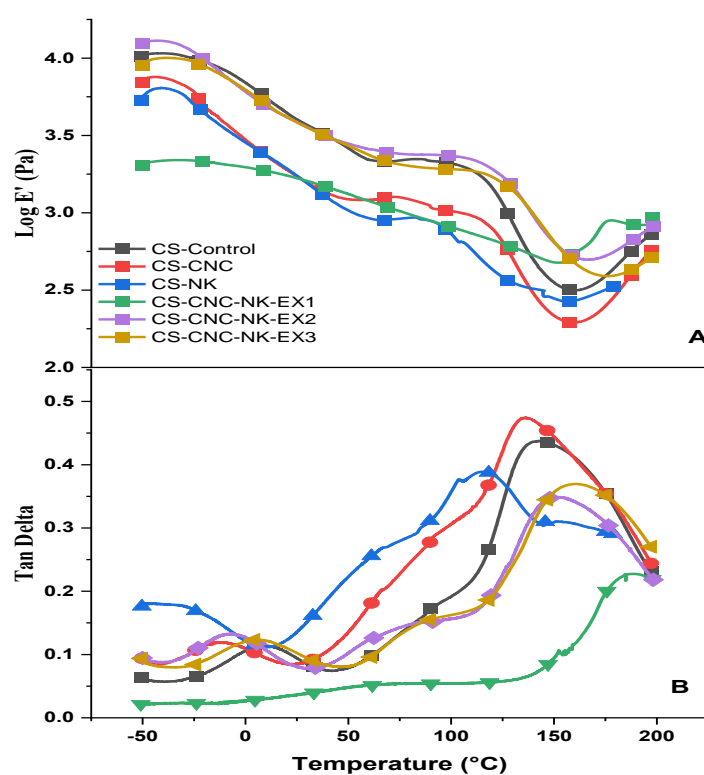


Figure 3.22. DMA Analysis

(a) Effect of temperature on $\log E'$ and (b) $\tan \delta$ of CS, CS-CNC, CS-NK, CS-CNC-NK-EX1, CS-CNC-NK-EX2 and CS-CNC-NK-EX3 Composites.

3.4 Conclusion

Present experimental findings suggest much improved properties of synthesized composites as compared to chitosan control. Mechanical analysis results showed that extract loaded films reinforced with both nano fillers showed 59% increase in tensile strength of chitosan films. However, a remarkable increase of 63% was seen in T.S of CNC reinforced polyphenol composites. Extract incorporated films depicted excellent barrier properties (42% decrease in WVP), a two-fold increase in opacity, an enhanced thermal stability and glass transition temperature as compared to neat chitosan films. Polyphenol composites displayed only 22% decrease in WVP and 38% increase in opacity. Extract loaded composites were found to be more thermally stable as compared to polyphenol composites. Among all blends, *M. piperita* incorporated films reinforced with both CNC and NK and Quercetin incorporated films reinforced with CNC were found to exhibit best mechanical, thermal and barrier characteristics.

***In vitro* Biological Activities of**
Phyto-assisted Chitosan
Nanocomposites

(Chapter # 4)

4.1 Introduction

Problems of food poisoning and spoilage by either micro-organisms or UV rays are causing a vulnerable threat to human health and safety (He *et al.*, 2020). In an effort to overcome these detrimental effects, scientists have been continuously making several attempts to inhibit microbial growth and oxidative damage through the use of antibacterial chemical agents, antibiotics and synthetic antioxidants (Cai *et al.*, 2022). However, microbial resistance by antibiotics has gradually limited their widespread use and synthetic antioxidants also seem to be rejected by consumers due to their toxicological concerns (Akarca, 2019). Therefore, active packaging carrying natural antimicrobial and antioxidant substances have gained consumer's attention as they lack drug resistance and are nontoxic to use (Hu *et al.*, 2019).

The main aim of the active packaging is to improve food quality and shelf life. The active agents inside the packaging film act as free radical scavengers or in activators of deleterious organisms by exerting either antioxidant or antimicrobial effect (Leistner, 2000). Biological polymers made of carbohydrates, proteins etc. (chitosan, cellulose, keratin etc.) and natural plant extracts are successfully used in the preparation of packaging films and coatings. Green plant extracts are mostly composed of diverse variety of polyphenols, flavonoids and alkaloids which once incorporated in the polymer matrix can exert their antioxidant/antimicrobial effect by slowly releasing these compounds into the film environment (Pisoschi *et al.*, 2018). Polyphenols are the plant compounds possessing an aromatic ring with two or more hydroxy group substituents and mostly found in fruits and vegetables, red wine, black tea, coffee, chocolate and olive oil etc. These polyphenols are safe to use and can be directly used as an additive in food industry. Several studies have been carried out to incorporate plant extracts as well as commercially available plant polyphenols in biopolymer-based packaging films to act as anti-microbial, antioxidant as well as cross linking agent (Zhang W. *et al.*, 2021). In context of chitosan films, pine apple peel polyphenols (Jatav *et al.*, 2022), tea polyphenols (Gao L. *et al.*, 2021), potato peel polyphenols (Ma *et al.*, 2022), Quercus polyphenol extract (Oberlintner *et al.*, 2021) has been added recently. To assess food quality, a beef fillet shelf life was found to increase when packaged with an active chitosan film incorporated with poly lysine (Alirezalu *et al.*, 2021). Magnolol,

classified as lignin, was incorporated in chitosan film and these active films were found to inhibit microbial growth when applied for chilled pork preservation (Song *et al.*, 2021). In another study, sensory attributes of baby carrots were evaluated by dipping/spraying them with chitosan films solution (Leceta I *et al.*, 2015). Moreover, apple peel polyphenol incorporated novel chitosan coating was found to affect the storage of fresh strawberry by causing a 19% decrease in sample weight loss during storage period (Riaz *et al.*, 2021).

In same contribution, the synthesized chitosan films reinforced with CNC and NK and incorporated with selected plant extracts (*C. tamala*, *A. subulatum* and *M. piperita*) and polyphenols (quercetin, rutin, vanillic acid) were evaluated for their antioxidant and antimicrobial properties. Moreover, their effect on food quality was assessed by packaging baby carrots with these films. The effect of synthesized films on physical and sensory properties of packaged carrots was checked.

4.2 Materials and Methods

4.2.1 Total Phenolic Acid Content

Total phenolic content of films was observed using previously reported method with some modifications (Xu *et al.*, 2018). Film samples (10 mg) were cut in 1cm x1cm squares, placed in 1 ml acetic acid and stirred for 24 hours. 10 μ l aliquots of film solution was added to 10 fold diluted Folin–Ciocalteu reagent. Following 5 minutes' incubation, 98 μ l sodium carbonate (6%) was mixed and after incubation of 90 min at 25° C absorbance was recorded at 630 nm wavelength on a microplate reader. TPC was determined as μ g of gallic acid equivalents per mg of film.

4.2.2 Antioxidant activity

Antioxidant activity of extract and polyphenol loaded nano reinforced chitosan films was checked by DPPH assay using previously reported method (Khan *et al.*, 2021). Film samples (10 mg) were cut in 1cm x1cm squares, placed in 1ml acetic acid and stirred for 24 hours. Briefly, 190 μ l of DPPH (2 mg DPPH/ 50 ml methanol) was poured in each well of 96 well plate and then 10 μ l aliquot of film solution was mixed with DPPH solution in each well. The 96 well plate was then incubated for 30 min at 37°C

in dark. Absorbance was recorded at 517 nm on a microplate reader (Biotech, Elx-800, USA). DPPH discoloration from purple to yellow color was used to assess free radical scavenging activity of films. Ascorbic acid and acetic acid mixed with DPPH was used as positive control and negative controls respectively. Triplicates of each sample were recorded for DPPH activity.

4.2.3 Anti-bacterial activity

The antibacterial activity was assessed using disc diffusion assay (Ahmed *et al.*, 2017). The test bacterial strains cultures (i.e. *Bacillus subtilis* (ATCC-6633), *Staphylococcus aureus* (ATCC-6538), *Pseudomonas aeruginosa* (ATCC-15442) and *E. coli* (ATCC-25922) were obtained from the Pharmacy department, Quaid-i-Azam University, Islamabad, Pakistan. Each bacterial strain (100 µl) was streaked on nutrient agar respectively for antibacterial assay. Films (cut in equal circular discs) were directly placed on inoculated agar medium. Moreover, positive control (Ciprofloxacin, 20 µg/mL), and 1% acetic acid (negative control) were employed on agar plates and incubated (24 h; 37°C). Afterwards, plates were observed for particular antibacterial zones of inhibition (mm) on specific time intervals. Ciprofloxacin was used as positive control.

4.2.4 Anti-fungal activity

The antifungal activity of extracts was evaluated by the agar disc diffusion method (Ahmed *et al.*, 2017). The spores of test fungal strains *Fusarium solani* (FCBP- 0291), *Mucor* species (FCBP-0300), *Aspergillus niger* (FCBP-0198), and *Aspergillus flavus* (FCBP-0064) were procured from the department of Pharmacy, Quaid-i-Azam University, Islamabad, Pakistan. These strains were collected in solution (0.02% v/v tween 20 in H₂O) and the turbidity was adjusted according to McFarland 0.5 turbidity standard. Then, fungal strain (100 µL) was streaked on sabouraud dextrose agar. Films were cut in equal circular discs with a hole puncher and directly placed on inoculated agar medium. Terbinafine (20 µg/mL) used as positive control and 1% acetic acid as negative control were also employed on agar plates. Plates were incubated at 28 °C for 24–48 hours. Afterward, the average diameter (mm) of the growth inhibition zone around all the discs was measured and recorded.

4.2.5 Food quality analysis

Effect of synthesized films on food quality was judged by previously reported method (Leceta I *et al.*, 2015). Baby carrots were purchased from Canadian superstore at the analysis day. Each carrot was packed with polyphenol loaded chitosan films (by cutting films in the same size as that of carrots) for 5 days at room temperature. Experiment was performed in triplicates. Carrots packaged with commercially available packaging film worked as positive control whereas uncoated carrots were termed as negative control. Weight of carrots was noted at day 0 and day 7 and these were photographed to measure changes in color and texture.

4.3 Results

4.3.1 Total polyphenol content

Determination of total polyphenol content of films was used to evaluate and verify the incorporation of extract/polyphenol in the films. Fig 4.1(a) shows that chitosan control films exhibited negligible polyphenol content as compared to extract films. Moreover, *M. piperita* incorporated chitosan films displayed highest TPC which clearly shows increased entrapment of polyphenols in chitosan matrix in these films.

Fig 4.1(b) shows that Chitosan control, CNC and NK films exhibited least polyphenol content as compared to polyphenol composites films. Highest TPC was found in quercetin incorporated CNC films followed by rutin incorporated CNC films. However, NK reinforced films depicted least TPC suggesting decreased polyphenol entrapment in these films.

Total phenolic content of these composite films came out to be directly related to their DPPH scavenging potential. Films showing higher total phenolic content also displayed strong antioxidant potential.

Fig.4.1 Total polyphenol content and DPPH activity of films

(a) Extract incorporated films (b) Polyphenol incorporated films

4.3.2 Anti-oxidant activity

Fig 4.1(a) shows that chitosan control exhibited some scavenging activity (22%) however extract films displayed highest (70%) DPPH free radical scavenging. Among all composites, *M. piperita* incorporated extract (CS-CNC-NK-EX3) films were found to have greater antioxidant activity than other films. Fig 4.1(b) shows that both CNC and nano keratin alone did not show significant effect on antioxidant potential but when mixed with polyphenols these films exhibited good free radical scavenging ability. Specifically, quercetin when mixed with chitosan and CNC showed strong scavenging potential (70%) followed by CS-NK-Q (57%) and CS-CNC-R (53%).

4.3.3 Antibacterial activity

Extract and polyphenol incorporated films were screened against four bacterial strains i-e *S. aureus*, *B. subtilis* (Gram positive strains), *E. coli* and *P. aeruginosa*, (Gram negative strains). *M. piperita* (EX3) and *A. subulatum* (EX2) incorporated films displayed antibacterial activity against *B. subtilis* and *P. aeruginosa* strains and slight activity against *S. aureus* was exhibited by *A. subulatum* films. Interestingly, no activity was shown against *E. coli* by any of the composites. Among CNC and NK reinforced polyphenol films, Quercetin and rutin incorporated CNC composites exhibited moderate antibacterial activity against *P. aeruginosa* (Fig.4.2). Vanillic acid composites displayed activity against *B. subtilis*. However, NK reinforced films didn't display antibacterial activity against any of these strains. Antibacterial zones of representative samples are shown in fig 4.3.

4.3.4 Antifungal activity

All films were screened for antifungal activity against four fungal strains i-e *A. flavus*, *A. niger*, *Mucor species* and *F. solani*. In case of extract incorporated films reinforced with CNC and NK, good antifungal activity was exhibited by *A. subulatum* (EX2) incorporated films against *Mucor* and *A. flavus*. *C. tamala* (EX1) films also showed activity against *A. niger* (Fig 4.2).

Fig 4.2. Anti-bacterial and antifungal Zone of inhibition (mm) of films

In case of polyphenol incorporated composites, quercetin incorporated CNC reinforced composites showed inhibition against all tested strains (with an exception of *A. flavus*) (Fig.4.2). Rutin incorporated CNC reinforced composites exhibited activity against *Mucor spp.* and *A. flavus*. However, none of the extract or polyphenol incorporated composites showed inhibition against *F. solani*. Antifungal zones of representative samples are shown in figure 4.4.

4.3.5 Relationship analysis between DPPH scavenging and antimicrobial activity

Antibacterial activity of extract incorporated films was found to correlate with DPPH scavenging results. Since film showing highest DPPH scavenging potential (i-e CS-CNC-NK-EX3) depicted highest inhibitory zone against *P. aeruginosa* and *B. subtilis*. Same correlation was seen in antibacterial activity of CS-CNC-Q & CS-CNC-R films against *P. aeruginosa*.

In antifungal assay, CS-CNC-NK-EX2 film (showing 2nd highest scavenging potential i.e. 67%), CS-CNC-Q & CS-CNC-R films (showing 70% &53% DPPH scavenging respectively) exhibited highest inhibitory zones against *A.flavus* and *Mucor spp.*

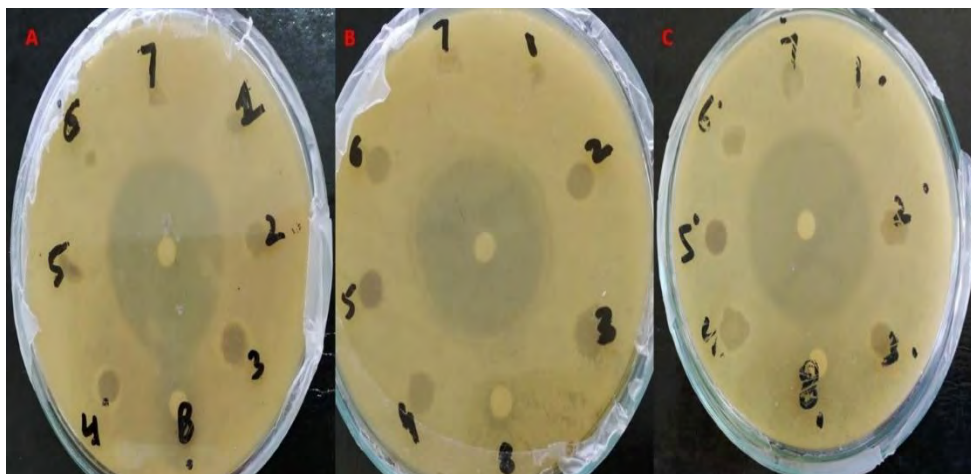


Fig 4.3 Plates showing Antibacterial zones of films

a). *B. subtilis* (b). *S. aureus* (C). *P. aeruginosa* (1,2 and 3 are CS-CNC-NK-EX1, CS-CNC-NK-EX2 and CS-CNC-NK-EX3 films 4,5,6 are CS-CNC-VA, CS-CNC-Q and CS-CNC-R films, 7 is CS control film) and 8 is 1% acetic acid.

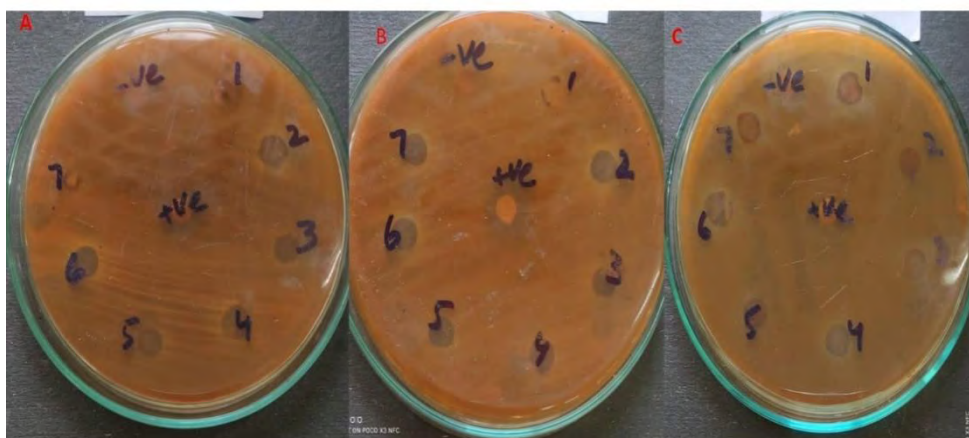


Fig 4.4 Plates showing Antifungal zones of films

(a). *Mucor sp.* (b). *A. Flavus* (c). *A. niger*

1,2 and 3 are CS-CNC-NK-EX1, CS-CNC-NK-EX2 and CS-CNC-NK-EX3 films 4,5,6 are CS-CNC-VA, CS-CNC-Q and CS-CNC-R films, 7 is CS control film)

4.3.6 Food quality

To analyze the packaging effects of synthesized films, baby carrots were coated with film pieces. Changes in physical appearance and weight were determined over a 7 day period.

Fig.4.5 Percentage weight loss of baby carrots packaged with extract incorporated films

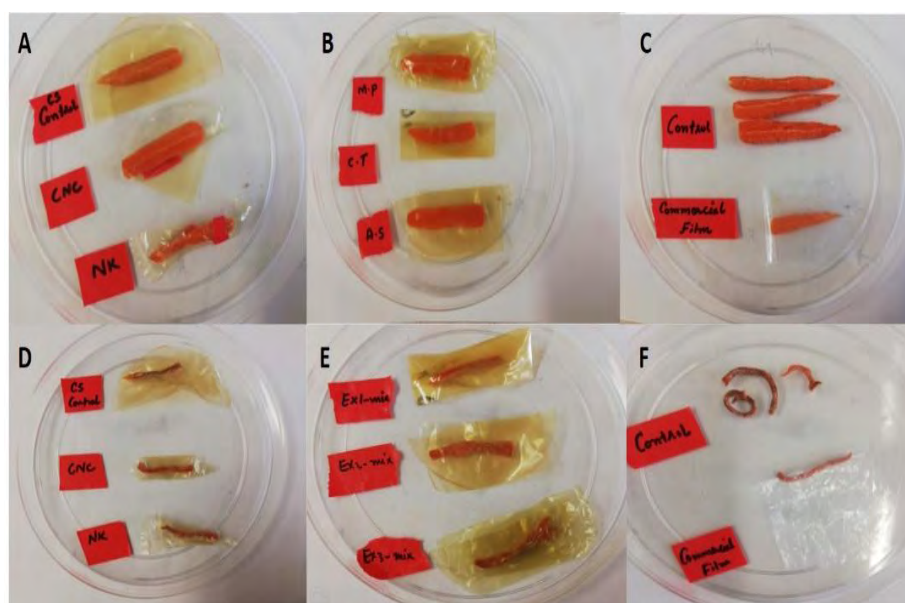


Fig 4.6 Baby carrots packaging with extract incorporated films
(a) (b) and (c) at day 0; (d), (e) and (f) at day 7

With the progression of storage time the weight loss of quercetin incorporated chitosan films and *M. piperita* incorporated films was found to be less as compared to control chitosan and commercial coatings shown in figure 4.5 and 4.7. It is evident from the physical appearance of carrots after 7 days of storage that carrots packed with extracts and polyphenol nanocomposite films were having better acceptability and appearance than control as shown in Fig 4.6 & 4.8.

Fig.4.7 Percentage weight loss of baby carrots packaged with polyphenol incorporated films

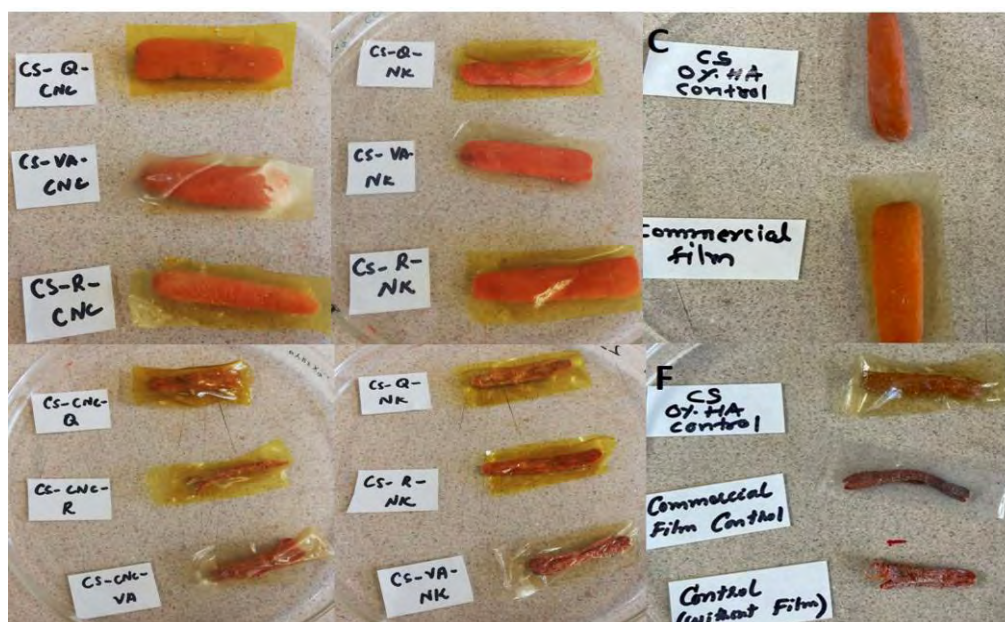


Fig 4.8 Baby carrots packaging with polyphenol incorporated films

(a) (b) and (c) at day 0; (d), (e) and (f) at day 7

4.4 Conclusion

In vitro biological assays were carried out to confirm the biological applications of synthesized nanocomposite films. Our results show that both extract and polyphenol films exhibited higher polyphenol content as compared to control which indicates incorporation of extract/polyphenol in the synthesized films. The films having higher TPC were found to have higher antioxidant activity. Very promising results were obtained for antioxidant activity of synthesized films (i.e. 70 % free radical scavenging) however the antimicrobial activity of films was found to be moderate. Specifically, *M. piperita* and quercetin incorporated nanocomposite films displayed best DPPH scavenging and provided least weight loss of baby carrots while determining the food quality. Overall, in vitro analysis of synthesized chitosan phyto-assisted nanocomposite films suggested their applications for improving antioxidant, antimicrobial properties and thus they can be helpful in extending shelf life of food products.

Biodegradability and Toxicity

(Chapter # 5)

5.1 Introduction

Plastic waste induced pollution has recently caused a trend of using biodegradable polymers for food packaging. Chitosan, obtained from de-acetylated chitin, has gained much attention in this regard due to its bio-compatibility, biodegradability and non-toxicity (Oberlintner *et al.*, 2021). However, its hydrophilic characteristics like high water vapor permeability (Aguirre-Loredo *et al.*, 2016) has led researchers to use blend films (i-e chitosan with nano reinforcements and plant extract addition) for improved packaging.

Biodegradability and toxicity are the main concerns while synthesizing blend films for food packaging. Chitosan based products are extensively studied for degradation in human body as well as in biomedical uses (Matica *et al.*, 2017). There are reports on chitosan degradation in aquatic environment, however, degradation mechanism in terrestrial environment is still not fully known. Heat, stress, UV rays, hydrolysis, oxidation and biological processes can cause degradation of chitosan as reported earlier (Prashanth *et al.*, 2005). Therefore, environmental conditions, chemical interactions within polymeric complex and type of microorganism can affect the degradation process. Chitosan film degradation may take few weeks to months entirely depending on its molecular weight, degree of acetylation, relative environmental humidity, type of acid and crosslinking agent used etc. The bio-degradation of composite/blend films comprise on degradation by hydrolysis followed by microbial attack on fragmented films and their conversion into biomass, carbon dioxide and water. So far more than 90 species of bacteria and fungi have been discovered that can degrade the plastics (Gan *et al.*, 2021). Recently, *Ophiocordyceps heteropoda*, *E.roggenkampii* and *Enterobacter kobei* has been reported as the chitosan composite film degrading microbes (Gan *et al.*, 2021). Moreover, the effect of cross linkers such as glutaraldehyde has also been reported to decrease the chitosan film weight loss percentage in a soil assay, probably due to greater stability of cross linked films owing to formation of imine linkage (Pavoni *et al.*, 2021). Therefore, biodegradability of packaging films may vary depending on raw materials, chemical modifications and final chemical structure of composite films (Rujnić-Sokele & Pilipović, 2017). The biodegradability can be assessed by keeping the films in industrial/garden soil and determining the weight loss

of films during the burial period as a measure of biodegradability (Oberlintner *et al.*, 2021). The analysis of biodegraded chitosan films has pronounced importance in designing drug delivery systems. For this purpose, lysozyme (found in body fluids) also represents a good fit to evaluate in vitro degradation of chitosan as chitosan is reported to degrade in human body by lysozyme (Lončarević *et al.*, 2017).

Inside the gastro intestinal tract, chitosan-based nanocomposites may undergo several alterations due to mechanical, ionic and acidic conditions in the stomach. Once in intestine nanostructures commence to breakdown by raising pH allowing the loaded components to be absorbed. Nanocomposites may be absorbed in GIT depending on the size, shape and surface characteristics. Nanoparticles of size <400 nm can pass through mucosal epithelial cells and cationic chitosan composites can be absorbed due to mucus negative charge. This may result in inflammation, oxidative stress due to nanoparticle build up (Zhang & Chen, 2019). Similarly, CNC (200-300 nm) may have prolonged blood circulation and delayed clearance by macrophage system (Mahmoud *et al.*, 2010). Though the chitosan exhibit in situ gelling, biocompatibility, muco-adhesion, hydrophilic character and cellulose shows low toxicity (Zhang & Chen, 2019), the composite films comprising of chitosan with even plant bioactive agent, CNC or any other nanoparticle must be checked for their in vitro and in vivo toxicity. Humans and rodents cell lines from liver, skin and lungs are often used as in vitro models to evaluate cytotoxicity. However, in vivo experiments are mostly done in rats, rabbits and even human volunteers to determine body response to nanocomposites (Zhang & Chen, 2019). For example, chitosan subcutaneous doses (5 to 50 mg/kg/day) have been reported to induce cytotoxicity in rabbits and dogs however, oral chitosan dose up to 6.75 g/day displayed no clinical side effects in human volunteers (Jain & Jain, 2015).

Considering above mentioned importance, the biodegradability of synthesized chitosan nanocomposites was carried out by soil assay and lysozyme assay. Moreover, in vitro toxicity of films was evaluated by hemo-compatibility test and oral dose of films was given to rats to determine in vivo toxicity.

5.2 Materials and methods

5.2.1 Materials

Lysozyme (source: chicken egg white) was bought from Sigma Aldrich. Sodium chloride, sodium bi phosphate, potassium phosphate and potassium chloride for preparation of phosphate buffer saline were purchased from Sigma Aldrich. Formalin (10%), Saline (9%), purple and yellow top tubes were used for blood collection.

5.2.2 Bio-degradation studies

(a). Soil biodegradation assay

The biodegradability of prepared films was assessed by previously reported composting test (Oberlintner *et al.*, 2021). The soil was obtained from Dollar store (Edmonton, Canada). In a plastic tray, 250 g soil was placed and pre-weighed film samples (2cm x 2cm) were buried far from each other at 3 cm depth for 2 weeks. After day 7th and 14th, the films were taken out and their weight loss was calculated.

(b). Lysozyme degradation assay

Degradation of prepared films in lysozyme was checked by following a previously reported procedure (Lončarević *et al.*, 2017). Small pieces of films (1cm x 1cm) were weighed (initial weight= w_i) and soaked in lysozyme/PBS solution (1mg/ml) for two weeks at 37°C. After 7 and 14days film pieces were taken out and oven dried at 105°C until constant weight was achieved (final weight= w_f).

The relative soil and lysozyme degradation was calculated by using following formula.

$$D(\%) = \frac{w_i - w_f}{w_i} * 100 \quad \text{Eq.5.1}$$

5.2.3 Toxicity analysis

(a). In-vitro toxicity

Hemo-compatibility analysis was performed following a recently reported method (Kaczmarek *et al.*, 2019), to check the in vitro toxicity on RBCs. 3 ml fresh venous blood was collected from human volunteers and centrifuged for 10 minutes at 3000 rpm. Three times washing of pellet with phosphate buffer saline (pH 7.4) was carried

out via centrifugation. Afterwards, a 10 % v/v suspension of pellet was prepared in PBS referred as RBC suspension. To study the impact of synthesized films on red blood cells (RBCs), washed RBCs were treated with PBS solution containing films in the form of squares (0.5cm × 0.5 cm). The samples were incubated for 1 hour at 37°C followed by centrifugation at 1000 rpm for 10 minutes. The supernatant was collected and 100 µl of this supernatant was added to micro titer well plate to measure optical density (OD) at 540 nm. Here, PBS was used as the negative control and 1% triton X-100 as the positive control. The percentage of hemolysis was determined based on the hemoglobin (Hb) released into the supernatants. The hemolysis ratio was calculated as follows:

$$\% \text{ Hemolysis} = \frac{\text{Sample}_{\text{abs}} - \text{Negative control}_{\text{abs}}}{\text{Positive control}_{\text{abs}} - \text{Negative control}_{\text{abs}}}$$

Eq .5.2.

(b). In-vivo toxicity

Animals

Adult Sprague dawley rats were kept in aluminum cages (grade 304) and a controlled environment of natural 12/12 h light/dark cycle, humidity (50–60%) and temperature (21 ± 2 °C) was provided. All rats were given tap water and standard diet at the Animal House, Quaid-i-Azam University (QAU) Islamabad, Pakistan. Rats were housed in this environment for 7 days before the toxicity analysis. The BCH 464 protocol for laboratory animals was followed under the Institutional Animal Ethics Committee (QAU Islamabad) recommendations.

Study Design

All rats were first weighed and marked with numbers. Total four groups were made having 6 male rats per group. The chitosan nanocomposite films were ground to powder and combined with standard rat feed at a single dose of 1000 mg kg⁻¹. Group 1 received standard commercial feed and was used as a negative control. The rats in group 2,3 and 4 were given 1000 mg kg⁻¹ single dose of CS-CNC-NK-EX2, CS-CNC-NK-EX3 and CS-CNC-Q films respectively.

Acute Oral Toxicity Study

The acute toxicity study was undertaken according to the Organization for Economic Cooperation and Development (OECD) guidelines 425 and followed a recently reported method applied for evaluating CNC toxicity (Torlopov *et al.*, 2021). After overnight fasting, film powders were administered to treatment groups at single oral doses of 1000 mg/kg, respectively in their feed. Control rats received standard (commercial) rat feed without film powder. After dosing, all animal groups were analyzed individually for any behavioral changes for first 30 min, then at 2, 4, 6, 10 and 24 h following treatment. Moreover, rats were inspected for 14 days for any signs of morbidity, mortality or toxicity during this whole experimental period. LD50 was calculated according to (OECD) guidelines 425 and body weight was measured initially before dosing and on day 0, 7 and 14 after dosing.

On the 14th day, rats were fasted for 15-16 hours before blood collection. Then they were anesthetized with chloroform and for each rat 3 ml of blood was collected by cardiac puncture. Afterwards, centrifugation of the blood samples was done at 3000rpm (4°C) for 15 minutes and sera were collected. Liver function was evaluated by measuring the total bilirubin, AST, ALT and ALP levels in blood samples whereas renal function was assessed by measuring urea, creatinine and uric acid using a blood chemistry analyzer.

5.3 Results

5.3.1 Biodegradability analysis

For extract incorporated films, results show that chitosan control displayed more weight loss at day 7 (26.5%) and 14 (33%) as compared to extract films (25% and 30% respectively) when films were exposed to lysozyme. Contrastingly, in soil environment these nanocomposite films were quickly degraded in 7 days and displayed 63% higher weight loss than control (Fig 5.1). Overall, CS-CNC-NK-EX1 films displayed highest weight loss in soil and lysozyme respectively.

In case of polyphenol incorporated composites, NK films displayed least weight loss both in soil and lysozyme (with the exception of CS-Q-NK films in soil), whereas Q-

CNC and R-CNC depicted highest weight loss % in soil (57% and 89% respectively) as well as in lysozyme studies (55% and 74% respectively). Overall, both extract and polyphenol composite films showed more degradation in soil as compared to lysozyme (Fig 5.2).

Fig. 5.1 Soil and Lysozyme degradation of the extract incorporated chitosan nanocomposites

Fig 5.2 Soil and Lysozyme degradation of polyphenol incorporated chitosan nanocomposites

5.3.2 Characterization of degraded films

(a). SEM analysis

SEM microphotographs were studied to see the extent of film's biodegradation in soil and lysozyme, taken after 14 days' exposure to both soil and lysozyme.

The morphology of different extract incorporated films in soil and lysozyme is given in figure 5.3(a-c) and 5.3 (d-f) respectively. Bigger, deeper holes and large cavities in some films can be found when exposed to soil, which seem to be more randomly distributed than in lysozyme exposed samples. Small cracks were found in lysozyme degraded samples therefore it is evident that biodegradability was improved in soil environment as compared to lysozyme. These SEM scanning results are correlated with weight loss evaluation in biodegradability assay (Fig 5.1 & 5.2).

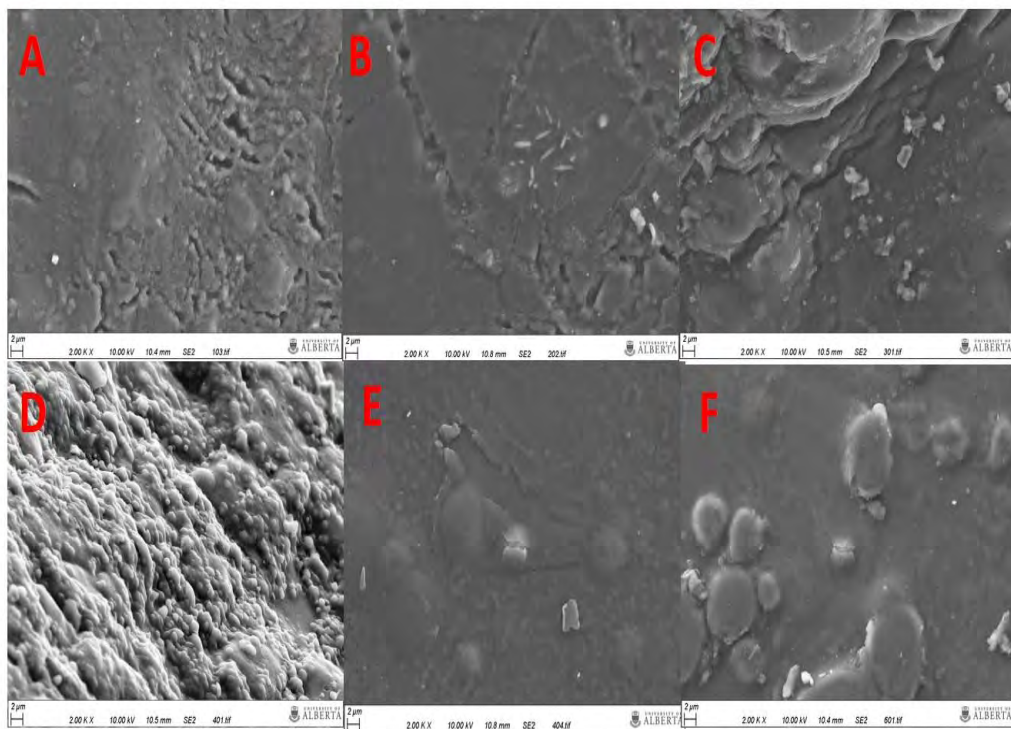


Fig.5.3 SEM images of degraded extract incorporated films

Soil degraded films: a). CS-CNC-NK-EX1 a). CS-CNC-NK-EX2 c). CS-CNC-NK-EX3

lysozyme degraded films: d). CS-CNC-NK-EX1 e). CS-CNC-NK-EX2 f). CS-CNC-NK-EX3

Similar results were found in case of polyphenol loaded composites i-e deeper holes and cracks can be seen in soil degradation SEM pictures (a, b and c of fig 5.4) as compared to smaller cracks in lysozyme degradation with the exception of CS-CNC-

VA (e of fig 5.4). Both fig 5.3 and 5.4 clearly represent cracked surface of extract and polyphenol loaded composites representing their degradation.

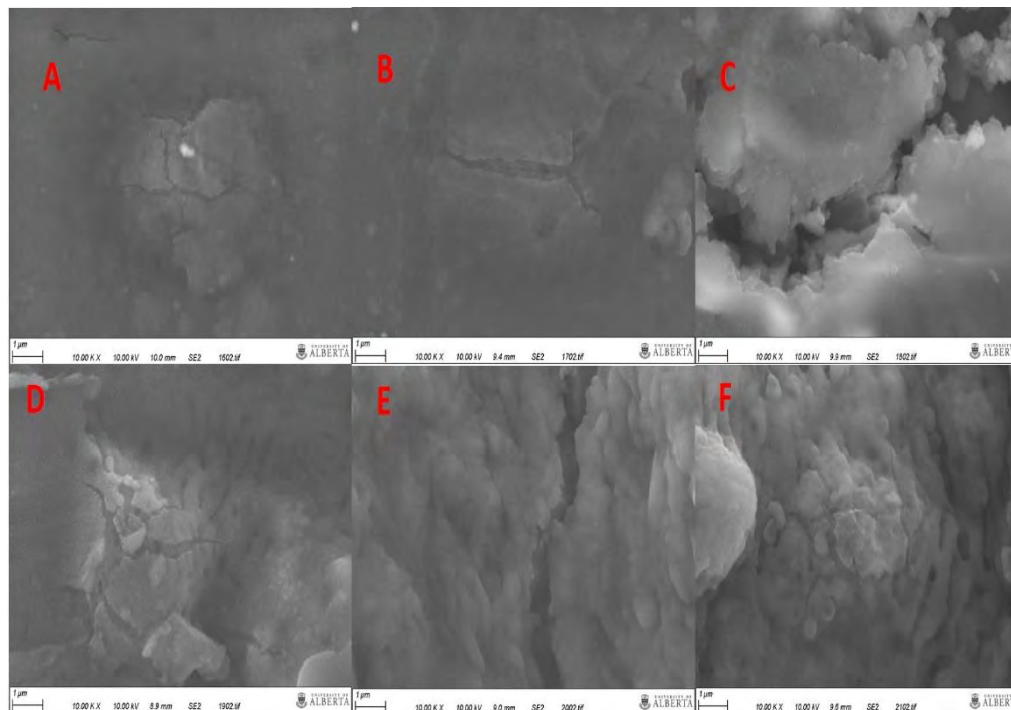


Fig. 5.4 SEM images of degraded polyphenol incorporated films

Soil degraded films: a). CS-CNC-Q a). CS-CNC-VA c). CS-CNC-R

lysozyme degraded films: d). CS-CNC-Q e). CS-CNC-VA f). CS-CNC-R

(b). FTIR Analysis

To identify some film-soil interactions FTIR analysis of degraded films was conducted however, those effects were not observed. Thus, the chitosan film degradation is likely to be related to the enzyme activity in the soil. In Fig. 5.5, the FTIR spectra of degraded chitosan composite films are given.

The chitosan films before degradation (shown in chapter 3) displayed a characteristic band of OH vibrations at 3280 cm^{-1} which was shifted to 3289 cm^{-1} in degraded control samples (Fig 5.4 and 5.6). The band around 1578 cm^{-1} corresponds to N–H vibrations

was shifted to 1674 cm^{-1} in degraded samples. A noticeable variation at around 1466 cm^{-1} was observed, which correlates to C-O stretching vibrations. Lysozyme incubated films displayed the presence of sharp amide I and II bands at 1648 and 1548 cm^{-1} and CS-CNC-NK-EX1 films exhibited a decrease in intensity of C-O, OH, N-H bands as compared to other composites.

Figure 5.5 FTIR analysis of degraded extract incorporated films

(a). Soil degraded (b) Lysozyme degraded

Fig 5.6 FTIR analysis of degraded Polyphenol incorporated CNC films

(a). Soil degraded (b) Lysozyme degraded

(c). TGA Analysis

TGA analysis (Fig 5.7) shows that after 14 days of soil burial CS-CNC-Q and CS-CNC-NK-EX1 composite films showed low thermal degradation temperature (249°C and 269°C respectively) as compared to chitosan control film (i-e 283 °C) and degraded chitosan film (259°C). This further confirms significant thermal modification in soil degraded composite films.

In lysozyme degradation (Fig 5.8), CS-CNC-NK-EX2 films showed early thermal degradation in lysozyme (258°C) as compared to soil (276°C). Similarly, polyphenol incorporated films displayed thermal degradation in lysozyme at low temperature i-e 258°C.

Fig 5.7.TGA Analysis of soil degraded films

Extract (a & b) and Polyphenol (c & d)

Fig 5.8.TGA Analysis of lysozyme degraded films

Extract (a & b) and Polyphenol (c & d) incorporated composites

(d). DSC Analysis

DSC analysis in fig 5.9 (a & c) shows that soil degraded extract and polyphenol incorporated films showed a slightly delayed water loss peak but earlier melting and denaturation temperature (261°C) (particularly in case of CS-CNC-NK-EX3 and CS-CNC-R) as compared to degraded chitosan sample. As shown in previous chapters before degradation composite films were denatured at 293°C.

In case of lysozyme degraded extract incorporated samples, no significant difference was seen in control and composite films degradation except for CS-CNC-NK-EX1 film which displayed early denaturation at 249°C (fig 5.9 b & d).

Fig. 5.9 DSC analysis of degraded films

Soil degraded (a & c) extract and polyphenol incorporated composites;
Lysozyme degraded (b & d) extract and polyphenol incorporated composites.

5.3.3 Toxicity studies

(a). In Vitro toxicity on RBCs

Safety of bio-nanocomposite films is also one of the issues concerned mostly by consumers. Hemo-compatibility assay was carried out to check whether the synthesized nanocomposite films are toxic to red blood cells (RBCs) causing hemolysis. ASTM F756-00 protocols have categorized the hemolytic assessment of samples as hemolytic, slightly hemolytic and non-hemolytic with $>5\%$, $< 5\%$ and $<2\%$ hemolysis percentage respectively (Pires *et al.*, 2018).

Results of hemo-compatibility assay demonstrate that less than 2% RBC hemolysis was shown by *A. subulatum* (EX2) and *M. piperita* (EX3) incorporated films (i-e CS-CNC-NK-EX2 and CS-CNC-NK-EX3) indicating their non-toxic character. Overall, all films depicted less than 5 % hemolysis as compared to control which clearly shows their safety for use in food packaging applications.

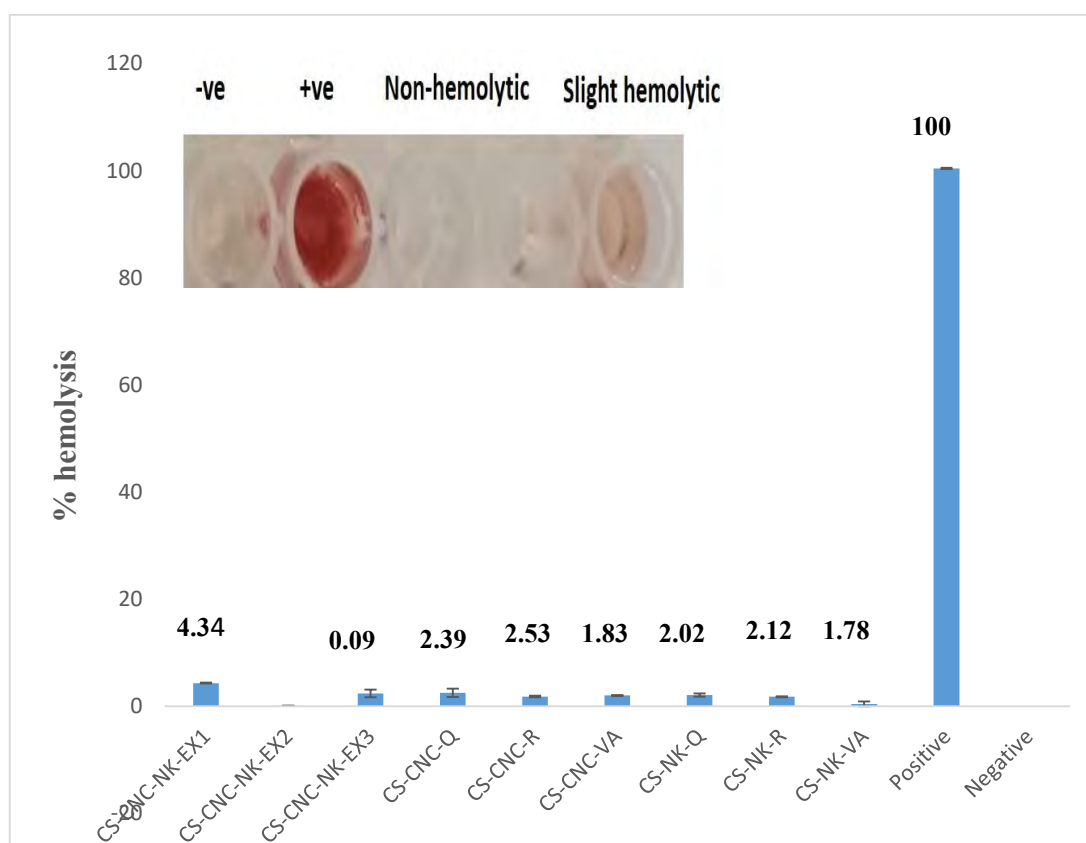


Fig 5.10 Hemo-compatibility assay

(b). Acute oral toxicity

The single dose of orally administered nanocomposite films at 1000 mg/kg did not cause death of any male or female rats during two weeks' observation period. All rats survived after single oral dose of CS-CNC-NK-EX2, CS-CNC-NK-EX3 and CS-CNC-Q films. The results suggest that acute administration of tested nanocomposite films did not cause mortality in 50% of rats at dose of 1000 mg/kg. Therefore, LD50 of films could not be assessed and can be regarded as e greater than 1000 mg/kg (as an experiment upper limit) in acute toxicity assessment.

Visual daily inspection for two weeks did not show any signs of discomfort, distress or any sufferings. Animals responded quite normally during handling and none of them showed diarrhea, changes in locomotor activity, change in food consumption pattern or any adverse clinical signs of toxicity. Moreover, upon oral administration of films, the normal increase in body weight was seen similar to control rats (Table 5.1).

Table 5.1. Body weight changes in films treated rats

Rats Groups	Weight (in gram) after oral dose		
	0 days	7 days	14 days
Control	213.3±19.7	217±15.1	218.5±13.6
CS-CNC-NK-EX2	220±28.3	219.5±21.1	221.7±14.7
CS-CNC-NK-EX3	215±36.2	215±25.9	219±28.3
CS-CNC-Q	211.7±25.6	218.5±22.5	222±24.1

Data represents mean ± SD (n=6)

The hematological parameters evaluated in rats with oral feed of nanocomposite films were found to be in normal ranges (Table 5.2). No significant difference was found in blood parameters as compared to control suggesting the non-toxicity of synthesized nanocomposite films.

Table 5.2 Hematological parameters of rats fed with films

Parameters	Control	CS- EX2	CS- EX3	Q-CNC
WBC (10 ³ cells/mm ³)	9.5 ± 0.05 ^a	8.2±1.33 ^b	9.2 ± 0.36 ^{ab}	8.9 ± 0.71 ^{ab}
RBC (mil/ mm ³)	6.8 ± 0.07 ^a	6.6 ± 0.4 ^a	6.6 ± 0.4 ^a	6.6 ± 0.31 ^a
Platelets (10 ³ cells/mm ³)	869.3 ± 6.7 ^a	856.8 ± 22 ^a	876.2 ± 12.3 ^a	875 ± 10.4 ^a
HGB (g/dL)	13.4± 0.2 ^a	13.1 ± 0.41 ^a	13.3 ± 0.2 ^a	13.5 ± 0.07 ^a
HCT (%)	35.8 ± 0.3 ^{ab}	34.4 ± 3 ^b	35.7 ± 0.8 ^{ab}	37.4 ± 0.2 ^a
MCV (fL)	52.5 ± 0.1 ^a	52 ± 0.3 ^a	54.2 ± 3.1 ^a	53.7 ± 0.7 ^a
MCH (pg)	19.4 ± 0.1 ^a	19.5 ± 0.3 ^a	19.4 ± 1.3 ^a	19.3 ± 0.3 ^a
MCHC (g/dL)	36.7 ± 0.1 ^a	37± 0.3 ^a	37.2 ± 0.6 ^a	36.6 ± 0.3 ^a
MPV (fL)	7.2 ± 0.3 ^{ab}	7.2 ± 0.3 ^{ab}	6.9 ± 0.17 ^b	7.4 ± 0.3 ^a
PCT (%)	0.6 ± 0.05 ^a	0.65 ± 0.04 ^{ab}	0.64 ± 0.08 ^{ab}	0.72 ± 0.05 ^a
POLYMORH (%)	17.7 ± 0.5 ^a	16.3 ± 4.3 ^a	16.7 ± 1.4 ^a	16.8 ±3.4 ^a
LYM (%)	70.7 ± 0.6 ^{ab}	68 ± 3.2 ^b	71.7 ±1.9 ^a	72 ±1.4 ^a
MON (%)	8.3 ± 0.6 ^a	7.8 ± 0.8 ^a	7.7± 0.8 ^a	7.8 ±0.8 ^a
Eosino (%)	2.7 ± 0.6 ^a	3± 0.9 ^a	3.2 ± 0.4 ^a	3.3 ±0.8 ^a

Data represents mean ± SD. Mean in the same row following same letter are not significantly different (P>0.05)

Liver function parameters specifically liver enzymes such as ALT and AST were not significantly different from control, suggesting that normal functioning of liver was not compromised by oral ingestion of tested films (Fig 5.11).

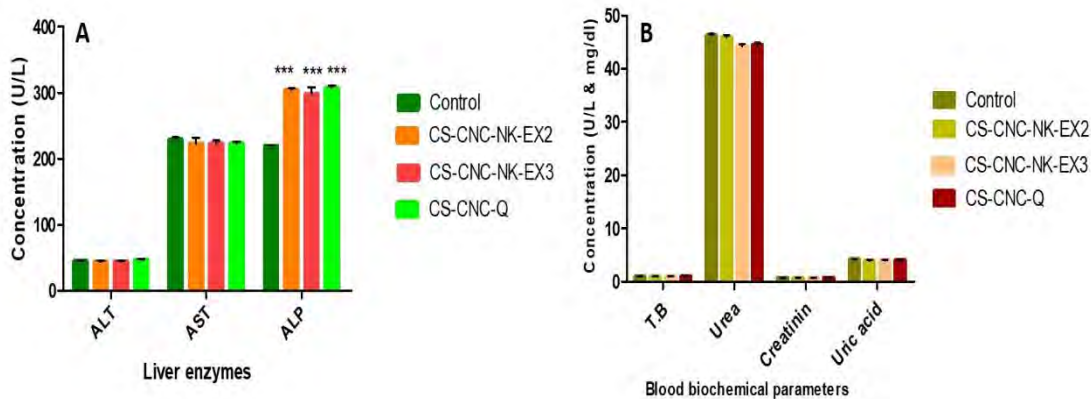


Fig.5.11 Liver and Blood biochemical parameters profile of film treated rats

(a). Liver enzymes profile and (b). Blood biochemical parameters, Differences between the control and films (CS-CNC-NK-EX2, CS-CNC-NK EX3 and CS-CNC-Q) treated animals in acute toxicity treatment groups were evaluate using one-way ANOVA and bonferroni posttest via graph pad prism 5, Bars represent mean \pm SD, all parameters were statistically non-significant ($P > 0.05$) whereas *** indicates $P < 0.001$ for alkaline phosphatase being highly significant.

However, a significantly increased ($P < 0.001$) level of alkaline phosphatase was found in film treated rats as compared to control which may be not be considered as a sign of liver toxicity because of other parameters in normal range. Total bilirubin was also tested along with liver enzymes and was found to be in normal range of 0.9-1 mg/dl in control as well as film treated rats indicating no disturbance in liver function. With the help of biochemical assays, the parameters indicating kidney function such as urea, uric acid and creatinine did not show significant differences (Fig 5.11), evidencing that these films at tested dose did not affect kidney function.

5.4 Conclusion

Biodegradability of synthesized films was analyzed in soil and lysozyme. All chitosan nanocomposite films displayed quick and increased degradation in soil as compared to lysozyme. Among all synthesized films, CS-CNC-NK-EX2 composites exhibited highest weight loss in both soil and lysozyme. Thermal analysis of degraded films showed that synthesized nanocomposites films thermally degrade at low temperatures than chitosan control. SEM analysis also confirmed degradation in soil and lysozyme by the presence of cracks and holes in degraded film samples. Results of hemocompatibility assay proved the safety and nontoxic effect of synthesized films on RBCs as all films exhibited less than 5% hemolysis, while *A. subulatum*, *M. piperita* and vanillic acid films showed the least hemolysis (<2%). In vivo acute oral toxicity analysis further confirmed that the prepared films are non-toxic and fall under GHS category- 5 as their LD50 exceeds than 1000 mg/kg body weight. Single oral dose of synthesized films (1000 mg/kg) exhibited no adverse effect on hematological parameters as well as on normal functioning of both liver and kidney. Overall, no mortality or tissue related toxicity was observed upon oral dose of tested films therefore these films can be regarded as safe for food packaging applications

Discussion

(Chapter # 6)

6.1 Discussion

Biodegradable polymers such as chitosan have been used as food packaging material however their use is limited due to low mechanical, barrier and antioxidant properties and high hydrophilic nature of neat chitosan. Therefore, nano-reinforcements along with incorporation of green extracts in chitosan comes out to be suitable alternative (Souza *et al.*, 2017; Xu *et al.*, 2018). Therefore, this study was carried out to synthesize chitosan blend films with two nano fillers and edible plant extracts/polyphenols to improve chitosan film properties.

Previous researchers have reported that addition of 3-5% CNC into chitosan improves the tensile strength and barrier characteristics of chitosan owing to strong interaction between chitosan matrix and CNC (Xu *et al.*, 2018). Chitosan scaffolds with nano keratin have also been reported to give a porous structure to chitosan matrix along with increased percentage swelling and improved protein adsorption ability (Saravanan *et al.*, 2013). A variety of natural constituents like thyme extract, pomegranate peel extract, grape pomace extracts and polyphenols like Quercetin, vanillin (Stroescu *et al.*, 2015) and tea polyphenols have been incorporated in chitosan films to improve their antioxidant/antimicrobial properties (Siripatrawan & Harte, 2010; Xu *et al.*, 2018). In this study, Chitosan was blended together with CNC, nano keratin, edible plant extracts and their polyphenols. The individual as well as combined effect of nano fillers along with extract/polyphenol addition was checked on film's mechanical, barrier, thermal and biological characteristics to improve the shelf life. Moreover, biodegradability and toxicity of films was determined and effect of packaging film on food quality was evaluated.

6.2 Screening, *in vitro* activities and molecular docking of the plant extracts

The integration of antioxidant and antimicrobial compounds from natural herbs into the food packaging films and coatings are the attributes of active packaging (Kapetanakou & Skandamis, 2016). Such kind of active packaging was reported earlier where incorporation of garlic skin extract and CNC in chitosan films not only improved the barrier properties but also improved antibacterial activity of the film due to extract addition (Salim *et al.*, 2022). In this contribution, eight edible plants (i.e. *C. zeylanicum*,

C. tamala, *A. subulatum*, *T. foenum graecum*, *M. piperita*, *C. sativum*, *L. sativa* and *B. oleraceae*) were screened for their antioxidant and antimicrobial properties in order to be incorporated in chitosan films.

Ethanollic plant extracts were prepared from above mentioned plants. Varying percentage yield was shown by all plant extracts, perhaps due to differences in their variable solubility and phytochemical composition (Ahmed *et al.*, 2017). It is evident from total polyphenolic content and total reducing power assay that *C. tamala*, *C. zeylanicum*, *M. piperita* and *A. subulatum* exhibited highest polyphenol content as well as significant reducing power. The reducing power of *C. zeylanicum* leaf and bark extracts can be due to the di- and mono-hydroxyl replacements in the aromatic ring, which have potent hydrogen donating capacities as described in a previous report (Abeysekera *et al.*, 2013). Plants with high phenolic content are mostly targeted by pharmacists to treat infections (Prasad *et al.*, 2009). Significant antioxidant property of studied plants may be due to polyphenols as they are reported to scavenge OH group due to nucleophilicity of phenolic groups which aids in their antioxidant activity (Pan *et al.*, 2023). The least IC₅₀ was exhibited by *C. tamala* in case of DPPH assay which further suggest the use of this plant in chitosan film to expand shelf life of readily oxidized food products.

In antibacterial assay, all plants exhibited slight zones of inhibition against *E. coli* (except *T. foenum graecum* and *M. piperita*) and *S. aureus* (except *C. tamala* and *M. piperita*). These activities might be due to the presence of polyphenols and flavonoids in the studied extracts. Although phenolic compounds reveal various antimicrobial mechanisms, most of them do this by supporting damage to the function of either cell membrane or wall (Ngolong Ngea *et al.*, 2021). In antifungal assay, all plant extracts showed inhibition against *F. solani*, with a highest zone of inhibition by *C. zeylanicum*. The antifungal ability of *C. zeylanicum* bark powder and its essential oils against *Fusarium oxysporum* is well documented (Kowalska *et al.*, 2020). There are reports of *C. zeylanicum* methanol, n-hexane, and aqueous extracts to show inhibition against *Alternaria solani* (Yeole *et al.*, 2014). To the best of our knowledge, there is no report presenting the antifungal effects of ethanol extract of *C. zeylanicum* and *A. subulatum* against *Fusarium solani*, which we observed in our study. *C. zeylanicum* and *A. subulatum* ethanolic extracts showed moderate inhibition against the growth of both

Aspergillus species. In a previous report, methanolic extract of *A. subulatum* exhibited a considerably higher zone of inhibition (i.e. 19 mm) against *A. niger* (Agnihotri & Wakode, 2010). This can be due to different experimental conditions and different solvent system used. Extract of *M. piperita* inhibited the growth of two fungal strains, i.e., *A. niger* and *F. solani*. *M. piperita* extract has already been shown to cause inhibitory effects against radial fungal growth and aflatoxin production by Aspergillus species (Skrinjar *et al.*, 2009). *A. subulatum* and *M. piperita* exhibited antifungal activity against *A. niger* even at lowest MIC (50 µg/ml) which shows that these extracts can be incorporated in chitosan films to resist fungal growth. The significant antioxidant potential of these plants might also be the reason for their antifungal efficacy, as plant flavonoids are reported to inhibit biofilm formation by stimulating membrane disturbances, which reduces the fungal cell size and causes leakage of intracellular components (Lee *et al.*, 2018). In response to infection, Phenols are also oxidized to their respective quinones which can further inactivate the fungal/bacterial enzymes. Polyphenols have ortho para directing groups (which tend to donate electrons) which may contribute to their antioxidant as well as antimicrobial properties thus they can serve as anti- mycotoxins (Appell *et al.*, 2020).

HPLC results reveal that rutin, vanillic acid and quercetin were the most common polyphenols in selected plants. Docking analysis results were also consistent with the hypothesis that the studied plants showed antimicrobial efficacy due to presence of polyphenols (like rutin and quercetin) which inhibit fungi most probably by acting similar to azole drugs. This is because lowest binding energy was shown by rutin and quercetin against two major drug targeted fungal enzymes i.e. CYP51(sterol 14 α -demethylase; used for sterol biosynthesis in fungi) and NDK (nucleoside diphosphokinase; used for spore development and pathogenicity (Wang Y. *et al.*, 2019)). Interestingly the K_d values of rutin (-9.4) and quercetin (-8) against fungal CYP51 were comparable with terbinafine (-8.9). In line with these results, another study reported that rutin was among the seven plant molecules showing excellent binding energy against CYP51 (Jadhav *et al.*, 2020). Fluconazole and ketoazole have also been reported to show binding affinity values of -7.6 and -10, respectively, with fungal alpha demethylase (Mhatre & Patravale, 2021). It indicates that rutin can inhibit CYP51 either alone or in combination with the above-mentioned drugs. Rutin and quercetin have also been reported to enhance the antifungal activity of amphotericin

B (Azeem *et al.*, 2022). Quercetin has been found to exhibit individual or synergic antifungal properties with fluconazole (an inhibitor of fungal fatty acid synthase) (Al Aboody & Mickymaray, 2020). In addition to CY51 inhibition, quercetin and rutin showed a significant binding affinity with NDK, which attributes to their dual mechanism of action. Moreover, the antifungal efficacy of these polyphenols also supports the structure-activity relationship analysis, revealed by a previous researcher who discovered that phenolic compounds possessing a low electrophilicity index have good antifungal activities (Appell *et al.*, 2020). The inhibition of these two enzymes (involved in major pathogenesis pathways of fungi) by plant extract polyphenols is only a predicted antifungal mechanism as various limitations of docking exist in literature like scoring functions do not provide any quantitative reliability as some of them consider protein as rigid body and some as flexible bodies so they do not give accurate free energies. Therefore, docking results need to be to be rescored via MM/GBSA (Molecular mechanics/generalized-born surface area) or by running molecular dynamics stimulations of the docking results which will be a more authentic approach (Desta *et al.*, 2020).

On the basis of results of above assays, three plant extracts i-e *C. tamala*, *A. subulatum*, *M. piperita* and three polyphenols i-e quercetin, rutin and vanillic acid were selected for incorporation in chitosan films in order to exert their antioxidant and antimicrobial effect.

6.3 Synthesis and characterization of phyto-assisted chitosan nanocomposites

Chitosan is a chitin derived versatile polymer, obtained from fishing industry waste. It has demonstrated antimicrobial and anti-inflammatory properties and has been rendered as non-toxic, bio-compatible and biodegradable among other polymers. Chitosan possesses protonated amino groups, hydroxyl and carboxyl groups which have facilitated its compatibility with other natural or synthetic compounds therefore it is a widely investigated polymer for the preparation of low-cost composite films for food packaging (Azmana *et al.*, 2021).

In this connection, this study is based on synthesis of chitosan nanocomposites reinforced with CNC (Cellulose nanocrystals from cellulose) and NK (nano keratin from keratin). The use of nano metric compounds has been evaluated in recent studies

for reinforcement of natural polymers like chitosan. It has been noticed that particle size reduction of reinforcing agent helps the polymer and nanoparticles to disperse more homogeneously and causes an increase in the surface of the reinforcements, such as nano keratin, nano clay and nano cellulose (Kuttalam *et al.*, 2021). Low reinforcement load (1-5%) has been reported to improve barrier, thermal and mechanical properties of packaging films. Similar was found in current study as 3% CNC and 0.3% NK came out to be optimal concentration of nanoparticles used for making chitosan composite films with improved barrier properties. Predominantly, films with 3% CNC-CS demonstrated significantly high T.S (65.5 Mpa). However, %E was seen to be gradually increased by addition of nano-keratin to chitosan in CS-NK films. This increase in tensile strength due to CNC addition may be due to much similarity in structure of cellulose and chitosan as compared to chitosan and keratin structure which allows more strong bonding of chitosan with CNC than keratin (Tran & Mututuvvari, 2015). Chitosan being cationic (having amino groups) and CNC being anionic (having hydroxyl groups) in nature, when blended together spontaneously form a polyelectrolyte complex owing to strong electrostatic/ hydrogen bonding/ Van der Waals forces etc. It eventually leads to increased tensile strength and most often decrease in % elongation (Wildan & Lubis, 2021; Xu *et al.*, 2018). Addition of CNC to chitosan films has been previously reported to improve barrier properties of chitosan films. For example, previous researchers have investigated that 5% and 20% (w/v) CNC addition to chitosan leads to enhancement of tensile properties (Khan *et al.*, 2012; Mujtaba *et al.*, 2017).

Synergistic addition of two nano-fillers (without extract) was found to decrease the tensile strength. However, the addition of extract remarkably improved the tensile strength of chitosan films reinforced by both CNC and NK, in spite of already reported trend of decreased tensile strength of chitosan films upon extract addition (Gao Z. *et al.*, 2021). This enhanced tensile strength may be due to increased intermolecular interactions including physical and chemical crosslinking. However, decrease in elongation upon extract addition is might be due to increasing interactions such as increased hydrogen bonding and other crosslinking reactions (Nadira *et al.*, 2022). Therefore, it can be predicted that extracts might have served as cross linkers with chitosan, CNC and NK to increase the film's strength. The OH groups of plant polyphenols are reported to react with Chitosan amino groups through electrostatic interaction, ester linkage and hydrogen bonding (Zhao *et al.*, 2022). Polyphenols from plant extracts might serve as cross linker in chitosan nano-composites while the ratio

of extract and chitosan is of great importance in this regard. Different mechanisms of crosslinking are reported, such as aldehyde group of cinnamaldehyde and hydroxyl group of polyphenols can react with amino groups resulting in formation of a Schiff base and conversion of chitosan to imino chitosan. (Gao Z. *et al.*, 2021; Moalla *et al.*, 2021). In case of polyphenol loaded composites, CNC reinforced composites displayed significant increase in tensile strength as compared to NK reinforcements which shows more strong interaction of Chitosan with CNC as compared with NK.

Mechanical strength confirmation of films was followed by evaluation of their barrier properties such as WVP and opacity. Recently, a decrease in WVP of chitosan film was reported upon addition of *Prunella L.* extract (Erken *et al.*, 2022). However, in our findings, adding extracts to CS-CNC and CS-NK films individually was found to enhance the WVP. Interestingly, when both CNC and NK were blended in chitosan film incorporated with extract, the 42% decrease in water permeability of the bio-nanocomposite film was achieved (especially in case of CS-CNC-NK-EX3 and CS-CNC-NK-EX2) as compared to control. It may be credited to the enhanced hydrogen bonding interactions between the chitosan matrix, glycerol, cellulose nanocrystal and nano keratin with OH groups of these extracts causing a free O–H groups decline and thus causing the low diffusion of water molecules (Huang *et al.*, 2020). Due to this network, water vapors track a tortuous path via chitosan matrix around the nanoparticles and extract components, thereby it leads to enhance the path length for water molecules' diffusion and thus decrease the permeability (Rhim *et al.*, 2006). Polyphenol loaded CNC composites also displayed lower WVP as compared to both chitosan control and NK reinforced polyphenol composites which may be due to strong hydrogen bonding interactions in these composites.

The opacity of films was evaluated as another barrier property. CNC reinforced quercetin nanocomposites displayed 38% increase in opacity while presence of extract in individual CNC and NK film exhibited no significant effect on opacity which is in contrast to a finding of garlic extract addition (Salim *et al.*, 2022). However, when both CNC and nano-keratin were mixed with chitosan-extracts film solution their opacity was found to be doubled especially with *C. tamala* addition. It may be due to blockage of light path through the chitosan matrix owing to a strong contact between CNC, NK, extract and chitosan (Yadav M. *et al.*, 2020). Opacity is found to be directly proportional to the homogenous dispersion of the film components and depends on internal structure of film (Abdollahi *et al.*, 2012). A Surge in film's opacity can be a

desired characteristic for food packaging in case of light sensitive food items as it might help to inhibit lipid oxidation induced by UV light (Vejdan *et al.*, 2016). The decrease in transparency of CNC film can be due to the increase in light scattering by the CNC (Cao *et al.*, 2009). However, decreased transparency in case of extract loaded composites reinforced by both nano fillers might be due to presence of polyphenols interactions in films as reported earlier (Zeng *et al.*, 2020).

Structure insights of the films were exhibited by FTIR and XRD. In FTIR spectra, the peak shift and change in peak intensity represent the contact between chitosan, CNC, NK and extracts. Hydrogen bonding interactions in CS-CNC-NK-EX composites represent a significant rise in peak intensity and a broader OH peak at 3280.2cm^{-1} (as compared to control film). Moreover, the intensity and sharpening of the peaks at 1578.6 (Amide II) slightly increased in presence of extracts, particularly in case of EX3. Schiff base formation is reported to show peak around $1690\text{-}1590\text{ cm}^{-1}$ and occurs due to C=N bonding (Su *et al.*, 2016). It clearly represents the role of extracts as cross linkers in chitosan nanocomposites reinforced by CNC and NK. Moreover, C=O stretching vibration as obvious in control film (1648 cm^{-1}), CS-CNC-NK-EX1 (1641cm^{-1}) and CS-CNC-NK-EX2 (1659 cm^{-1}) was absent in CS-CNC-NK-EX3 film. It may be because all C=O group present in CS-CNC-NK-EX3 film were occupied in making hydrogen bonds. In case of extract loaded individual reinforcements (CNC/NK), a decrease in peak intensity for OH associated vibrations (3258 cm^{-1}) were seen which suggest that adding both nano filler in presence of extract might result in more interactions between nano filler and matrix as compared to individual additions. Moreover, the increased intensity and peaks sharpening in case of CNC- reinforced polyphenol composites show the stronger intermolecular interactions and thus higher tensile strength as compared to NK reinforced polyphenol composites.

XRD analysis was carried out to see extent of above FTIR interpreted interactions in prepared films. Our results show that CNC-NK-EX3 films displayed new peak (7.05°) which shows additional crystallinity regions revealing more interaction of chitosan and nanoparticles. Moreover, in CNC-NK-EX3 films, particular CNC peak (34.6°) disappearance is the indication of more dispersion of CNC in these composites (Xu *et al.*, 2018). It is reported that nano filler has the tendency to modify the degree and crystallinity rate (Cao *et al.*, 2017). Mechanical properties also enhance due to reinforcement supported by strong interactions between polymer (chitosan) and

nanoparticles (CNC and NK) and development of new crystallinity regions (Zubair & Ullah, 2020). XRD results are consistent with greater tensile strength of CS-CNC-NK-EX3 films. Furthermore, in CS-CNC-Q composites a new peak belonging to quercetin appeared at 12.2° (Yadav S. *et al.*, 2020) and it implies that the strong interaction among quercetin, CNC and chitosan has affected the quercetin crystallinity and a change in both the angle and intensity of quercetin reflection peaks has occurred (De Arruda *et al.*, 2017). In case of CS-NK-Q and CS-NK-VA new peak appearance suggests the good compatibility and interaction among components of these composites. Moreover, Incorporation of polyphenols to chitosan was found to increase the chitosan peak intensity in both CNC and NK reinforced composites which suggest that their addition helps in ordering of chitosan chains during oven drying (Xu *et al.*, 2018).

The chemical bonding of CS control, CS-CNC, CS-NK, CS-CNC-NK-EX1, CS-CNC-NK-EX2 and CS-CNC-NK-EX3 was estimated via XPS analysis. Gradual increase in oxygen and nitrogen atoms was obvious in case of CS-CNC-NK-EX2 which can be due to homogenous dispersion of CNC and NK in these nanocomposites (Kaur *et al.*, 2018). According to previous reports, neat CNC was found to have three peaks with binding energy at 287.6, 286.3, and 284.6eV appearing due to C=O/O-C-O, C-O-C/C-OH and C-C/C-H, respectively (Kaboarani & Riedl, 2015). However, in current study when CNC was mixed with chitosan it displayed surface modification by showing four peaks. The presence of an additional peaks at 286.98 ev in CS-CNC-NK-EX2 composites might have been created during CNC and NK dispersion (Kaboarani & Riedl, 2015). Peak at 285.4 ev appears in CS-CNC-NK-EX2 due to -C-O bond owing to 20% glycerol. While peak at 283.1 ev determines C-C bonds of chitosan as reported earlier (Ye *et al.*, 2021). Moreover, C-C, C-H bonds' intensity (at 282.5, 283.1, 283.9 ev) can be due to alkanes (C-H groups) attached to CNC /NK during modification.

In an effort to explore the surface morphology, SEM results suggest that change in surface morphology from smooth to rough surface can be due to increase in interfacial tension due to change in film thickness following incorporation of nano fillers and extract. The cross-section analysis shows roughness that is mainly due to addition of nanoparticles (CNC and NK) which either intercalate/exfoliate with chitosan matrix along with plasticizer and polyphenol molecules of extracts. Some aggregation or clumping areas were seen in cross section of CS-CNC-NK-EX2 which indicate more

sonication to improve dispersion. SEM results are consistent with good mechanical strength of these chitosan derived composites, because well dispersed nanoparticles are found to enhance the strength of layered matrix (Jose *et al.*, 2014). In case of polyphenol composites, both intercalated (increased interlayer spacing) and exfoliated morphologies can be predicted. TEM analysis also confirmed that the adding CNC and NK into the CS matrix caused a homogeneous composite to be formed, in which the individual components are strongly connected by hydrogen bonds (Kang *et al.*, 2018). uniform CNC distribution in nanocomposite films is actually known to be responsible for improved physico-mechanical properties (Yadav & Chiu, 2019). In our study, significantly enhanced physical and mechanical properties of prepared nanocomposites may also be due to partial exfoliation of nano fillers in chitosan matrix which occurs due to superior interaction between chitosan chains and nano cellulose/nano-keratin (i.e. via forming a hydrogen bond network) and is evident from disappeared interlayer spacing diffraction peak in XRD analysis and expanded inter gallery spacing in TEM analysis. Similar enhancement in physical and mechanical properties was reported by a previous researcher in case of graphene oxide containing rubber composites (Malas & Das, 2015).

Considering the above structural attributes, thermal analysis of films was carried out. During TGA analysis, CS-CNC-NK-EX3 films displayed 70% loss at a delayed temperature i.e. at 287°C. It shows the stronger interaction of CNC, NK and EX3 within the chitosan matrix and thus more thermal stability as compared to composites reinforced with one filler (either CNC /NK). The DTG (derivative of mass loss) curve represents rate of maximum weight loss and shows two or three regions of weight loss due to weak or strong interactions between extracts, chitosan and nanoparticles. The regions having less interaction of nanoparticles, extract and glycerol with the chitosan demonstrate early weight loss (Paydayesh *et al.*, 2022). Chitosan, CNC and NK exhibited three weight loss points. Initial slight weight loss observed at 50-100°C due to moisture loss (evaporation of loosely bound water), next weight loss occurred over a range of 140°C to 395°C due to degradation of Chitosan, glycerol, CNC, NK and extract components (Xu *et al.*, 2018). CNC degradation is reported to occur at 240°C - 335°C and is due to glycosidic bond cleavage, breakdown reactions with C=O, water, and low-volatility compounds (Mujtaba *et al.*, 2017; Taherimehr *et al.*, 2021) while major degradation of chitosan occurs at 140°C -310°C due to de-acetylation and

glycosidic linkage cleavage resulting in its de-polymerization. A final weight loss occurred at a temperature of 395–600 °C. This is due to breakdown of char into low molecular weight gas products (Bonilla *et al.*, 2018). In case of CNC reinforcement, TGA results indicated that addition of quercetin and rutin increased maximum thermal degradation temperature of chitosan-CNC film (283.1°C to 286.9°C). This higher thermal stability of rutin and quercetin loaded films is consistent with previous reports of rutin loaded CS/PVA films and quercetin loaded chitosan films (Narasagoudr *et al.*, 2020). Moreover, polyphenol loaded films show 70% weight loss only at 1°C higher temperature than control. It can be due to reduced mobility of CS/CNC chains in film forming solution due to polyphenol's incorporation (El Miri *et al.*, 2015). Furthermore, higher char residue was obtained in case of CS-NK-VA films (34%), which could be due to a different mechanism of degradation in these films due to difference in composition.

TGA was followed by DSC to detect thermal transitions of composite films. The first peak at 109°C appeared due to solvent (water, acetic acid) evaporation and second peak (210°C) was attributed to melting of crystalline structure of chitosan, glycerol, CNC, NK and extract components representing “melting temperature (T_m)” (Rao & Johns, 2008). Third peak at 293°C represented the phase inversion temperature of chitosan showing its decomposition. Delayed moisture peak in Extract loaded composites may be due to better interactions of two nanoparticles (CNC and NK) with the polar groups of chitosan in these composites, making this moisture loss difficult. In a study conducted earlier, the melting temperature was reduced by adding tea extract but our results were contrasting to this (Peng *et al.*, 2013). As higher T_m (i.e. 250°C) was achieved for CS-CNC-NK-EX3 and CS-CNC-NK-EX2 films. It might indicate that incorporation/mixing of two nano fillers has profound impact on the amorphous region of chitosan matrix (Kouser *et al.*, 2020) and might produce a delayed temperature shift in T_m of bio-nanocomposites. This is in agreement with previous reports where extract was found to have plasticizing effect and was not found to be involved in increasing thermal stability. Films having only CNC as nano filler also represented an intermediate T_m instead of increased T_m value (Xu *et al.*, 2018; Yadav M. *et al.*, 2020). The reduction in T_m of polyphenol loaded composited reinforced with either CNC/NK also confirms the above interpretation.

Polymer chain mobility is generally associated with its thermal transitions, among such transitions glass transition is of prime importance that is mainly determined from $\tan \delta$ curve of DMA analysis (Qian *et al.*, 2019). The steady drop in storage modulus (E') just like the synthetic polymers was observed in CS-CNC-NK-EX composites. The CS-CNC-NK-EX3 films showing delayed glass transition temperature (T_g) represented the higher values of E' and literature reports indicate that higher storage modulus is due to more stable interactions between nano filler and matrix (Kaur *et al.*, 2018).

This mixed nano-reinforcement effect is also supported by XRD and mechanical analysis as CS-CNC-NK-EX3 composite also displayed new peaks in XRD and highest tensile strength in tensile analysis. Two transitions were seen in bio-nanocomposite films that may be attributed to the presence of glycerol as it is reported to produce a disordered structure with two glass transitions (Chen & Zhang, 2006; Zubair *et al.*, 2019) that can be seen as glycerol rich and chitosan rich regions. The transitions obtained in all composites represented a good interaction of glycerol with chitosan. CS-CNC-NK-EX3 films showed two transition peaks which may be because of two nano fillers intercalated/exfoliated into chitosan matrix leading to enhanced glass transition temperature (T_g). Moreover, some $\tan \delta$ peaks were broad while others were found narrow/sharp in current study. Literature supports the point that position of $\tan \delta$ peak may vary from the bulk and may shift to higher temperatures with addition of nano fillers (Tomaszewska *et al.*, 2021). It is generally believed that during strong interactions, T_g associated $\tan \delta$ peaks shift to higher temperatures due to constrained polymer molecules close to filler. Previous reports also show broadening of $\tan \delta$ peak indicating the heterogeneity of polymer dynamics and some authors reported the inhomogeneity due to two distinct T_g as a reason of broad $\tan \delta$ peaks. Additives can also contribute change in a nanocomposite dynamic as they often help in filler dispersion in the polymer matrix (Bustamante-Torres *et al.*, 2021).

6.4 *In vitro* biological activities of phyto-assisted chitosan nanocomposites

The use of nano-packaged and antioxidant or antimicrobial compounds loaded films are responsible for sustainability of food supply chain. Literature shows significant enhancement in antioxidant/antimicrobial characteristics of chitosan films by addition of polyphenols, essential oils and plant extracts (Flórez *et al.*, 2022). Grafting of *p*-coumaric acid on cellulose nanocrystals was recently reported in a pectin coating which

not only improved the barrier properties but also inhibited the browning of fresh cut fruits (Wu *et al.*, 2022). Another study reported the incorporation of nettle leaf extract in chitosan films to improve the guava fruit shelf life by the antimicrobial effect of extract (Kalia *et al.*, 2021).

Hence, the synthesized nanocomposite films in this study were tested for their antioxidant antimicrobial and food quality attributes. To confirm the presence/loading of extract/polyphenols, total phenolic assay was carried out which clearly shows that films loaded with plant extract/polyphenols were having higher TPC than films without extract/polyphenols. Films showing higher total phenolic content (*M. piperita* and quercetin loaded films) also displayed strong antioxidant potential in DPPH assay. It is consistent with previous reports when grape pomace extract was added to chitosan CNC film it resulted in strong antioxidant potential due to increase in polyphenol content (Xu *et al.*, 2018). Similarly, another study reported that scavenging degree was found to be directly proportional to polyphenol content (TPC) when pomegranate peel extract and mint extract were added to chitosan-PVA films (Kanatt *et al.*, 2012). DPPH assay revealed that CNC and nano keratin alone did not show significant effect on antioxidant potential but when mixed with polyphenols these films exhibited good free radical scavenging ability. Decolorization of DPPH (stable free radical) and reduction in absorbance occurs when it reacts with antioxidants. The extent of reduction in color and absorbance depends on hydrogen donating capacity of film's antioxidants. Chitosan control exhibited some scavenging activity that is attributed to the use of low molecular weight chitosan (having active amino and hydroxyl groups in polymer chain) (Xing *et al.*, 2008) in current study. Among extract loaded films, *M. piperita* films displayed significant DPPH scavenging. In case of polyphenol loaded films, quercetin when mixed with chitosan and CNC showed strong scavenging potential (70%) followed by CS-NK-Q (57%) and CS-CNC-R (53%). It may be attributed to previously reported strong DPPH scavenging potential of quercetin and rutin. The difference in antioxidant potential of these films may be due to difference in the position and number of hydroxyl groups in specific loaded polyphenol as well as loading efficiency of polyphenols (Zeng *et al.*, 2020).

Nanocomposite films were further checked for their antimicrobial activity. *M. piperita* and *A. subulatum* films displayed moderate antibacterial activity against *B. subtilis* and

P. aeruginosa which may be due to their higher polyphenol content and good antioxidant potential. It is consistent with recently reported antibacterial effect of mint leaf extract based hydrogel films against *P. aeruginosa* (Mojally *et al.*, 2022). NK reinforced films didn't display antibacterial activity against the tested strains but quercetin and rutin incorporated CNC composites exhibited moderate antibacterial activity against *P. aeruginosa*. It might be due to slow release of quercetin and rutin from films because control chitosan film did not show any inhibition zones against these bacteria. Literature also proves the bacteriostatic activity of quercetin against both gram positive and gram negative bacteria, most probably by promoting damage to the bacterial cell membrane/cell wall function (Mandal *et al.*, 2017). These results suggest the release of quercetin and rutin from films to encounter antibacterial effect, as both of these polyphenols are not only known to cause prevention of biofilms but also reported to enhance the bactericidal effect of amphotericin B (Nguyen & Bhattacharya, 2022).

The results of antifungal assay demonstrated moderate antifungal activity of quercetin and rutin incorporated CNC reinforced composites against *Mucor*. It is in accordance with antifungal activity of rutin and quercetin reported in previous studies. These polyphenols may cause either mitochondrial dysfunction, DNA damage or induction of apoptosis for exhibiting their antifungal effect (Nguyen & Bhattacharya, 2022). NK reinforced composites might have not inhibited these strains due to difference in their structure as compared to polyphenol CNC composites. These polyphenols differ from each other only in hydroxyl group substitutions and difference of nano filler results in different structure as well which may affect their antimicrobial properties (Han, 2009). Moreover, among extract loaded films *C. tamala* and *A. subulatum* displayed good antifungal activity against *Mucor* and *A. niger* respectively which correlate with already reported antifungal potential of these extracts (Khanzada *et al.*, 2021). It may be due to their polyphenol content which might serve as anti-mycotoxins by damaging cell wall or cell membrane (Christ-Ribeiro *et al.*, 2019).

In order to evaluate the food quality, baby carrots were coated with synthesized composites for a week. Our results showed that carrots packaged with chitosan nanocomposite films exhibited less quality changes as compared to neat chitosan film and control samples. Moreover, least weight loss was exhibited by quercetin and *M.*

piperita loaded chitosan films. However, unwrapped baby carrots were shrunk and unacceptable for eating. The least weight changes in nanocomposite film packaged carrot over a period of 7 days might be due to good antioxidant and antimicrobial activity of these films (CS-CNC-Q and CS-CNC-NK-EX3) as discussed earlier in current study. Polyphenols from these films might have slowly released from these films and have exerted their antioxidant effect to increase the shelf life of carrots. Therefore, it clearly shows that packaging by the synthesized films decreased the weight loss of carrots and increased the overall acceptability.

6.5 Biodegradability and toxicity

Chitosan is being used in gene therapy due to its biocompatibility and low cytotoxicity (Sharma *et al.*, 2019). Chitosan films can be easily degraded into non-toxic counterparts and it is well determined that chitosan degradation depends on its de-acetylation degree and molecular mass or any modifications within its structure (Matica *et al.*, 2017). The degradation of chitosan based films can occur either through action of enzymes or chemicals and it mentions the breakdown of the chitosan polymer into smaller monomers (D-glucosamine, N-acetyl-glucosamine) (Sanchez-Salvador *et al.*, 2021). Lysozyme comes out to be main enzyme used for studying in vitro degradation of chitosan. However, in vivo degradation of chitosan can be studied via oral administration or subcutaneous/intravenous injections of chitosan to laboratory animals (Matica *et al.*, 2017).

In current study, biodegradability of synthesized chitosan nanocomposite films was compared both in lysozyme and soil. Our results show that all synthesized films (extract/polyphenol loaded) displayed increased degradation in soil than lysozyme. Soil microflora includes a mixture of microbial population including bacteria, protozoa, fungi and actinomycetes acting together while degradation (Singh G. P. *et al.*, 2022). The comparative low degradation in lysozyme may be because chitosan degradation in lysozyme mainly depends on pH of dissolving medium, lysozyme is only active at a pH of 6-9. Similar results have been reported in an earlier study showing inactivation of lysozyme because the initial pH of solution was not as required for enzyme activity that eventually resulted only chitosan dissolution in lysozyme instead of cleavage (Lončarević *et al.*, 2017). Another reason of this difference in degradation rate is the presence of chitosanase enzymes produced by soil bacteria which is more specific in

cleaving chitosan as compared to lysozyme as they cleave β -1,4-glycosidic linkage of chitosan to release chito-oligosaccharides (Liu *et al.*, 2009). Moreover, CNC reinforced polyphenol loaded films and extract loaded films exhibited increased degradation than control and NK reinforced polyphenol loaded films. It may be because chitosan film degradation highly depends on chemical modifications in their structure (Islam *et al.*, 2019). Furthermore, the different degradation rates of synthesized composite films may be due to difference in their molecular weight and degree of crystallinity. The degradation of all films was found to increase by increasing incubation time it may be because longer reaction time causes more water to diffuse from the soil into nanocomposite films causing them to swell and increase biodegradation (Kuo *et al.*, 2006).

SEM analysis was carried out to confirm the surface degradation. Correlating with above results, SEM images exhibited more degradation in soil as evident from large and deep holes in soil buried samples. It may also be because of unavailability of acetyl groups of chitosan in modified composites which are required for lysozyme binding and function (Lončarević *et al.*, 2017). FTIR analysis of degraded lysozyme incubated composites revealed the strong interaction of lysozyme with the films due to presence of sharp amide I and II bands at 1648 and 1548 cm^{-1} . As the FTIR spectrum of lysozyme has been previously shown to exhibit characteristic amide -I band at 1640 cm^{-1} (C=O; amide I) and 1525 cm^{-1} (-NH₂; amide II) of polypeptide chain (Sowjanya *et al.*, 2013). A decrease in intensity of C-O, OH, N-H bands was found in case of CS-CNC-NK-EX1 as compared to other films which correlates with increased % degradation of these composites. The decreased concentration of C-O bonds indicates the decomposition of chitosan into smaller units (Lončarević *et al.*, 2017). However, the entire mechanism of degradation could not be understood based on FT-IR results only.

To confirm the decreased thermal stability of degraded films, TGA and DSC analysis were carried out. TGA analysis showed that all composite films samples after exposure to soil or lysozyme showed degradation at lower temperatures than neat control. This indicates the effect of soil microflora and lysozyme action on breakdown of bonds in composite films leading to quick degradation.

DSC analysis of soil degraded nanocomposite films showed low melting temperatures and early denaturation as compared to both degraded and non-degraded neat chitosan

films. It is consistent with previous findings, where the lower melting point of soil degraded samples was reported (Vasile *et al.*, 2018). Original crystallinity of control chitosan was seen at 293°C while CS-CNC-NK-EX1 films displayed lower melting temperature and early degradation temperature (249°C) which is correlated with highest weight loss percentage after soil burial. It may be because a composite film biodegradability is promoted by many factors like higher molecular weight, amorphous structure, increased hydrophilicity as well presence of additives (Vasile *et al.*, 2018). Similar Increase in crystallinity was observed in case of soil degraded soy protein isolate, chicken feather derived CNC/MMT composites and PLA/ATBC/CS3 composite films depicted by previous researchers (Kaur *et al.*, 2018; Luzi *et al.*, 2015). This may suggest the early attack of soil microflora on amorphous region first during degradation of films.

In addition to biodegradability, toxicity of nanocomposite films is another important feature that needs be analyzed. In vitro hemo-compatibility is a required characteristic of polymer based materials such as sols, gels and nanocomposites specially when using for food packaging applications as they would be in contact with the food that is consumed by humans (Wijesinghe *et al.*, 2020). It is also considered as a measure of in vitro toxicity as polymers used in biomedical applications should not cause blood coagulation, thrombosis and red blood cell hemolysis. Therefore, in vitro compatibility with blood and some coagulation tests should be performed to see the influence of the nanocomposites on whole blood (Ni *et al.*, 2021). RBC's hemolysis is associated with some prothrombic changes as also seen in some hemolytic disorders (e.g sickle cell anemia) and is also characterized by the presence of free hemoglobin. Free hemoglobin is known to cause vasoconstriction by binding to nitric oxide and removing nitrogen oxide. It also increases the platelets reactivity and platelet adhesion to fibrinogen. This free hemoglobin released from RBC hemolysis can be measured spectrophotometric ally to help determine the hemolysis percentage (Torlopov *et al.*, 2021). ASTM F756-00 protocols have categorized the samples as hemolytic, slightly hemolytic and non-hemolytic with >5%, < 5% and <2% hemolysis percentage respectively (Pires *et al.*, 2018). Results of hemolytic assay suggest the non-hemolytic behavior of *A. subulatum*, *M. piperita* and vanillic acid incorporated films which depicts the safety of these nanocomposite films. Whereas all other film compositions exhibited slightly hemolytic character. This difference in hemolytic activity is dependent on the structure and

composition of nanocomposites. Several factors have impact on the hemolytic activity of nanocomposites such as their shape, charge, size, surface roughness and surface modification. A previous research has shown that surface changes can efficiently lessen the hemolytic activity of bare mesoporous silica nanoparticles (MSNs) (He *et al.*, 2010).

In vitro toxicity evaluation was followed by in vivo acute oral toxicity to further determine the safety of films. Throughout the two weeks' observation period all film treated rats behaved normally as that of control with a steady increase in body weight and no death was recorded. The hematopoietic system is regarded as the most susceptible to be targeted by the toxic substances, therefore, it was used in our study to evaluate the physiological and infectious status of rats. All the hematological parameters were found to be in the normal range after oral administration of films which indicated that these films pose no adverse effect on blood. This may be deduced because altered number of leukocytes or platelets usually indicate hepatic inflammation (Suljević *et al.*, 2022) which was not found in our study.

Clinical biochemistry analysis helps to investigate the toxicity effects on tissues, particularly on kidney and liver (Han *et al.*, 2016). In an effort to evaluate any hepatotoxicity caused by the films, liver function parameters were tested. The elevated serum levels of AST and ALT indicate the hepatocellular damage or cirrhosis. Estimation of ALT is considered more specific marker of liver damage as compared to AST. Literature reports also declare AST/ALT ratio in differentiating alcoholic from non-alcoholic liver diseases (Isa *et al.*, 2022). In our study, ALT, AST and total bilirubin levels were not altered in film treated rats indicating normal liver functioning. However, alkaline phosphatase levels were found to be elevated which might not arise from liver. This may be because ALP is found in high concentration in other organs like bone, kidney, placenta and intestine too so it is not a liver specific marker determining hepatotoxicity. Moreover, ALP levels can be moderately high in other pathological conditions like bone diseases, hodgkin lymphoma, heart failure or other infections. (Vishawanath *et al.*, 2023). The rise of ALT along with ALP should be concerning towards liver damage which was not seen in our study. Moreover, healthy state of all rats throughout the experiment also indicate that changes in ALP do not implicate hepatocellular injury, any alterations in bone metabolism or infection. Our results are in agreement with a recent study which reported that oral administration of

PLA/Ci/Lig-Np films resulted in higher ALP levels in rats which does not correspond to liver damage due to normal AST/ALT levels (Cerro *et al.*, 2021).

Kidney function parameters (such as urea, uric acid, creatinine and bilirubin) are considered as important markers for determining nephrotoxicity (Ali *et al.*, 2022). All these renal parameters of chitosan nanocomposite film treated rats were not found significantly different from the control group. It suggests that prepared chitosan nanocomposite film or their degradation metabolites did not induce renal changes at tested dose.

The obtained results are in agreement with another quercetin oral delivery study, which stated that 50 mg/ kg dose of quercetin to mice for 14weeks (98 days) can be regarded as safe with no effects on any organ function (Cunningham *et al.*, 2022). Moreover, CNC has also been proved to be non-toxic in an acute toxicity study where its LD50 was reported to be greater than 2000 mg/kg (Torlopov *et al.*, 2021). As far as Chitosan oral toxicity is concerned it was found to be nontoxic and was declared to have LD50 comparable to sucrose of >16 g/kg in oral administration to mice (Kean & Thanou, 2010). In another study, chitosan oral LD50 was reported to be 1.5 g/kg body weight in rats. Chitosan is regarded as non-toxic FDA approved biopolymer, however modifications in chitosan can make it either less toxic or more toxic. A nanocomposite size and surface charge greatly determines its toxicity in vivo. The modifications that do not affect the charge density on chitosan molecule usually do not cause toxic effects (Kean & Thanou, 2010). Therefore, non-toxic/biocompatible nature of prepared nanocomposite films can be concluded from the healthy state of rats in our study with no mortality as well as normal blood and organ function parameters upon oral ingestion of film

Conclusion and Future Prospective

Conclusion

The present study explains an efficient and low cost method for development of chitosan phyto-assisted nanocomposite food packaging films. Films with different ratios and combinations of nano fillers, plant extracts and polyphenols were synthesized and evaluated for their mechanical, barrier, thermal and biological properties. Our results indicate that addition of both CNC and NK (nano fillers) along with extract incorporation can result in 59% increase in tensile strength, 42% decrease in water vapor permeability, two-fold increase in opacity and enhanced thermal stability of chitosan films. Whereas, polyphenol incorporation in chitosan CNC films can bring about a bit more increased tensile strength (63%) with only 22% decreased water vapor permeability and 38% increase in opacity. Moreover, both polyphenol and extracts incorporated films were found to exhibit 70% free radical scavenging and moderate antimicrobial activities to be used as an active packaging for food preservation. The prepared nanocomposite films exhibited quick degradation in both soil and lysozyme confirming their biodegradability. *In vitro* hemo-compatibility analysis also proved the slight to non-hemolytic nature of prepared films confirming their safety. *In vivo* acute oral toxicity assay further confirmed that prepared films have no toxic effect and are biocompatible. Furthermore, the effect of prepared films on baby carrot packaging was also found to cause least weight changes in baby carrots over time thus ensuring the quality. Therefore, it can be concluded that data presented in this study can be potentially used to promote the synthesis of more active packaging films based on natural compounds, as well as different combination of nano fillers and additive can be tried to see their effect on properties of packaging films.

Future prospective

- Future studies can be carried out to see the release of extracts and polyphenols from the packaging films and interaction with food components
- Compression molding, electrospinning can be tried to make these films and a comparison can be drawn in properties of films synthesized through different techniques.

- Encapsulation techniques can be used to encapsulate particular therapeutic compound in these films for their use as nutritional supplement; however, their edible safe doses need to be determined.
- Further *in vivo* toxicity analysis can be carried out to determine safety of the prepared films.

References

REFERENCES

- Abdollahi, M., Rezaei, M., & Farzi, G. (2012). Improvement of active chitosan film properties with rosemary essential oil for food packaging. *International journal of food science & technology*, 47(4), 847-853.
- Abeysekera, W., Premakumara, G., & Ratnasooriya, W. (2013). In vitro antioxidant properties of leaf and bark extracts of ceylon cinnamon (*Cinnamomum zeylanicum* Blume). *Tropical Agricultural Research*, 24 (2), 128 - 138
- Adarsh, A., Chettiyar, B., Kanthesh, B., & Raghu, N. (2020). Phytochemical screening and antimicrobial activity of "Cinnamon zeylanicum". *International Journal of Pharmaceutical Research and Innovation*, 13, 22-33.
- Agarwal, H., Nakara, A., Menon, S., & Shanmugam, V. (2019). Eco-friendly synthesis of zinc oxide nanoparticles using *Cinnamomum Tamala* leaf extract and its promising effect towards the antibacterial activity. *Journal of Drug Delivery Science and Technology*, 53, 101212.
- Agnihotri, S., & Wakode, S. (2010). Antimicrobial activity of essential oil and various extracts of fruits of greater cardamom. *Indian journal of pharmaceutical sciences*, 72(5), 657.
- Aguirre-Loredo, R. Y., Rodríguez-Hernández, A. I., Morales-Sánchez, E., Gómez-Aldapa, C. A., & Velazquez, G. (2016). Effect of equilibrium moisture content on barrier, mechanical and thermal properties of chitosan films. *Food Chemistry*, 196, 560-566.
- Ahmad, A. A., & Sarbon, N. M. (2021). A comparative study: Physical, mechanical and antibacterial properties of bio-composite gelatin films as influenced by chitosan and zinc oxide nanoparticles incorporation. *Food bioscience*, 43, 101250.
- Ahmadi, S., Hivechi, A., Bahrami, S. H., Milan, P. B., & Ashraf, S. S. (2021). Cinnamon extract loaded electrospun chitosan/gelatin membrane with antibacterial activity. *International Journal of Biological Macromolecules*, 173, 580-590.
- Ahmed, M., Fatima, H., Qasim, M., & Gul, B. (2017). Polarity directed optimization of phytochemical and in vitro biological potential of an indigenous folklore: *Quercus dilatata* Lindl. ex Royle. *BMC complementary and alternative medicine*, 17(1), 1-16.
- Akarca, G. (2019). Composition and antibacterial effect on food borne pathogens of *Hibiscus sarrattensis* L. calyces essential oil. *Industrial crops and products*, 137, 285-289.
- Al Aboody, M. S., & Mickymaray, S. (2020). Anti-fungal efficacy and mechanisms of flavonoids. *Antibiotics*, 9(2), 45.
- Algburi, A., Asghar, A., Huang, Q., Mustfa, W., Javed, H. U., Zehm, S., & Chikindas, M. L. (2021). Black cardamom essential oil prevents *Escherichia coli* O157: H7 and *Salmonella Typhimurium* JSG 1748 biofilm formation through inhibition of quorum sensing. *Journal of Food Science and Technology*, 58(8), 3183-3191.
- Alghuthaymi, M. A., Diab, A. M., Elzahy, A. F., Mazrou, K. E., Tayel, A. A., & Moussa, S. H. (2021). Green biosynthesized selenium nanoparticles by cinnamon extract and their antimicrobial activity and application as edible coatings with nano-chitosan. *Journal of Food Quality*, 2021.
- Ali, A., Ali, A., Ahmad, W., Amir, M., Ashraf, K., Wahab, S., Alam, P., & Ahamad, A. (2022). Nephroprotective effect of polyphenol-rich extract of *Costus spicatus* in cisplatin-induced nephrotoxicity in Wistar albino rats. *3 Biotech*, 12(9), 189.
- Alirezalu, K., Pirouzi, S., Yaghoubi, M., Karimi-Dehkordi, M., Jafarzadeh, S., & Khaneghah, A. M. (2021). Packaging of beef fillet with active chitosan film incorporated with ϵ -polylysine: An assessment of quality indices and shelf life. *Meat Science*, 176, 108475.
- Alvarez, M. V., Ponce, A. G., & Moreira, M. d. R. (2013). Antimicrobial efficiency of chitosan coating enriched with bioactive compounds to improve the safety of fresh cut broccoli. *LWT-Food Science and Technology*, 50(1), 78-87.

- An, J., Bi, Y.-Y., Yang, C.-X., Hu, F.-D., & Wang, C.-M. (2013). Electrochemical study and application on rutin at chitosan/graphene films modified glassy carbon electrode. *Journal of Pharmaceutical Analysis*, 3(2), 102-108.
- Appell, M., Tu, Y.-S., Compton, D. L., Evans, K. O., & Wang, L. C. (2020). Quantitative structure-activity relationship study for prediction of antifungal properties of phenolic compounds. *Structural Chemistry*, 31(4), 1621-1630.
- Arfat, Y. A., Benjakul, S., Prodpran, T., Sumpavapol, P., & Songtipya, P. (2014). Properties and antimicrobial activity of fish protein isolate/fish skin gelatin film containing basil leaf essential oil and zinc oxide nanoparticles. *Food Hydrocolloids*, 41, 265-273.
- Ashraf, S. A., Siddiqui, A. J., Abd Elmoneim, O. E., Khan, M. I., Patel, M., Alreshidi, M., Moin, A., Singh, R., Snoussi, M., & Adnan, M. (2021). Innovations in nanoscience for the sustainable development of food and agriculture with implications on health and environment. *Science of the Total Environment*, 768, 144990.
- Avella, M., De Vlieger, J. J., Errico, M. E., Fischer, S., Vacca, P., & Volpe, M. G. (2005). Biodegradable starch/clay nanocomposite films for food packaging applications. *Food Chemistry*, 93(3), 467-474.
- Awasthi, S. K., Kumar, M., Kumar, V., Sarsaiya, S., Anerao, P., Ghosh, P., Singh, L., Liu, H., Zhang, Z., & Awasthi, M. K. (2022). A comprehensive review on recent advancements in biodegradation and sustainable management of biopolymers. *Environmental Pollution*, 307, 119600.
- Azarmi-Atajan, F., & Sayyari-Zohan, M. H. (2020). Alleviation of salt stress in lettuce (*Lactuca sativa* L.) by plant growth-promoting rhizobacteria. *Journal of Horticulture and Postharvest Research*, 3(7), 67-78.
- Azeem, M., Hanif, M., Mahmood, K., Ameer, N., Chughtai, F. R. S., & Abid, U. (2022). An insight into anticancer, antioxidant, antimicrobial, antidiabetic and anti-inflammatory effects of quercetin: A review. *Polymer Bulletin*, 80, 241-262.
- Azeredo, H. M., Mattoso, L. H. C., Avena-Bustillos, R. J., Filho, G. C., Munford, M. L., Wood, D., & McHugh, T. H. (2010). Nanocellulose reinforced chitosan composite films as affected by nanofiller loading and plasticizer content. *Journal of Food Science*, 75(1), 1-7.
- Azizi, S., Ahmad, M. B., Ibrahim, N. A., Hussein, M. Z., & Namvar, F. (2014). Cellulose nanocrystals/ZnO as a bifunctional reinforcing nanocomposite for poly (vinyl alcohol)/chitosan blend films: fabrication, characterization and properties. *International journal of molecular sciences*, 15(6), 11040-11053.
- Azmana, M., Mahmood, S., Hilles, A. R., Rahman, A., Arifin, M. A. B., & Ahmed, S. (2021). A review on chitosan and chitosan-based bionanocomposites: Promising material for combatting global issues and its applications. *International Journal of Biological Macromolecules*, 185, 832-848.
- Baig, M. W., Nasir, B., Waseem, D., Majid, M., Khan, M. Z. I., & Haq, I.-u. (2020). Withametelin: a biologically active withanolide in cancer, inflammation, pain and depression. *Saudi Pharmaceutical Journal*, 28(12), 1526-1537.
- Bakshi, P. S., Selvakumar, D., Kadirvelu, K., & Kumar, N. (2020). Chitosan as an environment friendly biomaterial—a review on recent modifications and applications. *International Journal of Biological Macromolecules*, 150, 1072-1083.
- Balti, R., Mansour, M. B., Sayari, N., Yacoubi, L., Rabaoui, L., Brodu, N., & Massé, A. (2017). Development and characterization of bioactive edible films from spider crab (*Maja crispata*) chitosan incorporated with *Spirulina* extract. *International Journal of Biological Macromolecules*, 105, 1464-1472.
- Beyki, M., Zhavah, S., Khalili, S. T., Rahmani-Cherati, T., Abollahi, A., Bayat, M., Tabatabaei, M., & Mohsenifar, A. (2014). Encapsulation of *Mentha piperita* essential oils in chitosan—

- cinnamic acid nanogel with enhanced antimicrobial activity against *Aspergillus flavus*. *Industrial crops and products*, 54, 310-319.
- Bi, F., Zhang, X., Bai, R., Liu, Y., Liu, J., & Liu, J. (2019). Preparation and characterization of antioxidant and antimicrobial packaging films based on chitosan and proanthocyanidins. *International Journal of Biological Macromolecules*, 134, 11-19.
- Bonilla, J., Poloni, T., Lourenço, R. V., & Sobral, P. J. (2018). Antioxidant potential of eugenol and ginger essential oils with gelatin/chitosan films. *Food bioscience*, 23, 107-114.
- Bustamante-Torres, M., Romero-Fierro, D., Arcenales-Vera, B., Pardo, S., & Bucio, E. (2021). Interaction between filler and polymeric matrix in nanocomposites: Magnetic approach and applications. *Polymers*, 13(17), 2998.
- Cai, M., Wang, Y., Wang, R., Li, M., Zhang, W., Yu, J., & Hua, R. (2022). Antibacterial and antibiofilm activities of chitosan nanoparticles loaded with *Ocimum basilicum* L. essential oil. *International Journal of Biological Macromolecules*, 202, 122-129.
- Cao, W., Li, Z., Sheng, G., & Jiang, X. (2017). Insulating property of polypropylene nanocomposites filled with nano-MgO of different concentration. *IEEE Transactions on Dielectrics and Electrical Insulation*, 24(3), 1430-1437.
- Cao, X., Dong, H., Li, C. M., & Lucia, L. A. (2009). The enhanced mechanical properties of a covalently bound chitosan-multiwalled carbon nanotube nanocomposite. *Journal of Applied Polymer Science*, 113(1), 466-472.
- Cazón, P., & Vázquez, M. (2020). Mechanical and barrier properties of chitosan combined with other components as food packaging film. *Environmental Chemistry Letters*, 18(2), 257-267.
- Cerro, D., Bustos, G., Villegas, C., Buendia, N., Truffa, G., Godoy, M. P., Rodríguez, F., Rojas, A., Galotto, M. J., & Constandil, L. (2021). Effect of supercritical incorporation of cinnamaldehyde on physical-chemical properties, disintegration and toxicity studies of PLA/lignin nanocomposites. *International Journal of Biological Macromolecules*, 167, 255-266.
- Chatterjee, N. S., Panda, S. K., Navitha, M., Asha, K., Anandan, R., & Mathew, S. (2015). Vanillic acid and coumaric acid grafted chitosan derivatives: improved grafting ratio and potential application in functional food. *Journal of Food Science and Technology*, 52(11), 7153-7162.
- Chen, P., Xie, F., & McNally, T. (2021). Understanding the effects of montmorillonite and sepiolite on the properties of solution-cast chitosan and chitosan/silk peptide composite films. *Polymer International*, 70(5), 527-535.
- Chen, P., Xie, F., Tang, F., & McNally, T. (2021). Influence of plasticiser type and nanoclay on the properties of chitosan-based materials. *European Polymer Journal*, 144, 110225.
- Chen, P., & Zhang, L. (2006). Interaction and properties of highly exfoliated soy protein/montmorillonite nanocomposites. *Biomacromolecules*, 7(6), 1700-1706.
- Chivrac, F., Pollet, E., & Averous, L. (2009). Progress in nano-biocomposites based on polysaccharides and nanoclays. *Materials Science and Engineering: R: Reports*, 67(1), 1-17.
- Christ-Ribeiro, A., Graça, C., Kupski, L., Badiale-Furlong, E., & de Souza-Soares, L. (2019). Cytotoxicity, antifungal and anti mycotoxins effects of phenolic compounds from fermented rice bran and *Spirulina* sp. *Process Biochemistry*, 80, 190-196.
- Cunningham, P., Patton, E., VanderVeen, B. N., Unger, C., Aladhami, A., Enos, R. T., Madero, S., Chatzistamou, I., Fan, D., & Murphy, E. A. (2022). Sub-chronic oral toxicity screening of quercetin in mice. *BMC Complementary Medicine and Therapies*, 22(1), 1-12.
- Das, P. P., Chaudhary, V., Ahmad, F., & Manral, A. (2021). Effect of nanotoxicity and enhancement in performance of polymer composites using nanofillers: A state-of-the-art review. *Polymer Composites*, 42(5), 2152-2170.

- Das, S., Singh, V. K., Dwivedy, A. K., Chaudhari, A. K., Upadhyay, N., Singh, P., Sharma, S., & Dubey, N. K. (2019). Encapsulation in chitosan-based nanomatrix as an efficient green technology to boost the antimicrobial, antioxidant and in situ efficacy of *Coriandrum sativum* essential oil. *International Journal of Biological Macromolecules*, *133*, 294-305.
- Dayarian, S., Zamani, A., Moheb, A., & Masoomi, M. (2014). Physico-mechanical properties of films of chitosan, carboxymethyl chitosan, and their blends. *Journal of Polymers and the Environment*, *22*(3), 409-416.
- de Arruda, I. N. Q., Pereira, V. A., & Stefani, R. (2017). Application of chitosan matrix for delivery of rutin. *Journal of the Iranian Chemical Society*, *14*(3), 561-566.
- Desta, I. T., Porter, K. A., Xia, B., Kozakov, D., & Vajda, S. (2020). Performance and its limits in rigid body protein-protein docking. *Structure*, *28*(9), 1071-1081. e1073.
- Díaz-Montes, E., & Castro-Muñoz, R. (2021). Edible films and coatings as food-quality preservers: An overview. *Foods*, *10*(2), 249.
- Diyana, Z., Jumaidin, R., Selamat, M. Z., Ghazali, I., Julmohammad, N., Huda, N., & Ilyas, R. (2021). Physical properties of thermoplastic starch derived from natural resources and its blends: a review. *Polymers*, *13*(9), 1396.
- Drishya, S., Dhanisha, S. S., & Guruvayoorappan, C. (2022). Antioxidant-rich fraction of *Amomum subulatum* fruits mitigates experimental methotrexate-induced oxidative stress by regulating TNF- α , IL-1 β , and IL-6 proinflammatory cytokines. *Journal of Food Biochemistry*, *46*(4), 13855.
- El Miri, N., Abdelouahdi, K., Zahouily, M., Fihri, A., Barakat, A., Solhy, A., & El Achaby, M. (2015). Bio-nanocomposite films based on cellulose nanocrystals filled polyvinyl alcohol/chitosan polymer blend. *Journal of Applied Polymer Science*, *132*(22).
- Erken, İ., Şahin, S., Karkar, B., Akça, B., & Özakin, C. (2022). Chitosan based edible film incorporating different *Prunella L.* extracts, characterization and their antioxidant properties. *Journal of Food Processing and Preservation*, *46*(7), e16658.
- Fernandes, B. C. N., Paulo, B. B., Guimarães, M. C., Sarantopoulos, C. I. G. d. L., de Melo, N. R., & Prata, A. S. (2022). Prospection of the use of encapsulation in food packaging. *Comprehensive Reviews in Food Science and Food Safety*, *21*(3), 2309-2334.
- Flórez, M., Guerra-Rodríguez, E., Cazón, P., & Vázquez, M. (2022). Chitosan for food packaging: Recent advances in active and intelligent films. *Food Hydrocolloids*, *124*, 107328.
- Foo, S. C., Yusoff, F. M., Ismail, M., Basri, M., Yau, S. K., Khong, N. M., Chan, K. W., & Ebrahimi, M. (2017). Antioxidant capacities of fucoxanthin-producing algae as influenced by their carotenoid and phenolic contents. *Journal of biotechnology*, *241*, 175-183.
- Gallego-Schmid, A., Mendoza, J. M. F., & Azapagic, A. (2019). Environmental impacts of takeaway food containers. *Journal of Cleaner Production*, *211*, 417-427.
- Gan, P. G., Sam, S. T., Abdullah, M., Omar, M. F., & Tan, W. K. (2021). Water resistance and biodegradation properties of conventionally-heated and microwave-cured cross-linked cellulose nanocrystal/chitosan composite films. *Polymer Degradation and Stability*, *188*, 109563.
- Gao, L., Zhu, T., He, F., Ou, Z., Xu, J., & Ren, L. (2021). Preparation and characterization of functional films based on chitosan and corn starch incorporated tea polyphenols. *Coatings*, *11*(7), 817.
- Gao, Z., Wang, C., & Li, Z. (2021). Effect of ethanol extract of black soybean coat on physicochemical properties and biological activities of chitosan packaging film. *Food Science and Biotechnology*, *30*(10), 1369-1381.
- Gautam, K., Vishvakarma, R., Sharma, P., Singh, A., Gaur, V. K., Varjani, S., & Srivastava, J. K. (2022). Production of biopolymers from food waste: Constrains and perspectives. *Bioresource Technology*, *361*, 127650.

- Gholamipourfard, K., Salehi, M., & Banchio, E. (2021). Mentha piperita phytochemicals in agriculture, food industry and medicine: Features and applications. *South African Journal of Botany*, *141*, 183-195.
- Gruppuso, M., Iorio, F., Turco, G., Marsich, E., & Porrelli, D. (2022). Hyaluronic acid/lactose-modified chitosan electrospun wound dressings—Crosslinking and stability criticalities. *Carbohydrate Polymers*, *288*, 119375.
- Hafsa, J., Ali Smach, M., Khedher, M. R. B., Charfeddine, B., Limem, K., Majdoub, H., & Rouatbi, S. (2016). Physical, antioxidant and antimicrobial properties of chitosan films containing Eucalyptus globulus essential oil. *LWT-Food Science and Technology*, *68*, 356-364.
- Haghighi, H., Licciardello, F., Fava, P., Siesler, H. W., & Pulvirenti, A. (2020). Recent advances on chitosan-based films for sustainable food packaging applications. *Food Packaging and Shelf Life*, *26*, 100551.
- Han, S. H., Suh, H. J., Hong, K. B., Kim, S. Y., & Min, S. C. (2016). Oral toxicity of cold plasma-treated edible films for food coating. *Journal of Food Science*, *81*(12), 52-57.
- Han, Y. (2009). Rutin has therapeutic effect on septic arthritis caused by Candida albicans. *International immunopharmacology*, *9*(2), 207-211.
- Hassan, W., Kazmi, S. Z., Noreen, H., Riaz, A., & Zaman, B. (2016). Antimicrobial activity of cinnamomum tamala leaves. *Journal of Nutritional Disorders & Therapy*, *6*(2), 1000190.
- He, F., Wang, W., Wu, M., Fang, Y., Wang, S., Yang, Y., Ye, C., & Xiang, F. (2020). Antioxidant and antibacterial activities of essential oil from Atractylodes lancea rhizomes. *Industrial crops and products*, *153*, 112552.
- He, Q., Zhang, J., Shi, J., Zhu, Z., Zhang, L., Bu, W., Guo, L., & Chen, Y. (2010). The effect of PEGylation of mesoporous silica nanoparticles on nonspecific binding of serum proteins and cellular responses. *Biomaterials*, *31*(6), 1085-1092.
- Hiremani, V. D., Goudar, N., Gasti, T., Khanapure, S., Vanjeri, V. N., Sataraddi, S., D'souza, O. J., Vootla, S. K., Masti, S. P., & Malabadi, R. B. (2022). Exploration of multifunctional properties of piper betel leaves extract incorporated polyvinyl alcohol-oxidized maize starch blend films for active packaging applications. *Journal of Polymers and the Environment*, *30*(4), 1314-1329.
- Hossain, A., Skalicky, M., Brestic, M., Mahari, S., Kerry, R. G., Maitra, S., Sarkar, S., Saha, S., Bhadra, P., & Popov, M. (2021). Application of nanomaterials to ensure quality and nutritional safety of food. *Journal of Nanomaterials*, *2021*.
- Hu, B., Liu, X., Zhang, C., & Zeng, X. (2017). Food macromolecule based nanodelivery systems for enhancing the bioavailability of polyphenols. *Journal of food and drug analysis*, *25*(1), 3-15.
- Hu, W., Li, C., Dai, J., Cui, H., & Lin, L. (2019). Antibacterial activity and mechanism of Litsea cubeba essential oil against methicillin-resistant Staphylococcus aureus (MRSA). *Industrial crops and products*, *130*, 34-41.
- Huang, D., Zhang, Z., Zheng, Y., Quan, Q., Wang, W., & Wang, A. (2020). Synergistic effect of chitosan and halloysite nanotubes on improving agar film properties. *Food Hydrocolloids*, *101*, 105471.
- Huq, T., Salmieri, S., Khan, A., Khan, R. A., Le Tien, C., Riedl, B., Frascini, C., Bouchard, J., Uribe-Calderon, J., & Kamal, M. R. (2012). Nanocrystalline cellulose (NCC) reinforced alginate based biodegradable nanocomposite film. *Carbohydrate Polymers*, *90*(4), 1757-1763.
- Ilyas, R. A., Aisyah, H. A., Nordin, A. H., Ngadi, N., Zuhri, M. Y. M., Asyraf, M. R. M., Sapuan, S. M., Zainudin, E. S., Sharma, S., & Abral, H. (2022). Natural-Fiber-Reinforced Chitosan, Chitosan Blends and Their Nanocomposites for Various Advanced Applications. *Polymers*, *14*(5), 874.

- Isa, A., Muhammad, M., Hudu, A., Jamba, B., & Magaji, M. (2022). Hepatotoxic Evaluation of Carboxymethylcellulose in Adult Wistar Rats. *Journal of Medical and Basic Scientific Research*, 3(2), 33-40.
- Islam, N., Dmour, I., & Taha, M. O. (2019). Degradability of chitosan micro/nanoparticles for pulmonary drug delivery. *Heliyon*, 5(5), e01684.
- Isogai, A. (2021). Emerging nanocellulose technologies: Recent developments. *Advanced Materials*, 33(28), 2000630.
- Jadhav, A. K., Khan, P. K., & Karuppaiyil, S. M. (2020). Phytochemicals as potential inhibitors of lanosterol 14 α -demethylase (CYP51) enzyme: An in silico study on sixty molecules. *International Journal of Applied Pharmaceutics*, 12(4), 18-30.
- Jafarzadeh, S., Jafari, S. M., Salehabadi, A., Nafchi, A. M., Kumar, U. S. U., & Khalil, H. A. (2020). Biodegradable green packaging with antimicrobial functions based on the bioactive compounds from tropical plants and their by-products. *Trends in food science & technology*, 100, 262-277.
- Jain, A., & Jain, S. K. (2015). Environmentally responsive chitosan-based nanocarriers (CBNs). *Handbook of polymers for pharmaceutical technologies, biodegradable polymers*, 3, 105.
- Jatav, J., Tarafdar, A., Saravanan, C., & Bhattacharya, B. (2022). Assessment of Antioxidant and Antimicrobial Property of Polyphenol-Rich Chitosan-Pineapple Peel Film. *Journal of Food Quality*, 2022.
- Jiang, L., Luo, Z., Liu, H., Wang, F., Li, H., Gao, H., & Zhang, H. (2021). Preparation and characterization of chitosan films containing lychee (*Litchi chinensis* sonn.) pericarp powder and their application as active food packaging. *Foods*, 10(11), 2834.
- John, M. J., & Thomas, S. (2008). Biofibres and biocomposites. *Carbohydrate Polymers*, 71(3), 343-364.
- Jose, T., George, S. C., Maria, H. J., Wilson, R., & Thomas, S. (2014). Effect of bentonite clay on the mechanical, thermal, and pervaporation performance of the poly (vinyl alcohol) nanocomposite membranes. *Industrial & Engineering Chemistry Research*, 53(43), 16820-16831.
- Kaboorani, A., & Riedl, B. (2015). Surface modification of cellulose nanocrystals (CNC) by a cationic surfactant. *Industrial Crops and Products*, 65, 45-55.
- Kaczmarek, B., Nadolna, K., Owczarek, A., Michalska-Sionkowska, M., & Sionkowska, A. (2019). The characterization of thin films based on chitosan and tannic acid mixture for potential applications as wound dressings. *Polymer Testing*, 78, 106007.
- Kalia, A., Kaur, M., Shami, A., Jawandha, S. K., Alghuthaymi, M. A., Thakur, A., & Abd-Elsalam, K. A. (2021). Nettle-Leaf extract derived ZnO/CuO nanoparticle-biopolymer-based antioxidant and antimicrobial nanocomposite packaging films and their impact on extending the post-harvest shelf life of guava fruit. *Biomolecules*, 11(2), 224.
- Kanatt, S. R., Rao, M., Chawla, S., & Sharma, A. (2012). Active chitosan–polyvinyl alcohol films with natural extracts. *Food Hydrocolloids*, 29(2), 290-297.
- Kang, X., Kuga, S., Wang, C., Zhao, Y., Wu, M., & Huang, Y. (2018). Green preparation of cellulose nanocrystal and its application. *ACS Sustainable Chemistry & Engineering*, 6(3), 2954-2960.
- Kapetanakou, A. E., & Skandamis, P. N. (2016). Applications of active packaging for increasing microbial stability in foods: Natural volatile antimicrobial compounds. *Current Opinion in Food Science*, 12, 1-12.
- Kaur, M., Arshad, M., & Ullah, A. (2018). In-situ nanoreinforced green bionanomaterials from natural keratin and montmorillonite (MMT)/cellulose nanocrystals (CNC). *ACS Sustainable Chemistry & Engineering*, 6(2), 1977-1987.
- Kean, T., & Thanou, M. (2010). Biodegradation, biodistribution and toxicity of chitosan. *Advanced drug delivery reviews*, 62(1), 3-11.

- Khan, A., Khan, R. A., Salmieri, S., Le Tien, C., Riedl, B., Bouchard, J., Chauve, G., Tan, V., Kamal, M. R., & Lacroix, M. (2012). Mechanical and barrier properties of nanocrystalline cellulose reinforced chitosan based nanocomposite films. *Carbohydrate Polymers*, *90*(4), 1601-1608.
- Khan, M., Tareq, F., Hossen, M., & Roki, M. (2018). Green synthesis and characterization of silver nanoparticles using *Coriandrum sativum* leaf extract. *Journal of Engineering Science and Technology*, *13*(1), 158-166.
- Khan, Y., Khan, S. M., ul Haq, I., Farzana, F., Abdullah, A., Abbasi, A. M., Alamri, S., Hashem, M., Sakhi, S., & Asif, M. (2021). Antioxidant potential in the leaves of grape varieties (*Vitis vinifera* L.) grown in different soil compositions. *Arabian Journal of Chemistry*, *14*(11), 103412.
- Khanzada, B., Akhtar, N., Okla, M. K., Alamri, S. A., Al-Hashimi, A., Baig, M. W., Rubnawaz, S., AbdElgawad, H., Hirad, A. H., & Haq, I.-U. (2021). Profiling of Antifungal Activities and In Silico Studies of Natural Polyphenols from Some Plants. *Molecules*, *26*(23), 7164.
- Kouser, S., Sheik, S., Nagaraja, G., Prabhu, A., Prashantha, K., D'souza, J. N., Navada, K. M., & Manasa, D. (2020). Functionalization of halloysite nanotube with chitosan reinforced poly (vinyl alcohol) nanocomposites for potential biomedical applications. *International Journal of Biological Macromolecules*, *165*, 1079-1092.
- Kowalska, J., Tyburski, J., Krzysińska, J., & Jakubowska, M. (2020). Cinnamon powder: an in vitro and in vivo evaluation of antifungal and plant growth promoting activity. *European Journal of Plant Pathology*, *156*(1), 237-243.
- Kumar, S., Ye, F., Dobretsov, S., & Dutta, J. (2019). Chitosan nanocomposite coatings for food, paints, and water treatment applications. *Applied Sciences*, *9*(12), 2409.
- Kuo, P.-C., Sahu, D., & Yu, H. H. (2006). Properties and biodegradability of chitosan/nylon 11 blending films. *Polymer Degradation and Stability*, *91*(12), 3097-3102.
- Kurek, M., Garofulić, I. E., Bakić, M. T., Ščetar, M., & Uzelac, V. D. (2018). Development and evaluation of a novel antioxidant and pH indicator film based on chitosan and food waste sources of antioxidants. *Food Hydrocolloids*, *84*, 238-246.
- Kuttalam, K. C., Karuppiyah, G., Palaniappan, M., Santulli, C., & Palanisamy, S. (2021). Mechanical and Impact Strength of Nanoclay-Filled Composites: A Short Review. *Journal of Materials Science Research and Reviews*, *7*, 7-20.
- Lavorgna, M., Attianese, I., Buonocore, G., Conte, A., Del Nobile, M. A., Tescione, F., & Amendola, E. (2014). MMT-supported Ag nanoparticles for chitosan nanocomposites: structural properties and antibacterial activity. *Carbohydrate Polymers*, *102*, 385-392.
- Leceta, I., Molinaro, S., Guerrero, P., Kerry, J., & De la Caba, K. (2015). Quality attributes of map packaged ready-to-eat baby carrots by using chitosan-based coatings. *Postharvest Biology and Technology*, *100*, 142-150.
- Leceta, I., Peñalba, M., Arana, P., Guerrero, P., & De La Caba, K. (2015). Ageing of chitosan films: Effect of storage time on structure and optical, barrier and mechanical properties. *European Polymer Journal*, *66*, 170-179.
- Lee, H., Woo, E.-R., & Lee, D. G. (2018). Apigenin induces cell shrinkage in *Candida albicans* by membrane perturbation. *FEMS yeast research*, *18*(1), foy003.
- Lee, S.-Y., Mohan, D. J., Kang, I.-A., Doh, G.-H., Lee, S., & Han, S. O. (2009). Nanocellulose reinforced PVA composite films: effects of acid treatment and filler loading. *Fibers and Polymers*, *10*(1), 77-82.
- Leistner, L. (2000). Basic aspects of food preservation by hurdle technology. *International journal of food microbiology*, *55*(1-3), 181-186.
- Leite, L. S. F., Pham, C., Bilatto, S., Azeredo, H. M., Cranston, E. D., Moreira, F. K., Mattoso, L. H. C., & Bras, J. (2021). Effect of tannic acid and cellulose nanocrystals on antioxidant and antimicrobial properties of gelatin films. *ACS Sustainable Chemistry & Engineering*, *9*(25), 8539-8549.

- Liu, J., Boo, W.-J., Clearfield, A., & Sue, H.-J. (2006). Intercalation and exfoliation: a review on morphology of polymer nanocomposites reinforced by inorganic layer structures. *Materials and Manufacturing Processes*, 21(2), 143-151.
- Liu, J., Liu, S., Wu, Q., Gu, Y., Kan, J., & Jin, C. (2017). Effect of protocatechuic acid incorporation on the physical, mechanical, structural and antioxidant properties of chitosan film. *Food Hydrocolloids*, 73, 90-100.
- Liu, J., Meng, C.-g., Liu, S., Kan, J., & Jin, C.-h. (2017). Preparation and characterization of protocatechuic acid grafted chitosan films with antioxidant activity. *Food Hydrocolloids*, 63, 457-466.
- Liu, J., Song, F., Chen, R., Deng, G., Chao, Y., Yang, Z., Wu, H., Bai, M., Zhang, P., & Hu, Y. (2022). Effect of cellulose nanocrystal-stabilized cinnamon essential oil Pickering emulsions on structure and properties of chitosan composite films. *Carbohydrate Polymers*, 275, 118704.
- Liu, Y.-L., Jiang, S., Ke, Z.-M., Wu, H.-S., Chi, C.-W., & Guo, Z.-Y. (2009). Recombinant expression of a chitosanase and its application in chitosan oligosaccharide production. *Carbohydrate Research*, 344(6), 815-819.
- Liu, Y., Wang, S., & Lan, W. (2018). Fabrication of antibacterial chitosan-PVA blended film using electrospray technique for food packaging applications. *International Journal of Biological Macromolecules*, 107, 848-854.
- Lončarević, A., Ivanković, M., & Rogina, A. (2017). Lysozyme-induced degradation of chitosan: the characterisation of degraded chitosan scaffolds. *Journal of Tissue Repair and Regeneration*, 1, 12-22.
- López de Dicastillo, C., Garrido, L., Velásquez, E., Rojas, A., & Gavara, R. (2021). Designing biodegradable and active multilayer system by assembling an electrospun polycaprolactone mat containing quercetin and nanocellulose between polylactic acid films. *Polymers*, 13(8), 1288.
- López de Dicastillo, C., Velásquez, E., Rojas, A., Guarda, A., & Galotto, M. J. (2020). The use of nanoadditives within recycled polymers for food packaging: Properties, recyclability, and safety. *Comprehensive Reviews in Food Science and Food Safety*, 19(4), 1760-1776.
- Luzi, F., Fortunati, E., Puglia, D., Petrucci, R., Kenny, J., & Torre, L. (2015). Study of disintegrability in compost and enzymatic degradation of PLA and PLA nanocomposites reinforced with cellulose nanocrystals extracted from *Posidonia Oceanica*. *Polymer Degradation and Stability*, 121, 105-115.
- Ma, Y., Zhao, H., Ma, Q., Cheng, D., Zhang, Y., Wang, W., Wang, J., & Sun, J. (2022). Development of chitosan/potato peel polyphenols nanoparticles driven extended-release antioxidant films based on potato starch. *Food Packaging and Shelf Life*, 31, 100793.
- Mahmoud, K. A., Mena, J. A., Male, K. B., Hrapovic, S., Kamen, A., & Luong, J. H. (2010). Effect of surface charge on the cellular uptake and cytotoxicity of fluorescent labeled cellulose nanocrystals. *ACS applied materials & interfaces*, 2(10), 2924-2932.
- Mal, D., Gharde, S., & Chatterjee, R. (2018). Chemical constituent of *Cinnamomum tamala*: An important tree spices. *International journal of current microbiology and applied sciences*, 7(4), 648-651.
- Malas, A., & Das, C. K. (2015). Effect of graphene oxide on the physical, mechanical and thermo-mechanical properties of neoprene and chlorosulfonated polyethylene vulcanizates. *Composites Part B: Engineering*, 79, 639-648.
- Mandal, S. M., Dias, R. O., & Franco, O. L. (2017). Phenolic compounds in antimicrobial therapy. *Journal of medicinal food*, 20(10), 1031-1038.
- Matica, A., Menghiu, G., & Ostafe, V. (2017). BIODEGRADABILITY OF CHITOSAN BASED PRODUCTS. *New Frontiers in Chemistry*, 26(1), 75-86.

- Merino, D., Mansilla, A. Y., Gutiérrez, T. J., Casalongué, C. A., & Alvarez, V. A. (2018). Chitosan coated-phosphorylated starch films: Water interaction, transparency and antibacterial properties. *Reactive and Functional Polymers*, *131*, 445-453.
- Mhatre, S., & Patravale, V. (2021). Drug repurposing of triazoles against mucormycosis using molecular docking: A short communication. *Computers in Biology and Medicine*, *136*, 104722.
- Moalla, S., Ammar, I., Fauconnier, M.-L., Danthine, S., Blecker, C., Besbes, S., & Attia, H. (2021). Development and characterization of chitosan films carrying Artemisia campestris antioxidants for potential use as active food packaging materials. *International Journal of Biological Macromolecules*, *183*, 254-266.
- Mohammed, M. A., Syeda, J. T., Wasan, K. M., & Wasan, E. K. (2017). An overview of chitosan nanoparticles and its application in non-parenteral drug delivery. *Pharmaceutics*, *9*(4), 53.
- Mohebi, E., & Shahbazi, Y. (2017). Application of chitosan and gelatin based active packaging films for peeled shrimp preservation: A novel functional wrapping design. *LWT-Food Science and Technology*, *76*, 108-116.
- Mojally, M., Sharmin, E., Obaid, N. A., Alhindi, Y., & Abdalla, A. N. (2022). Polyvinyl alcohol/corn starch/castor oil hydrogel films, loaded with silver nanoparticles biosynthesized in Mentha piperita leaves' extract. *Journal of King Saud University-Science*, *34*(4), 101879.
- Mouhoub, A., Guendouz, A., Belkamel, A., El Alaoui Talibi, Z., Ibsouda Koraichi, S., El Modafar, C., & Delattre, C. (2022). Assessment of the antioxidant, antimicrobial and antibiofilm activities of essential oils for potential application of active chitosan films in food preservation. *World Journal of Microbiology and Biotechnology*, *38*(10), 1-16.
- Moustafa, H., Youssef, A. M., Darwish, N. A., & Abou-Kandil, A. I. (2019). Eco-friendly polymer composites for green packaging: Future vision and challenges. *Composites Part B: Engineering*, *172*, 16-25.
- Mujtaba, M., Salaberria, A. M., Andres, M. A., Kaya, M., Gunyakti, A., & Labidi, J. (2017). Utilization of flax (Linum usitatissimum) cellulose nanocrystals as reinforcing material for chitosan films. *International Journal of Biological Macromolecules*, *104*, 944-952.
- Mumtaza, M., & Munir, S. (2022). Isolation and purification of keratinase producing bacteria from poultry soil. *THE JOURNAL OF MICROBIOLOGY AND MOLECULAR GENETICS*, *3*(2), 123-132.
- Nadira, P., Mujeeb, V. A., Rahman, P. M., & Muraleedharan, K. (2022). Effects of cashew leaf extract on physicochemical, antioxidant, and antimicrobial properties of N, O-Carboxymethyl chitosan films. *Carbohydrate Polymer Technologies and Applications*, *3*, 100191.
- Nageswar, Y. V. D., Domingues, N. L., Katla, R., & Katla, R. (2021). Application of Chitosan-Based Catalysts for Heterocycles Synthesis and Other Reactions. *Polysaccharides: Properties and Applications*, 517-542.
- Narasagoudr, S. S., Hegde, V. G., Chougale, R. B., Masti, S. P., Vootla, S., & Malabadi, R. B. (2020). Physico-chemical and functional properties of rutin induced chitosan/poly (vinyl alcohol) bioactive films for food packaging applications. *Food Hydrocolloids*, *109*, 106096.
- Naseri, N., Algan, C., Jacobs, V., John, M., Oksman, K., & Mathew, A. P. (2014). Electrospun chitosan-based nanocomposite mats reinforced with chitin nanocrystals for wound dressing. *Carbohydrate Polymers*, *109*, 7-15.
- Nasir, B., Baig, M. W., Majid, M., Ali, S. M., Khan, M. Z. I., Kazmi, S. T. B., & Haq, I.-u. (2020). Preclinical anticancer studies on the ethyl acetate leaf extracts of Datura stramonium and Datura innoxia. *BMC Complementary Medicine and Therapies*, *20*(1), 1-23.

- Nasrollahzadeh, M., Sajjadi, M., Irvani, S., & Varma, R. S. (2021). Starch, cellulose, pectin, gum, alginate, chitin and chitosan derived (nano) materials for sustainable water treatment: A review. *Carbohydrate Polymers*, 251, 116986.
- Ngolong Ngea, G. L., Qian, X., Yang, Q., Dhanasekaran, S., Ianiri, G., Ballester, A. R., Zhang, X., Castoria, R., & Zhang, H. (2021). Securing fruit production: Opportunities from the elucidation of the molecular mechanisms of postharvest fungal infections. *Comprehensive Reviews in Food Science and Food Safety*, 20(3), 2508-2533.
- Nguyen, T. L. A., & Bhattacharya, D. (2022). Antimicrobial Activity of Quercetin: An Approach to Its Mechanistic Principle. *Molecules*, 27(8), 2494.
- Ni, Y., Shi, S., Li, M., Zhang, L., Yang, C., Du, T., Wang, S., Nie, H., Sun, J., & Zhang, W. (2021). Visible light responsive, self-activated bionanocomposite films with sustained antimicrobial activity for food packaging. *Food Chemistry*, 362, 130201.
- Oberlintner, A., Bajić, M., Kalčíková, G., Likozar, B., & Novak, U. (2021). Biodegradability study of active chitosan biopolymer films enriched with Quercus polyphenol extract in different soil types. *Environmental Technology & Innovation*, 21, 101318.
- Odagiri, N., Shirasu, K., Kawagoe, Y., Kikugawa, G., Oya, Y., Kishimoto, N., Ohuchi, F. S., & Okabe, T. (2021). Amine/epoxy stoichiometric ratio dependence of crosslinked structure and ductility in amine-cured epoxy thermosetting resins. *Journal of Applied Polymer Science*, 138(23), 50542.
- Okura, H., Wada, M., & Serizawa, T. (2014). Dispersibility of HCl-treated cellulose nanocrystals with water-dispersible properties in organic solvents. *Chemistry Letters*, 43(5), 601-603.
- Oladzadabbasabadi, N., Nafchi, A. M., Ariffin, F., Wijekoon, M. J. O., Al-Hassan, A., Dheyab, M. A., & Ghasemlou, M. (2022). Recent advances in extraction, modification, and application of chitosan in packaging industry. *Carbohydrate Polymers*, 277, 118876.
- Oluba, O. M., Obokare, O., Bayo-Olorunmeke, O. A., Ojeaburu, S. I., Ogunlowo, O. M., Irokanulo, E. O., & Akpor, O. B. (2022a). Fabrication, characterization and antifungal evaluation of polyphenolic extract activated keratin starch coating on infected tomato fruits. *Scientific reports*, 12(1), 4340.
- Oluba, O. M., Obokare, O., Bayo-Olorunmeke, O. A., Ojeaburu, S. I., Ogunlowo, O. M., Irokanulo, E. O., & Akpor, O. B. (2022b). Fabrication, characterization and antifungal evaluation of polyphenolic extract activated keratin starch coating on infected tomato fruits. *Scientific reports*, 12(1), 1-12.
- Oluba, O. M., Osayame, E., & Shoyombo, A. O. (2021). Production and characterization of keratin-starch bio-composite film from chicken feather waste and turmeric starch. *Biocatalysis and Agricultural Biotechnology*, 33, 101996.
- Ozdemir, M., & Floros, J. D. (2004). Active food packaging technologies. *Critical reviews in food science and nutrition*, 44(3), 185-193.
- Pal, N., Banerjee, S., Roy, P., & Pal, K. (2021). Cellulose nanocrystals-silver nanoparticles-reduced graphene oxide based hybrid PVA nanocomposites and its antimicrobial properties. *International Journal of Biological Macromolecules*, 191, 445-456.
- Pan, Y., Zhang, Y., Hou, M., Xue, J., Qin, R., Zhou, M., & Zhang, Y. (2023). Properties of polyphenols and polyphenol-containing wastewaters and their treatment by Fenton/Fenton-like reactions. *Separation and Purification Technology*, 123905.
- Panda, P. K., Dash, P., Yang, J.-M., & Chang, Y.-H. (2022). Development of chitosan, graphene oxide, and cerium oxide composite blended films: Structural, physical, and functional properties. *Cellulose*, 29(4), 2399-2411.
- Parvizpur, A., Ahmadiani, A., & Kamalinejad, M. (2006). Probable role of spinal purinoceptors in the analgesic effect of *Trigonella foenum* (TFG) leaves extract. *Journal of ethnopharmacology*, 104(1-2), 108-112.

- Paudel, K. R., Dua, K., Panth, N., Hansbro, P. M., & Chellappan, D. K. (2022). Advances in research with rutin-loaded nanoformulations in mitigating lung diseases. *Future Medicinal Chemistry*, *14*(18), 1293-1295.
- Pavoni, J. M. F., dos Santos, N. Z., May, I. C., Pollo, L. D., & Tessaro, I. C. (2021). Impact of acid type and glutaraldehyde crosslinking in the physicochemical and mechanical properties and biodegradability of chitosan films. *Polymer Bulletin*, *78*(2), 981-1000.
- Paydayesh, A., Mousavi, S. R., Estaji, S., Khonakdar, H. A., & Nozarinya, M. A. (2022). Functionalized graphene nanoplatelets/poly (lactic acid)/chitosan nanocomposites: Mechanical, biodegradability, and electrical conductivity properties. *Polymer Composites*, *43*(1), 411-421.
- Peng, Y., Wu, Y., & Li, Y. (2013). Development of tea extracts and chitosan composite films for active packaging materials. *International Journal of Biological Macromolecules*, *59*, 282-289.
- Perdones, Á., Vargas, M., Atarés, L., & Chiralt, A. (2014). Physical, antioxidant and antimicrobial properties of chitosan–cinnamon leaf oil films as affected by oleic acid. *Food Hydrocolloids*, *36*, 256-264.
- Phan, D.-N., Lee, H., Huang, B., Mukai, Y., & Kim, I.-S. (2019). Fabrication of electrospun chitosan/cellulose nanofibers having adsorption property with enhanced mechanical property. *Cellulose*, *26*(3), 1781-1793.
- Pires, A. L. R., de Azevedo Motta, L., Dias, A. M., de Sousa, H. C., Moraes, Â. M., & Braga, M. E. (2018). Towards wound dressings with improved properties: Effects of poly (dimethylsiloxane) on chitosan-alginate films loaded with thymol and beta-carotene. *Materials Science and Engineering: C*, *93*, 595-605.
- Pirsa, S., Karimi Sani, I., Pirouzifard, M. K., & Erfani, A. (2020). Smart film based on chitosan/Melissa officinalis essences/pomegranate peel extract to detect cream cheeses spoilage. *Food Additives & Contaminants: Part A*, *37*(4), 634-648.
- Pisoschi, A. M., Pop, A., Cimpeanu, C., Turcuş, V., Predoi, G., & Iordache, F. (2018). Nanoencapsulation techniques for compounds and products with antioxidant and antimicrobial activity-A critical view. *European journal of medicinal chemistry*, *157*, 1326-1345.
- Prasad, K. N., Yang, B., Dong, X., Jiang, G., Zhang, H., Xie, H., & Jiang, Y. (2009). Flavonoid contents and antioxidant activities from Cinnamomum species. *Innovative Food Science & Emerging Technologies*, *10*(4), 627-632.
- Prashanth, K. H., Lakshman, K., Shamala, T., & Tharanathan, R. (2005). Biodegradation of chitosan-graft-polymethylmethacrylate films. *International biodeterioration & biodegradation*, *56*(2), 115-120.
- Qian, Z., Cao, Z., Galuska, L., Zhang, S., Xu, J., & Gu, X. (2019). Glass transition phenomenon for conjugated polymers. *Macromolecular Chemistry and Physics*, *220*(11), 1900062.
- Qin, Y.-Y., Zhang, Z.-H., Li, L., Yuan, M.-L., Fan, J., & Zhao, T.-R. (2015). Physio-mechanical properties of an active chitosan film incorporated with montmorillonite and natural antioxidants extracted from pomegranate rind. *Journal of food science and technology*, *52*(3), 1471-1479.
- Rajabinejad, H., Patrucco, A., Caringella, R., Montarsolo, A., Zoccola, M., & Pozzo, P. D. (2018). Preparation of keratin-based microcapsules for encapsulation of hydrophilic molecules. *Ultrasonics Sonochemistry*, *40*, 527-532.
- Rambabu, K., Bharath, G., Banat, F., Show, P. L., & Cocolletzi, H. H. (2019). Mango leaf extract incorporated chitosan antioxidant film for active food packaging. *International Journal of Biological Macromolecules*, *126*, 1234-1243.
- Rampone, S., Pagliarulo, C., Marena, C., Orsillo, A., Iannaccone, M., Trionfo, C., Sateriale, D., & Paolucci, M. (2021). In silico analysis of the antimicrobial activity of phytochemicals:

- Towards a technological breakthrough. *Computer Methods and Programs in Biomedicine*, 200, 105820.
- Rao, V., & Johns, J. (2008). Thermal behavior of chitosan/natural rubber latex blends TG and DSC analysis. *Journal of Thermal Analysis and Calorimetry*, 92(3), 801-806.
- Regiel-Futyra, A., Kus-Liśkiewicz, M., Sebastian, V., Irusta, S., Arruebo, M., Stochel, G. y., & Kyzioł, A. (2015). Development of noncytotoxic chitosan–gold nanocomposites as efficient antibacterial materials. *ACS applied materials & interfaces*, 7(2), 1087-1099.
- Rhim, J.-W., Hong, S.-I., Park, H.-M., & Ng, P. K. (2006). Preparation and characterization of chitosan-based nanocomposite films with antimicrobial activity. *Journal of agricultural and food chemistry*, 54(16), 5814-5822.
- Rhim, J.-W., & Ng, P. K. (2007). Natural biopolymer-based nanocomposite films for packaging applications. *Critical reviews in food science and nutrition*, 47(4), 411-433.
- Riaz, A., Aadil, R. M., Amoussa, A. M. O., Bashari, M., Abid, M., & Hashim, M. M. (2021). Application of chitosan-based apple peel polyphenols edible coating on the preservation of strawberry (*Fragaria ananassa* cv Hongyan) fruit. *Journal of Food Processing and Preservation*, 45(1), e15018.
- Rocha, O. B., do Carmo Silva, L., de Carvalho Júnior, M. A. B., de Oliveira, A. A., de Almeida Soares, C. M., & Pereira, M. (2021). In vitro and in silico analysis reveals antifungal activity and potential targets of curcumin on *Paracoccidioides* spp. *Brazilian Journal of Microbiology*, 52(4), 1897-1911.
- Rodríguez, G. M., Sibaja, J. C., Espitia, P. J., & Otoni, C. G. (2020). Antioxidant active packaging based on papaya edible films incorporated with *Moringa oleifera* and ascorbic acid for food preservation. *Food Hydrocolloids*, 103, 105630.
- Roy, S., Priyadarshi, R., & Rhim, J.-W. (2021). Development of multifunctional pullulan/chitosan-based composite films reinforced with ZnO nanoparticles and propolis for meat packaging applications. *Foods*, 10(11), 2789.
- Roy, S., & Rhim, J.-W. (2021a). Fabrication of bioactive binary composite film based on gelatin/chitosan incorporated with cinnamon essential oil and rutin. *Colloids and Surfaces B: Biointerfaces*, 204, 111830.
- Roy, S., & Rhim, J.-W. (2021b). Fabrication of chitosan-based functional nanocomposite films: Effect of quercetin-loaded chitosan nanoparticles. *Food Hydrocolloids*, 121, 107065.
- Rubilar, J. F., Cruz, R. M., Silva, H. D., Vicente, A. A., Khmelinskii, I., & Vieira, M. C. (2013). Physico-mechanical properties of chitosan films with carvacrol and grape seed extract. *Journal of Food Engineering*, 115(4), 466-474.
- Rubini, K., Boanini, E., Menichetti, A., Bonvicini, F., Gentilomi, G. A., Montalti, M., & Bigi, A. (2020). Quercetin loaded gelatin films with modulated release and tailored antioxidant, mechanical and swelling properties. *Food Hydrocolloids*, 109, 106089.
- Rujnić-Sokele, M., & Pilipović, A. (2017). Challenges and opportunities of biodegradable plastics: A mini review. *Waste Management & Research*, 35(2), 132-140.
- Sacui, I. A., Nieuwendaal, R. C., Burnett, D. J., Stranick, S. J., Jorfi, M., Weder, C., Foster, E. J., Olsson, R. T., & Gilman, J. W. (2014). Comparison of the properties of cellulose nanocrystals and cellulose nanofibrils isolated from bacteria, tunicate, and wood processed using acid, enzymatic, mechanical, and oxidative methods. *ACS applied materials & interfaces*, 6(9), 6127-6138.
- Salim, M. H., Kassab, Z., Abdellaoui, Y., García-Cruz, A., Soumare, A., Ablouh, E.-h., & El Achaby, M. (2022). Exploration of multifunctional properties of garlic skin derived cellulose nanocrystals and extracts incorporated chitosan biocomposite films for active packaging application. *International Journal of Biological Macromolecules*, 210, 639-653.

- Sameen, D. E., Ahmed, S., Lu, R., Li, R., Dai, J., Qin, W., Zhang, Q., Li, S., & Liu, Y. (2021). Electrospun nanofibers food packaging: Trends and applications in food systems. *Critical Reviews in Food Science and Nutrition*, 1-14.
- Sanchez-Salvador, J. L., Balea, A., Monte, M. C., Negro, C., & Blanco, A. (2021). Chitosan grafted/cross-linked with biodegradable polymers: A review. *International Journal of Biological Macromolecules*, 178, 325-343.
- Saravanan, S., Sameera, D., Moorthi, A., & Selvamurugan, N. (2013). Chitosan scaffolds containing chicken feather keratin nanoparticles for bone tissue engineering. *International Journal of Biological Macromolecules*, 62, 481-486.
- Sarul, D. S., Arslan, D., Vatansever, E., Kahraman, Y., Durmus, A., Salehiyan, R., & Nofar, M. (2021). Preparation and characterization of PLA/PBAT/CNC blend nanocomposites. *Colloid and Polymer Science*, 299(6), 987-998.
- Scopelliti, M. (2021). X-Ray Photoelectron Spectroscopy. *Spectroscopy for Materials Characterization*, 351-382.
- Shah, Y. A., Bhatia, S., Al-Harrasi, A., Afzaal, M., Saeed, F., Anwer, M. K., Khan, M. R., Jawad, M., Akram, N., & Faisal, Z. (2023). Mechanical Properties of Protein-Based Food Packaging Materials. *Polymers*, 15(7), 1724.
- Shahid, S., Leghari, A. A., Farid, M. S., Saeed, M., Anwar, S., Anjum, R., Saeed, N., & Abbas, Z. (2021). Role of active food packaging developed from microencapsulated bioactive ingredients in quality and shelf life enhancement: A review. *Journal of American Science*, 17(2), 12-28.
- Shameli, K., Ahmad, M. B., Zargar, M., Yunus, W. M. Z. W., Ibrahim, N. A., Shabanzadeh, P., & Moghaddam, M. G. (2011). Synthesis and characterization of silver/montmorillonite/chitosan bionanocomposites by chemical reduction method and their antibacterial activity. *International journal of nanomedicine*, 6, 271.
- Sharma, D., Arora, S., dos Santos Rodrigues, B., Lakkadwala, S., Banerjee, A., & Singh, J. (2019). Chitosan-based systems for gene delivery *Functional chitosan* (pp. 229-267): Springer.
- Silva, A. O., Cunha, R. S., Hotza, D., & Machado, R. A. F. (2021). Chitosan as a matrix of nanocomposites: A review on nanostructures, processes, properties, and applications. *Carbohydrate Polymers*, 272, 118472.
- Singh, B. K., Chaudhari, A. K., Das, S., Tiwari, S., & Dubey, N. K. (2022). Preparation and characterization of a novel nanoemulsion consisting of chitosan and Cinnamomum tamala essential oil and its effect on shelf-life lengthening of stored millets. *Pesticide Biochemistry and Physiology*, 187, 105214.
- Singh, G. P., Bangar, S. P., Yang, T., Trif, M., Kumar, V., & Kumar, D. (2022). Effect on the Properties of Edible Starch-Based Films by the Incorporation of Additives: A Review. *Polymers*, 14(10), 1987.
- Siripatrawan, U., & Harte, B. R. (2010). Physical properties and antioxidant activity of an active film from chitosan incorporated with green tea extract. *Food Hydrocolloids*, 24(8), 770-775.
- Siripatrawan, U., & Vitthayakitti, W. (2016). Improving functional properties of chitosan films as active food packaging by incorporating with propolis. *Food Hydrocolloids*, 61, 695-702.
- Skrinjar, M., Mandic, A., Misan, A., Sakac, M., Saric, L. C., & Zec, M. (2009). Effect of Mint (*Mentha piperita* L.) and Caraway (*Carum carvi* L.) on the growth of some toxigenic *Aspergillus* species and Aflatoxin B1 production. *Matica Srpska Proceedings for Natural Sciences*, 131-139.
- Song, X., Liu, L., Wu, X., Liu, Y., & Yuan, J. (2021). Chitosan-Based Functional Films Integrated with Magnolol: Characterization, Antioxidant and Antimicrobial Activity and Pork Preservation. *International journal of molecular sciences*, 22(15), 7769.

- Sorrentino, A., Gorrasi, G., & Vittoria, V. (2007). Potential perspectives of bio-nanocomposites for food packaging applications. *Trends in food science & technology*, 18(2), 84-95.
- Souza, V. G. L., Fernando, A. L., Pires, J. R. A., Rodrigues, P. F., Lopes, A. A., & Fernandes, F. M. B. (2017). Physical properties of chitosan films incorporated with natural antioxidants. *Industrial crops and products*, 107, 565-572.
- Sowjanya, J., Singh, J., Mohita, T., Sarvanan, S., Moorthi, A., Srinivasan, N., & Selvamurugan, N. (2013). Biocomposite scaffolds containing chitosan/alginate/nano-silica for bone tissue engineering. *Colloids and Surfaces B: Biointerfaces*, 109, 294-300.
- Sree, G. V., Rajasekaran, P., Bazaka, O., Levchenko, I., Bazaka, K., & Mandhakini, M. (2021). Biowaste valorization by conversion to nanokeratin-urea composite fertilizers for sustainable and controllable nutrient release. *Carbon Trends*, 5, 100083.
- Stroescu, M., Stoica-Guzun, A., Isopencu, G., Jinga, S. I., Parvulescu, O., Dobre, T., & Vasilescu, M. (2015). Chitosan-vanillin composites with antimicrobial properties. *Food Hydrocolloids*, 48, 62-71.
- Su, H., Jia, Q., & Shan, S. (2016). Synthesis and characterization of Schiff base contained dextran microgels in water-in-oil inverse microemulsion. *Carbohydrate Polymers*, 152, 156-162.
- Sudarsanan, D., Suresh Sulekha, D., & Chandrasekharan, G. (2021). Amomum subulatum induces apoptosis in tumor cells and reduces tumor burden in experimental animals via modulating pro-inflammatory cytokines. *Cancer Investigation*, 39(4), 333-348.
- Suljević, D., Mitrašinović-Brulić, M., Dervišević, A., & Fočak, M. (2022). Protective role of the dandelion extract against the blood–liver axis, cell membranes, and anemia disorder in sodium benzoate-exposed rats. *Cell Biochemistry and Function*, 40(8), 946-958.
- Sun, L., Sun, J., Chen, L., Niu, P., Yang, X., & Guo, Y. (2017). Preparation and characterization of chitosan film incorporated with thinned young apple polyphenols as an active packaging material. *Carbohydrate Polymers*, 163, 81-91.
- Taherimehr, M., YousefniaPasha, H., Tabatabaeekoloor, R., & Pesaranhajiabbas, E. (2021). Trends and challenges of biopolymer-based nanocomposites in food packaging. *Comprehensive Reviews in Food Science and Food Safety*, 20(6), 5321-5344.
- Tanabe, T., Okitsu, N., Tachibana, A., & Yamauchi, K. (2002). Preparation and characterization of keratin–chitosan composite film. *Biomaterials*, 23(3), 817-825.
- Tanase, C. E., & Spiridon, I. (2014). PLA/chitosan/keratin composites for biomedical applications. *Materials Science and Engineering: C*, 40, 242-247.
- Tang, C., Xiang, L., Su, J., Wang, K., Yang, C., Zhang, Q., & Fu, Q. (2008). Largely improved tensile properties of chitosan film via unique synergistic reinforcing effect of carbon nanotube and clay. *The Journal of Physical Chemistry B*, 112(13), 3876-3881.
- Tomaszewska, J., Sterzyński, T., Woźniak-Braszak, A., & Banaszak, M. (2021). Review of recent developments of glass transition in PVC nanocomposites. *Polymers*, 13(24), 4336.
- Tooryan, F., & Azizkhani, M. (2020). Effect of orange (*Citrus aurantium*) juice concentrate and chitosan coating enriched with fenugreek (*Trigonella foenum-graecum*) essential oil on the quality and shelf life of rainbow trout (*Oncorhynchus mykiss*) fillet During Storage In A Refrigerator. *Journal of Veterinary Research*, 75(2), 173-184.
- Torlopov, M. A., Drozd, N. N., Paderin, N. M., Tarabukin, D. V., & Udoratina, E. V. (2021). Hemocompatibility, biodegradability and acute toxicity of acetylated cellulose nanocrystals of different types in comparison. *Carbohydrate Polymers*, 269, 118307.
- Tran, C. D., & Mututuvvari, T. M. (2015). Cellulose, chitosan, and keratin composite materials. Controlled drug release. *Langmuir*, 31(4), 1516-1526.
- Vasanthi, H. R., Mukherjee, S., & Das, D. K. (2009). Potential health benefits of broccoli—a chemico-biological overview. *Mini reviews in medicinal chemistry*, 9(6), 749-759.

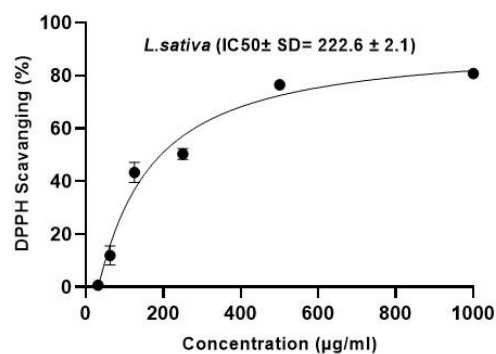
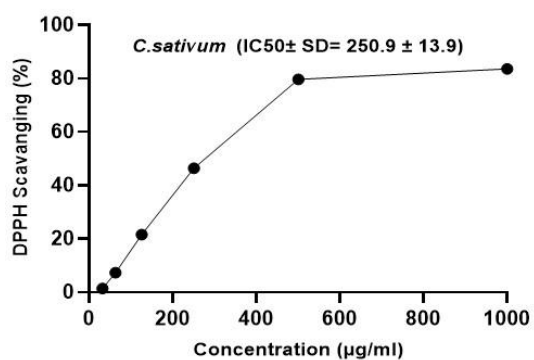
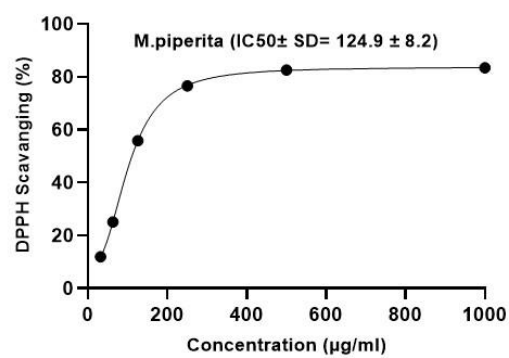
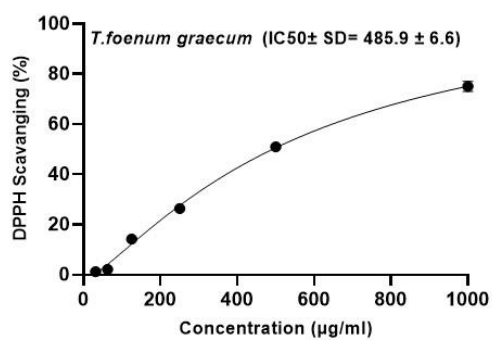
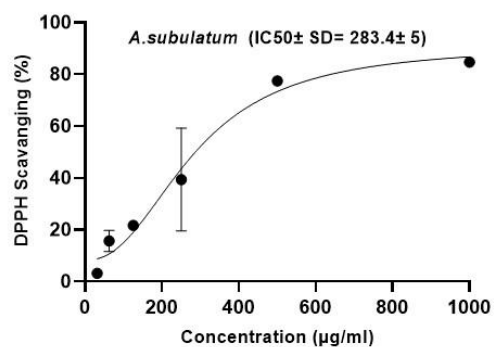
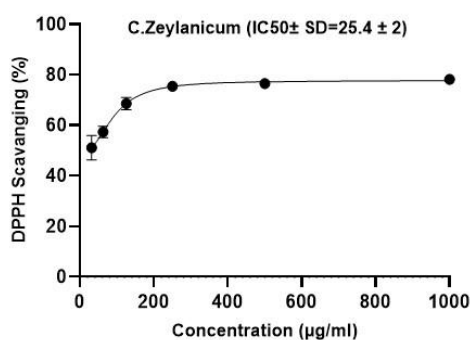
- Vasile, C., Pamfil, D., Râpă, M., Darie-Niță, R. N., Mitelut, A. C., Popa, E. E., Popescu, P. A., Draghici, M. C., & Popa, M. E. (2018). Study of the soil burial degradation of some PLA/CS biocomposites. *Composites Part B: Engineering*, *142*, 251-262.
- Vejdan, A., Ojagh, S. M., Adeli, A., & Abdollahi, M. (2016). Effect of TiO₂ nanoparticles on the physico-mechanical and ultraviolet light barrier properties of fish gelatin/agar bilayer film. *LWT-Food Science and Technology*, *71*, 88-95.
- Viacava, G. E., Gonzalez-Aguilar, G., & Roura, S. I. (2014). Determination of phytochemicals and antioxidant activity in butterhead lettuce related to leaf age and position. *Journal of Food Biochemistry*, *38*(3), 352-362.
- Vilela, C., Kurek, M., Hayouka, Z., Röcker, B., Yildirim, S., Antunes, M. D. C., Nilsen-Nygaard, J., Pettersen, M. K., & Freire, C. S. (2018). A concise guide to active agents for active food packaging. *Trends in food science & technology*, *80*, 212-222.
- Vinod, A., Sanjay, M., Suchart, S., & Jyotishkumar, P. (2020). Renewable and sustainable biobased materials: An assessment on biofibers, biofilms, biopolymers and biocomposites. *Journal of Cleaner Production*, *258*, 120978.
- Vishawanath, T., Sumana, S., & Sharanagouda, J. (2023). Application Of Enzymes In Disease Diagnosis. *ENZYMES-MECHANISMS AND ACTION*, 25-37.
- Visuvanathan, T., Than, L. T. L., Stanslas, J., Chew, S. Y., & Vellasamy, S. (2022). Revisiting *Trigonella foenum-graecum* L.: Pharmacology and Therapeutic Potentialities. *Plants*, *11*(11), 1450.
- Vlacha, M., Giannakas, A., Katapodis, P., Stamatis, H., Ladavos, A., & Barkoula, N.-M. (2016). On the efficiency of oleic acid as plasticizer of chitosan/clay nanocomposites and its role on thermo-mechanical, barrier and antimicrobial properties—Comparison with glycerol. *Food Hydrocolloids*, *57*, 10-19.
- Wang, Q., Tian, F., Feng, Z., Fan, X., Pan, Z., & Zhou, J. (2015). Antioxidant activity and physicochemical properties of chitosan films incorporated with *Lycium barbarum* fruit extract for active food packaging. *International Journal of Food Science & Technology*, *50*(2), 458-464.
- Wang, X., Yong, H., Gao, L., Li, L., Jin, M., & Liu, J. (2019). Preparation and characterization of antioxidant and pH-sensitive films based on chitosan and black soybean seed coat extract. *Food Hydrocolloids*, *89*, 56-66.
- Wang, Y., Wang, S., Nie, X., Yang, K., Xu, P., Wang, X., Liu, M., Yang, Y., Chen, Z., & Wang, S. (2019). Molecular and structural basis of nucleoside diphosphate kinase-mediated regulation of spore and sclerotia development in the fungus *Aspergillus flavus*. *Journal of Biological Chemistry*, *294*(33), 12415-12431.
- Wijesinghe, W., Mantilaka, M., Ruparathna, K., Rajapakshe, R., Sameera, S., & Thilakarathna, M. (2020). Filler matrix interfaces of inorganic/biopolymer composites and their applications. *Interfaces in Particle and Fibre Reinforced Composites*, 95-112.
- Wildan, M. W., & Lubis, F. I. (2021). Fabrication and characterization of chitosan/cellulose nanocrystal/glycerol bio-composite films. *Polymers*, *13*(7), 1096.
- Wu, Y., Wu, W., Farag, M. A., & Shao, P. (2022). Functionalized cellulose nanocrystal embedded into citrus pectin coating improves its barrier, antioxidant properties and potential application in food. *Food Chemistry*, 134079.
- Xiao, J. (2017). Dietary flavonoid aglycones and their glycosides: Which show better biological significance? *Critical reviews in food science and nutrition*, *57*(9), 1874-1905.
- Xiao, Y., Liu, Y., Kang, S., Wang, K., & Xu, H. (2020). Development and evaluation of soy protein isolate-based antibacterial nanocomposite films containing cellulose nanocrystals and zinc oxide nanoparticles. *Food Hydrocolloids*, *106*, 105898.
- Xing, R., Liu, S., Guo, Z., Yu, H., Zhong, Z., Ji, X., & Li, P. (2008). Relevance of molecular weight of chitosan-N-2-hydroxypropyl trimethyl ammonium chloride and their antioxidant activities. *European Journal of Medicinal Chemistry*, *43*(2), 336-340.

- Xu, C., Chen, W., Gao, H., Xie, X., & Chen, Y. (2020). Cellulose nanocrystal/silver (CNC/Ag) thin-film nanocomposite nanofiltration membranes with multifunctional properties. *Environmental Science: Nano*, 7(3), 803-816.
- Xu, Y., Willis, S., Jordan, K., & Sismour, E. (2018). Chitosan nanocomposite films incorporating cellulose nanocrystals and grape pomace extracts. *Packaging Technology and Science*, 31(9), 631-638.
- Yadav, M., Behera, K., Chang, Y.-H., & Chiu, F.-C. (2020). Cellulose nanocrystal reinforced chitosan based UV barrier composite films for sustainable packaging. *Polymers*, 12(1), 202.
- Yadav, M., & Chiu, F.-C. (2019). Cellulose nanocrystals reinforced κ-carrageenan based UV resistant transparent bionanocomposite films for sustainable packaging applications. *Carbohydrate Polymers*, 211, 181-194.
- Yadav, S., Mehrotra, G., Bhartiya, P., Singh, A., & Dutta, P. (2020). Preparation, physicochemical and biological evaluation of quercetin based chitosan-gelatin film for food packaging. *Carbohydrate polymers*, 227, 115348.
- Yang, K., Dang, H., Liu, L., Hu, X., Li, X., Ma, Z., Wang, X., & Ren, T. (2019). Effect of syringic acid incorporation on the physical, mechanical, structural and antibacterial properties of chitosan film for quail eggs preservation. *International Journal of Biological Macromolecules*, 141, 876-884.
- Yang, X., Zhang, H., Yuan, X., & Cui, S. (2009). Wool keratin: A novel building block for layer-by-layer self-assembly. *Journal of colloid and interface science*, 336(2), 756-760.
- Ye, Y., Zhang, T., Lv, L., Chen, Y., Tang, W., & Tang, S. (2021). Functionalization of chitosan by grafting sulfhydryl groups to intensify the adsorption of arsenite from water. *Colloids and Surfaces A: Physicochemical and Engineering Aspects*, 622, 126601.
- Yeole, G., Teli, N., Kotkar, H., & Mendki, P. (2014). Cinnamomum zeylanicum extracts and their formulations control early blight of tomato. *Journal of Biopesticides*, 7(2), 110.
- Yong, H., Wang, X., Bai, R., Miao, Z., Zhang, X., & Liu, J. (2019). Development of antioxidant and intelligent pH-sensing packaging films by incorporating purple-fleshed sweet potato extract into chitosan matrix. *Food Hydrocolloids*, 90, 216-224.
- Younus, I., Ismail, H., Rizvi, C. B., Dilshad, E., Saba, K., Mirza, B., & Tahir, M. (2019). Antioxidant, analgesic and anti-inflammatory activities of in vitro and field-grown Iceberg lettuce extracts. *Journal of Pharmacy & Pharmacognosy Research*, 7(5), 343-355.
- Yuan, G., Lv, H., Yang, B., Chen, X., & Sun, H. (2015). Physical properties, antioxidant and antimicrobial activity of chitosan films containing carvacrol and pomegranate peel extract. *Molecules*, 20(6), 11034-11045.
- Zahara, I., Arshad, M., Naeth, M. A., Siddique, T., & Ullah, A. (2021). Feather keratin derived sorbents for the treatment of wastewater produced during energy generation processes. *Chemosphere*, 273, 128545.
- Zarandona, I., Minh, N. C., Trung, T. S., de la Caba, K., & Guerrero, P. (2021). Evaluation of bioactive release kinetics from crosslinked chitosan films with Aloe vera. *International Journal of Biological Macromolecules*, 182, 1331-1338.
- Zarandona, I., Puertas, A., Dueñas, M., Guerrero, P., & de la Caba, K. (2020). Assessment of active chitosan films incorporated with gallic acid. *Food Hydrocolloids*, 101, 105486.
- Zeng, X., Yao, Y., Gong, Z., Wang, F., Sun, R., Xu, J., & Wong, C. P. (2015). Ice-templated assembly strategy to construct 3D boron nitride nanosheet networks in polymer composites for thermal conductivity improvement. *Small*, 11(46), 6205-6213.
- Zeng, Y., Song, J., Zhang, M., Wang, H., Zhang, Y., & Suo, H. (2020). Comparison of in vitro and in vivo antioxidant activities of six flavonoids with similar structures. *Antioxidants*, 9(8), 732.

- Zhang, G., Wang, Y., Wu, K., Zhang, Q., Feng, Y., Miao, Y., & Yan, Z. (2021). Exogenous application of chitosan alleviate salinity stress in lettuce (*Lactuca sativa* L.). *Horticulturae*, 7(10), 342.
- Zhang, H., & Chen, S. (2019). Nanoparticle-based methods for food safety evaluation *Evaluation Technologies for Food Quality* (pp. 817-835): Elsevier.
- Zhang, J., Zou, X., Zhai, X., Huang, X., Jiang, C., & Holmes, M. (2019). Preparation of an intelligent pH film based on biodegradable polymers and roselle anthocyanins for monitoring pork freshness. *Food Chemistry*, 272, 306-312.
- Zhang, L., Wang, H., Jin, C., Zhang, R., Li, L., Li, X., & Jiang, S. (2017). Sodium lactate loaded chitosan-polyvinyl alcohol/montmorillonite composite film towards active food packaging. *Innovative Food Science & Emerging Technologies*, 42, 101-108.
- Zhang, W., Jiang, H., Rhim, J.-W., Cao, J., & Jiang, W. (2021). Tea polyphenols (TP): a promising natural additive for the manufacture of multifunctional active food packaging films. *Critical reviews in food science and nutrition*, 1-14.
- Zhang, W., Li, X., & Jiang, W. (2020). Development of antioxidant chitosan film with banana peels extract and its application as coating in maintaining the storage quality of apple. *International Journal of Biological Macromolecules*, 154, 1205-1214.
- Zhang, X., Liu, Y., Yong, H., Qin, Y., Liu, J., & Liu, J. (2019). Development of multifunctional food packaging films based on chitosan, TiO₂ nanoparticles and anthocyanin-rich black plum peel extract. *Food Hydrocolloids*, 94, 80-92.
- Zhao, Q., Fan, L., Liu, Y., & Li, J. (2022). Fabrication of chitosan-protocatechuic acid conjugates to inhibit lipid oxidation and improve the stability of β -carotene in Pickering emulsions: Effect of molecular weight of chitosan. *International Journal of Biological Macromolecules*, 217, 1012-1026.
- Zhong, Y., & Li, Y. (2011). Effects of storage conditions and acid solvent types on structural, mechanical and physical properties of kudzu starch (*Pueraria lobata*)-chitosan composite films. *Starch-Stärke*, 63(9), 579-586.
- Zhu, F. (2021). Polysaccharide based films and coatings for food packaging: Effect of added polyphenols. *Food Chemistry*, 359, 129871.
- Ziani, K., Oses, J., Coma, V., & Maté, J. I. (2008). Effect of the presence of glycerol and Tween 20 on the chemical and physical properties of films based on chitosan with different degree of deacetylation. *LWT-Food Science and Technology*, 41(10), 2159-2165.
- Zubair, M., & Ullah, A. (2020). Recent advances in protein derived bionanocomposites for food packaging applications. *Critical reviews in food science and nutrition*, 60(3), 406-434.
- Zubair, M., Wu, J., & Ullah, A. (2019). Hybrid bionanocomposites from spent hen proteins. *ACS omega*, 4(2), 3772-3781.

Appendix

Dose response Curves of plant extracts showing DPPH activity



List of Publications

1. **Beenish Khanzada**, Nosheen Akhtar, Mohammad K. Okla, Saud A. Alamri, Abdulrahman Al-Hashimi, Muhammad Waleed Baig, Samina Rubnawaz, Hamada AbdElgawad, Abdurahman H. Hirad, Ihsan-Ul Haq and Bushra Mirza (2021). Profiling of Antifungal Activities and In Silico Studies of natural polyphenols. *Molecules*, Vol. 26:7164. DOI: <https://doi.org/10.3390/molecules26237164> **Impact factor: 4.148**
2. **Beenish Khanzada**, Bushra Mirza, Aman Ullah (2023). Chitosan based bio-nanocomposites packaging films with unique mechanical and barrier properties. *Food Packaging and Shelf life*, Vol.35 :101016 DOI: <https://doi.org/10.1016/j.fpsl.2022.101016> **Impact factor: 8.0**
3. **Beenish Khanzada**, Nosheen Akhtar, Ihsan ul haq, Bushra Mirza, Aman Ullah (2024). Polyphenol assisted nanoreinforced chitosan films with antioxidant and antimicrobial properties. *Food hydrocolloids*, Vol 153: 110010 DOI: <https://doi.org/10.1016/j.foodhyd.2024.110010> **Impact factor: 10.7**

Turnitin Originality Report

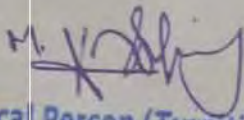
Synthesis, Characterization and Biological Applications of Phyto-assisted Chitosan Nanocomposites by Beenish
From PhD (PhD DRSML)

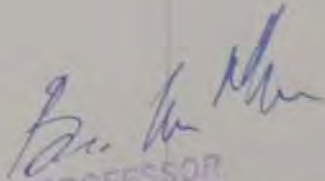


- Processed on 14-Jul-2023 08:27 PKT
- ID: 2130866438
- Word Count: 30801

Similarity Index
11%
Similarity by Source

Internet Sources:
7%
Publications:
7%
Student Papers:
3%


Focal Person (Turnitin)
Quaid-i-Azam University
Islamabad


PROFESSOR
Department of Biochemistry
Quaid-i-Azam University, Islamabad

sources:

- 1% match (student papers from 12-Mar-2023)
[Submitted to Universiti Teknologi Malaysia on 2023-03-12](#)
- < 1% match (Internet from 16-Apr-2023)
<https://www.mdpi.com/2223-7747/12/7/1495>
- < 1% match (Internet from 25-Oct-2022)
<https://www.mdpi.com/2073-4360/14/14/2905/html>
- < 1% match (Internet from 01-Apr-2023)
<https://www.mdpi.com/1420-3049/27/17/5604>
- < 1% match (Internet from 13-Mar-2022)
<https://www.mdpi.com/1420-3049/27/17/5604>
- < 1% match (Internet from 13-Mar-2020)
<https://www.mdpi.com/1420-3049/25/6/1269/html>
- < 1% match (Internet from 08-Jun-2022)
<https://www.mdpi.com/2304-8158/11/11/1118/html>
- < 1% match (Internet from 28-Apr-2023)
<https://www.mdpi.com/1420-3049/27/19/575>
- < 1% match (Internet from 10-Apr-2015)
<http://www.mdpi.com/1420-3049/20/3/4733/html>
- < 1% match (Internet from 30-Jun-2023)
<https://www.mdpi.com/2076-2607/11/6/1599>
- < 1% match (Internet from 28-Jun-2022)
<https://www.mdpi.com/2218-273X/12/6/855/html>
- < 1% match (Internet from 27-Dec-2021)
<https://bmccomplementmedtherapies.biomedcentral.com/articles/10.1186/s12906-020-02975-8>
- < 1% match (Internet from 28-Dec-2022)
<https://bmccomplementmedtherapies.biomedcentral.com/content/pdf/10.1186/s12906-015-0881-1.pdf>
- < 1% match (Internet from 21-Feb-2023)